



Utilization of Oxygen as a By-Product of Water Electrolysis

Nutzung von Sauerstoff als Nebenprodukt der Wasserelektrolyse

Term paper created at the TUM School of Engineering and Design of the Technical University of Munich.

Supervised by Prof. Dr.-Ing. Harald Klein

Johanna Hemauer, M.Sc.

Chair of Plant and Process Technology

Submitted by Amir Dastgheibifard, B.Sc.

Matr.-Nr. 03740543

Study program Chemical Engineering

City, Date Garching, April 6, 2025

Affidavit

I hereby declare in lieu of oath that I prepared the present work independently. Ideas adopted from external sources directly or indirectly are labeled accordingly.

This thesis was not submitted to another examination board.

Garching, April 6, 2025

Amir Dastgheibifard, B.Sc.

Abstract

Driven by the growing industrial and medical O_2 demand and expanding water electrolysis capacities, this term paper investigates the feasibility of utilizing electrolytically-produced O_2 across various industries. A comprehensive market and literature review compared O_2 demands with electrolysis production capacities both at a global and individual industrial plant level, further examining whether individual electrolysis systems can meet the O_2 purity and pressure needs of single oxygen-consuming industrial plants. Studying major oxygen-consuming sectors, fifty-two industrial plants across sixteen key industries were analyzed against projected electrolysis plant capacities until 2029. Beyond the quantitative and qualitative feasibility analysis of industrial-scale electrolysis O_2 integration, the future evolution of O_2 demand across various industries was also assessed.

Despite the limitation that electrolytically-produced O_2 cannot accommodate the global O_2 demand, the findings highlight its potential for direct implementation in individual oxygen-consuming plants. Notably, thirty-five of the fifty-two analyzed plants can have their O_2 demands met by a PEMWE stack capacity under 350 MW. The following cases were identified as those where electrolytically-produced O_2 can be integrated both quantitatively and qualitatively: on-land aquaculture, industrial and municipal wastewater treatment, pulp and paper mills, and several oxygen-enriched combustion processes, including those in magnesia, cement, and lime production, as well as in municipal solid waste incineration. Refineries employing O_2 enrichment in the Claus process for sulfur production and small to medium-sized ceramics manufacturing facilities represent additional direct use cases. Finally, the Ostwald process for nitric acid production and oxyfuel glass manufacturing plants can directly benefit from electrolysis O_2 as well.

Gasification, synthesis gas generation, healthcare, CAM manufacturing, and steel production applications require purification or significant pressurization before electrolytically-produced $\rm O_2$ can be utilized. Quantitatively, electrolysis $\rm O_2$ can benefit various sectors, including small-scale gasification and synthesis gas generation plants, healthcare facilities, and small to medium-sized CAM manufacturing plants. Furthermore, DRI-EAF steel mills up to an annual steel production capacity of $8 \cdot 10^6 \, \rm t$ can have their $\rm O_2$ demands met. In applications where both elemental products of electrolysis are needed, the $\rm H_2$ demand dictates the electrolysis capacity.

Several CO_2 -intensive and manufacturing industries are poised for emerging O_2 demand due to sustainability pressures, energy transition, and growing world population. While O_2 -intensive sectors like steelmaking may see declining O_2 demand with process changes, there appears to be a net increase in the demand for O_2 .

Contents

ΑI	tidav	IL							
Αŀ	ostrac	et							
Sy	mbo	ls							
1	Intro	Introduction							
2	The	ory							
	2.1	The P	rinciple a	and Functionality of Water Electrolysis					
	2.2	Other	Oxygen	Production Methods					
	2.3	Oxyge	en Applica	ation Industries					
		2.3.1	Direct (Oxygen Application					
			2.3.1.1	Iron and Steel Industry					
			2.3.1.2	Wastewater Treatment					
			2.3.1.3	Cathode Active Material Manufacturing					
			2.3.1.4	Healthcare					
			2.3.1.5	Oil and Gas Industry					
			2.3.1.6	Pulp and Paper Industry					
			2.3.1.7	Generation of Synthesis Gas					
			2.3.1.8	Nitric Acid Production					
			2.3.1.9	Aquaculture					
		2.3.2	Oxygen	in Combustion Processes					
			2.3.2.1	Glass Production					
			2.3.2.2	Cement Production					
			2.3.2.3	Waste Incineration					
			2.3.2.4	Ceramics Production					
			2.3.2.5	Production of Lime					
			2.3.2.6	Production of Magnesia					
			2.3.2.7	Power Generation					
		2.3.3	Summa	ry of Oxygen Demand, Pressure and Purity Requirements					
3	Qua	ntitativ	e Analysi	is of Oxygen Capacities and Demands					
3.1 Methodology									
						3.4	Oxyge	en Deman	nd at Plant Level
					4	Fea	sibility	Assessm	nent of Integrating Electrolytically-Produced Oxygen at
	an Industrial Scale								
4.1 Assessment Based on Demand and Capacities									

Co	Contents			
	4.2 4.3	Assessment Based on Pressure and Purity Values	50 52	
5	5 Summary and Outlook		54	
A	A Appendix			
Bi	bliog	raphy	64	

Symbols

Latin Symbols

 \dot{M} Mass flow $\frac{\mathrm{kg}}{\mathrm{s}}$

List of Abbreviations

AEMWE Anion exchange membrane water electrolysis

ASU Air separation unit
ATR Autothermal reforming
AWE Alkaline water electrolysis

BF Blast furnace

BOF Blast oxygen furnace
CAM Cathode active material
CAPEX Capital expenditure
CCT Combined cycle turbine

COPD Chronic obstructive pulmonary disease

DRI Direct reduced iron
EAF Electric arc furnace
FCC Fluid catalytic cracking
FID Final investment decision

GtL Gas-to-liquid

HBI Hot-briquetted iron

IGCC Integrated gasification combined cycle

LPG Liquefied petroleum gas NMC Nickel manganese cobalt OEA Oxygen-enriched air

OEC Oxygen-enriched combustion

OPEX Operating expenditure

PEMWE Proton exchange membrane water electrolysis

POX Partial oxidation PtG Power-to-gas

R&D Research and development SOEC Solid oxide electrolysis cells

SA Swing adsorption USD United States dollar

WWTP Wastewater treatment plants

1 Introduction

The energy transition relies on technologies capable of converting renewable electricity into chemical energy. Water electrolysis stands as a mature solution, ready for near-term deployment to facilitate this shift away from fossil fuels [Fahr et al. 2024]. The electrochemical splitting of water yields hydrogen and oxygen gases. While hydrogen is the target product for which electrolysis systems are deployed, the generated oxygen is commonly vented unused.

The ability to industrially valorize this oxygen by-product would not only improve the economic viability of the cost- and energy-intensive electrolysis systems, but also enhance resource efficiency. The growing importance of this idea is driven by rising global demand for oxygen gas and the concurrent expansion of global electrolysis capacities, leading to more and more oxygen that is produced electrolytically [MARKET.US 2024, IEA 2024].

This, therefore, motivates this term paper to delve into the intricacies of oxygen demand at both global and individual industrial plant levels.

First, market and literature research are conducted to compare and contrast the global oxygen demand vs. the global oxygen production capacity via water electrolysis. While this offers a broad perspective, a fundamental question remains: can a single electrolyzer satisfy the oxygen (O_2) demand of an individual oxygen-consuming industrial plant, considering its O_2 purity and pressure requirements?

To address this question, major oxygen-consuming industries are studied. Where feasible, the smallest and largest oxygen-consuming plants within each industry are identified, along with their purity and pressure requirements. Simultaneously, projected capacities of near-future individual electrolyzer plants are determined.

This data shall then allow for a quantitative comparison between individual electrolyzer systems and individual oxygen-consuming industrial plants, thereby facilitating the objective of this term paper: to determine a series of suitable use cases where the integration of electrolysis oxygen is both quantitatively and qualitatively feasible.

This industry-focused study would also enable an assessment of the future evolution of various sectors in terms of oxygen consumption, illustrating how demand within a given industry may decline, rise, or even emerge in the near future.

Oxygen production through water electrolysis, including the gas crossover phenomenon is contextualized in section 2.1, while section 2.2 explores industrial oxygen production more broadly. Section 2.3 explores oxygen-consuming industries, detailing their oxygen-related parameters, including the specific O_2 demand, as well as the required oxygen pressure and purity for each sector. This theoretical background is essential for assessing the industrial feasibility of integrating electrolytically-produced oxygen in chapter 4.

2.1 The Principle and Functionality of Water Electrolysis

Water electrolysis is an electrochemical process in which water is split into its elemental constituents using electrical energy, which creates a potential difference between the cathode (negative electrode) and the anode (positive electrode). This potential difference facilitates the required electron transfer essential for driving the non-spontaneous overall chemical reaction depicted by equation (C 2.1). [SMOLINKA & GARCHE 2022]

$$2 H_2 O \longrightarrow 2 H_2 + O_2$$
 (C 2.1)

It is evident from equation (C 2.1) that oxygen atoms in the initial H_2O molecules lose electrons (undergo oxidation), transitioning from an oxidation state of –II to 0, while the hydrogen atoms gain electrons and are reduced from +I to 0. The reaction, therefore, involves two distinct redox couples: H_2O/H_2 and H_2O/O_2 . [SMOLINKA & GARCHE 2022]

CARMO ET AL. 2013 and FAHR ET AL. 2024 list the predominant water electrolysis technologies including: alkaline electrolysis (AWE), proton exchange membrane water electrolysis (PEMWE), solid oxide electrolysis cells (SOEC), and anion exchange membrane water electrolysis (AEMWE).

These technologies differ in several key aspects, such as electrolyte type, membrane structure, ion transport mechanisms, operating conditions, catalysts, and overall technological maturity. AWE is distinguished by its two electrodes submerged in a liquid alkaline electrolyte, typically a 20-30% caustic potash (KOH) solution. A diaphragm separates the electrodes, ensuring the efficient and safe segregation of product gases while allowing the passage of hydroxide ions and water molecules. In PEMWE, on the other hand, the two electrodes are separated by a solid proton exchange membrane, which acts as both the electrolyte and a barrier between the product gases. Deionized

water is introduced at the anode, where it undergoes oxidation, releasing oxygen gas, protons, and electrons. The protons migrate through the membrane to the cathode, while the electrons travel via an external circuit. At the cathode, the protons and electrons combine to produce hydrogen gas. [SMOLINKA & GARCHE 2022]

Among water electrolysis technologies, AWE is the most established for large-scale applications, followed by PEMWE, SOEC, and AEM in descending order of technological maturity. [Fahr et al. 2024, Carmo et al. 2013]

Equation (C 2.1) represents the overall water electrolysis reaction regardless of the technology used.

Considering the stoichiometry of equation (C 2.1) and the molar masses of oxygen and hydrogen, it can be deduced that the mass flow of O_2 is eight times that of H_2 :

$$\dot{M}_{\rm O_2} = 8 \cdot \dot{M}_{\rm H_2} \,.$$
 (2.1)

To prevent the mixing of produced gases (oxygen and hydrogen) and their spontaneous recombination - which can pose explosion hazards and cause significant efficiency losses - each electrolyzer cell incorporates a separator, positioned between the two electrodes. This separator must allow free ion movement while restricting gas bubble transfer between compartments. However, due to various factors, some gas crossover still occurs in the cell and/or at the system level. Gas crossover refers to the unintended diffusion or leakage of hydrogen into the oxygen side (or vice versa) through the separator. Beyond efficiency losses, it poses a significant safety risk, as hydrogen concentrations of just 4% in the oxygen stream can create an explosive mixture. [SMOLINKA & GARCHE 2022]

Gas crossover means that neither product of water electrolysis in AWE or PEMWE is entirely pure. The hydrogen stream is contaminated with water and traces of oxygen, while the oxygen stream contains water and small amounts of hydrogen [Smolinka & Garche 2022]. Consequently, purification processes are essential when near-pure ($\geq 99.9\%$ by volume) hydrogen and oxygen gases are required.

Both Haug 2019 and Fahr et al. 2024 have investigated gas crossover in both AWE and PEMWE systems and suggested mitigation strategies. Both the hydrogen and oxygen sides can experience gas crossover:

- Hydrogen crossover is when the hydrogen generated at the cathode diffuses across the separator into the anode side (where oxygen is produced).
- Oxygen crossover is when the oxygen produced at the anode diffuses to the cathode side (where hydrogen is produced).

The crossover phenomenon is discussed in detail by Smolinka & Garche 2022, Haug 2019, and Fahr et al. 2024. Hydrogen crossover not only diminishes the overall efficiency of the cell but also introduces potential operational constraints due to safety concerns, as it heightens the risk of forming combustible or explosive gas mixtures. To

avoid this, the hydrogen volume content in the oxygen stream must remain below 2%, beyond which the electrolyzers are shut down.

Generally, in both AWE and PEMWE, hydrogen crossover increases significantly with decreasing current density and rising system pressure. This is driven by two key factors: first, lower current densities reduce the oxygen evolution rate, decreasing the dilution of permeating hydrogen and thereby increasing its relative concentration in the anodic gas stream. Second, elevated system pressures enhance gas solubility within the electrolyte, leading to greater hydrogen dissolution and subsequent permeation to the anodic side, ultimately resulting in higher measured hydrogen contamination. Supersaturation, which describes a higher concentration of dissolved hydrogen within the electrode boundary or catalyst layer than it would be expected through Henry's law, significantly increases diffusional hydrogen crossover in both AWE and PEMWE as well. Optimizing the geometric and structural properties of electrodes or catalyst layers offers a potential mitigation strategy to lessen the extent of supersaturation. [HAUG 2019]

In AWE, the rate and type of electrolyte circulation also affects the gas crossover flux. The anodic electrolyte cycle is the stream of electrolyte that circulates through the oxygen-producing half-cell, while the cathodic electrolyte cycle circulates through the hydrogen-producing half-cell. When the anodic and cathodic electrolyte cycles are maintained separately, the dissolved hydrogen generated at the cathode is prevented from mixing with the anodic electrolyte, resulting in much lower hydrogen contamination levels. In contrast, when the electrolyte cycles are mixed, the hydrogen produced at the cathode can combine with the anodic side, causing a significant increase in measured hydrogen content in the O_2 stream. [HAUG 2019]

In PEMWE, the 2% threshold is influenced by a delicate balance of membrane thickness, gas pressure, current density, and, to a lesser extent, temperature. While increasing membrane thickness can reduce hydrogen crossover, it is not a practical solution as it negatively impacts electrolyzer performance. An alternative approach to mitigating hydrogen crossover in PEMWE is the use of recombination catalysts, which facilitate the conversion of permeated hydrogen back into water. Hydrogen crossover is generally governed by both cell structure and operational parameters, such as current density, which varies with cell load and degradation. At high current densities, the cathode catalyst and transport layers significantly influence crossover flux, whereas at lower current densities, membrane thickness and cathode pressure play a more dominant role. This is because at high current densities, increased gas production leads to supersaturation and enhanced water drag effects in the cathode catalyst and transport layers, which significantly impact the crossover flux. In contrast, at lower current densities, gas production is lower, so the crossover is mainly governed by steady-state diffusion, where membrane thickness and cathode pressure become the dominant factors. [Haug 2019, Fahr et al. 2024]

In contrast, oxygen crossover to the cathode in PEMWE is typically less detrimental to efficiency and poses fewer safety concerns compared to hydrogen crossover. Due to reaction stoichiometry, oxygen in hydrogen is diluted twice as much as hydrogen in

oxygen. Additionally, most PEMWE systems operate at a differential pressure, with the anode often near atmospheric pressure. This results in a lower driving force for oxygen crossover compared to hydrogen. Furthermore, in PEMWE, the Pt-based catalyst at the cathode facilitates the recombination of oxygen and hydrogen into water, ensuring that only a fraction of the oxygen diffusing through the membrane reaches the gas phase on the cathode side. [FAHR ET AL. 2024]

Figure 2.1 summarizes the extent of hydrogen crossover for both PEMWE and AWE setups in various experiments conducted by HAUG 2019.

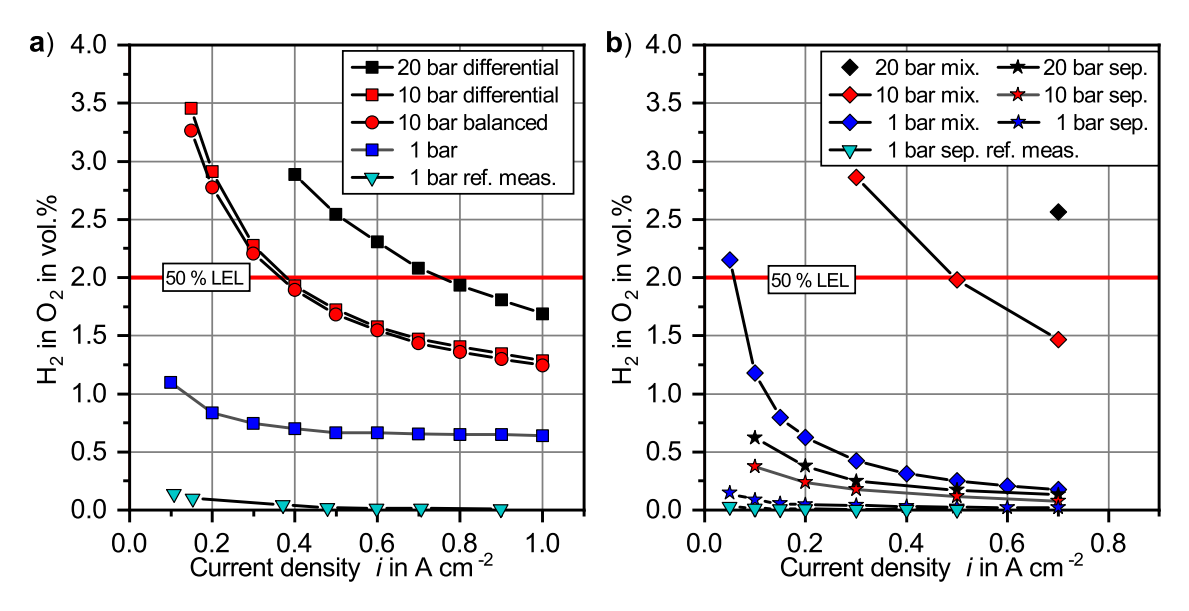


Figure 2.1: Hydrogen impurity in the oxygen stream as a function of current density for (a) PEMWE and (b) AWE setups at 60 ℃ under varying system pressures and electrolyte circulation strategies (for AWE) [Adapted from HAUG 2019]

As previously discussed, both electrolysis technologies clearly demonstrate a reduction in anodic hydrogen contamination as applied current density increases. In both cases, higher operating pressure results in increased hydrogen crossover. Notably, at a system or cathodic pressure of 10 bar, PEMWE exhibits no significant difference between differential and balanced pressure operation. In AWE, electrolyte circulation management appears to have a greater impact than operating pressure. Notably, PEMWE systems often utilize differential pressure operation, where near-atmospheric anode pressure reduces the oxygen crossover driving force [Fahr et al. 2024]. Similarly, AWE systems typically operate at equal anodic and cathodic pressures to minimize crossover [Martinez Lopez et al. 2023].

It is worth noting, as highlighted by Fahr Et al. 2024, that crossover values reported in the literature exhibit significant discrepancies. While measurements at near-zero current density tend to be consistent across studies, values at high current densities can vary considerably. These variations stem from differences in experimental setups, operating conditions, and modeling methodologies employed by different research groups.

In practice, the safe operation of both PEMWE and AWE systems, maintaining anodic hydrogen levels below 2 vol.%, can be achieved by implementing the operational

parameters and mitigation strategies recommended by Haug 2019 and Fahr et al. 2024. These include adjusting current densities, operating pressures, and optimizing the geometric and structural properties of cell components (for both technologies), application of recombination catalysts (PEMWE), placing thin interlayers within the separator or between the electrode and the separating unit (primarily for PEMWE), and implementing appropriate electrolyte circulation strategies (AWE).

Industrially, water electrolysis systems are primarily installed and operated to produce hydrogen rather than oxygen. In other words, hydrogen is the intended end product, while oxygen, as a by-product, is typically vented off [Bareiss et al. 2019].

Research conducted as a part of this term paper examined publicly available data on the oxygen pressure and purity levels of major PEMWE and AWE electrolysis stack manufacturers (electrolyzer outlet prior to further pressurization or treatment). Table 2.1 documents the results of this research.

Table 2.1: Comparison of oxygen outlet values across major electrolysis stack manufacturers (- if data is publicly unavailable)

Manufacturer Technology		O_2 pressure in barg	H_2 pressure in barg	O ₂ purity in vol.%	Stack efficiency in $\frac{MWh}{t_{H_2}}$	Source
ITM Power	PEMWE	1	30	-	50	ITM Power 2025
Nel ASA	PEMWE	1	30	-	53.2	NEL HYDRO- GEN 2019
Nel ASA	AWE	0.03	0.03	99.5	50	NEL HYDRO- GEN 2018
John Cock- erille	AWE	30	30	-	48	John Cock- erill 2025
Sunfire	AWE	30	30	-	50	Sunfire 2025
Quest One	PEMWE	-	30	-	51	QUEST ONE 2025
Siemens Energy	PEMWE	0.1	0.1	99.5-98	-	STEINHARDT 06.03.2025
Ohmium	PEMWE	1	10-30	-	-	Онміим 02.04.2025
Longi	AWE	-	16	-	47.8	LONGI 2025
Thyssenkrup	p AWE	-	0.3	-	50.07	THYSSENKRUPP NUCERA 2025
Peric	PEMWE	-	1-32	≥ 99.2	48	Peric 2025b
Peric	AWE	15-32	15-32	≥ 98.5	52.8	Peric 2025a

Stack efficiency refers to the power consumption of a stack required to produce a unit of hydrogen gas. In contrast, plant efficiency accounts for the power consumption of the stacks along with additional systems such as water purification, pumps, and other utilities essential for the operation of an electrolysis plant. For PEMWE systems (electrolysis plants), SMOLINKA & GARCHE 2022 delineates a power consumption span of 55.63 to 72 $\frac{\text{MW h}}{\text{tH}_2}$, while AWE plants range from 51.2 to 75.7 $\frac{\text{MW h}}{\text{tH}_2}$.

The total power consumption of an electrolysis plant can typically be estimated by increasing the stack power consumption by 6% to 12%, depending on the specific plant configuration. To convert the power consumption from $\frac{\text{MW}\,\text{h}}{\text{t}_{\text{H}_2}}$ to $\frac{\text{MW}\,\text{h}}{\text{t}_{\text{O}_2}}$, the value can be divided by eight, giving a range of 6.95 to 9 $\frac{\text{MW}\,\text{h}}{\text{t}_{\text{O}_2}}$ and 6.4 to 9.46 $\frac{\text{MW}\,\text{h}}{\text{t}_{\text{O}_2}}$ for PEMWE and AWE plants respectively.

The manufacturers were contacted via email, requesting the publicly unavailable data on O_2 outlet pressure and purity, but they declined to provide it.

Siemens Energy was the only manufacturer to respond positively to the request email, stating that the initial H₂ content in O₂ is less than 0.5%. However, toward the end of the stack's lifetime (approximately 10 years), this increases to below 2%. [Steinhardt 06.03.2025]

Particularly relevant are the outlet purity and pressure of the oxygen released from electrolysis stacks before further treatment. This information is essential for assessing how well these values align with the purity and pressure requirements of end users. Most stack efficiency and purity values assume 100% cell load and optimal performance at the beginning of the electrolysis system's lifetime.

Gustavsson et al. 2023 reports a study on the O_2 purity levels from different AWE manufacturers, which consistently report a purity of >98% by volume. The study also concludes that PEMWE systems deliver gases with a higher purity than AWE systems.

As evident from table 2.1, oxygen outlet pressures are generally lower than those of hydrogen, particularly in PEMWE that predominantly utilizes differential pressure operation. In contrast, AWE systems invariably employ balanced pressures. This fundamental difference arises from the robust nature of the solid polymeric membrane in PEMWE, which can withstand substantial pressure differentials across the electrochemical cells. AWE systems, however, with their less mechanically resilient diaphragms, are constrained to operate under balanced pressure conditions. Consequently, the maximum achievable oxygen output pressure in AWE systems is typically in the order of 30 bar. [Hancke et al. 2024, Colli et al. 2019]

In PEMWE, the oxygen outlet pressure is almost invariably maintained near atmospheric levels. This design choice is critical, as FAHR ET AL. 2024 discusses, because elevated oxygen pressures significantly amplify the rate of unwanted oxygen crossover through the membrane. This phenomenon is particularly detrimental to Faradaic efficiency due to the stoichiometry of the crossover reaction: a single oxygen molecule recombining with two hydrogen molecules at the cathode. Consequently, even trace amounts of oxygen permeation lead to a disproportionately large loss of efficiency. Increasing the pressure on the anode side enhances the solubility of oxygen in the liquid water present as well. This leads to a higher concentration of dissolved oxygen at the membrane interface, and subsequently, elevated oxygen pressures would increase both its solubility and diffusion rate across the membrane, resulting in a greater influx of oxygen into the hydrogen stream. Beyond the issue of crossover, high-pressure oxygen systems impose

more stringent demands on the mechanical strength of the electrolyzer components. This is especially true for the anode cell components, which must withstand the pressure exerted from the cathode side. To meet these requirements, thicker or reinforced membranes and porous transport layers may be necessary, leading to increased material costs and higher ohmic losses within the cell. [Fahr et al. 2024, Hancke et al. 2024] This explains why the majority of commercially available PEM electrolyzers are designed to deliver oxygen at near-atmospheric outlet pressures, necessitating a separate compression stage if higher oxygen pressures are required for downstream applications.

2.2 Other Oxygen Production Methods

Four primary methods of oxygen production, each with varying levels of industrial maturity and scale, can be named: cryogenic air separation, swing adsorption, membrane separation, and water electrolysis. [ECKL ET AL. 2025]

While oxygen production via water electrolysis was described in section 2.1, ECKL ET AL. 2025 summarizes the other three oxygen production methods.

Cryogenic air separation, the most widely used and advanced technology for high-purity ($\geq 99.5\%$ by volume) oxygen production, relies on the differing boiling points of air components such as nitrogen, oxygen, and argon. The process begins by compressing air to 4 to 10 bar, cooling it to ambient temperature, and then purifying it. As air, pre-cooled to near liquefaction in the cryogenic chamber, enters the distillation columns, both gaseous and liquid states of the components are available for separation based on their differing boiling points. This method produces high-purity liquid nitrogen and optionally argon as by-products, which can be sold with minimal additional costs. Some air separation units (ASU) have an oxygen production capacity of up to $3.65 \cdot 10^6 \,\mathrm{t}$ per year. The specific energy consumption is approximately $0.25 \, \frac{\mathrm{MWh}}{\mathrm{to}_2}$. The O₂ outlet pressure is near-atmospheric.

In swing adsorption (SA), oxygen is produced by passing air through a sieve bed, typically made of zeolites, which adsorb nitrogen. The process consists of two alternating steps occurring simultaneously in multiple sieve beds, controlled by valves: in the first step, nitrogen is adsorbed, and oxygen is directed to the storage tank; in the second step, the adsorbent is regenerated, and nitrogen is released. The regeneration phase is triggered either by reducing pressure or applying heat, depending on the technology type. Pressure swing adsorption and vacuum swing adsorption operate based on pressure changes, while temperature swing adsorption uses temperature variations. SA is less efficient in terms of economies of scale (and purity), which makes it better suited for small to medium-scale oxygen production, generally ranging from 7300 to 36500 tonnes per year. The specific energy consumption ranges from 0.4 to 0.89 $\frac{\text{MWh}}{\text{to}_2}$. O₂ outlet pressures can be as high as 4 bar.

The membrane separation process, a recent advancement in oxygen production technology, has seen significant progress in recent years. While different methods exist, they all share the same underlying principle: gas diffusion through a membrane. Membrane separation relies on a pressure difference to drive selective diffusion of certain components through the membrane while retaining others. In case of air, oxygen is separated from ambient air and retained upstream due to its high diffusivity, while nitrogen passes through and is collected downstream. As the permeate passes through the membrane, it experiences a pressure drop due to the membrane's resistance. This pressure differential is essential for controlling the separation rate and efficiency. Traditional polymeric membranes operate near ambient temperature conditions and produce oxygen-enriched air (OEA) with a purity of up to 40% by volume. If a second purification stage is added to this process, the purity level can reach 90%. The technology is recently developed and industrially immature with maximum production capacities of under 7300 tonnes per year. The specific energy consumption is similar to that of cryogenic air separation (0.23 $\frac{MWh}{to_2}$). The O₂ outlet pressure is near-atmospheric.

2.3 Oxygen Application Industries

Oxygen plays a vital role as a foundational feedstock across a wide range of industrial applications. The research conducted as part of this term paper identifies sixteen major industries or applications that currently require or may require oxygen in the future due to technical progress. A comprehensive quantitative demand analysis is presented in chapter 3.

This work builds upon the research of LOEFFLER 2022, who conducted a meticulous study of various industrial applications, drawing information and case studies from numerous sources. However, his analysis lacked a quantitative assessment, which this term paper aims to address.

Industries that utilize oxygen can be broadly categorized into two groups: those in which oxygen serves as a fundamental reactant or is directly used, and those in which it is primarily employed to enhance combustion.

2.3.1 Direct Oxygen Application

The research conducted for this paper has identified nine use cases where oxygen is directly required - either as a reactant, as part of a manufacturing or treatment process, or for direct use, such as in medical applications.

These nine use cases include:

- Iron and steel industry
- Medical oxygen
- Pulp and paper industry

- Wastewater treatment
- Oil and gas industry
- Cathode active material manufacturing
- Synthesis gas generation
- Nitric acid production
- Aquaculture.

The specific role of oxygen in each of these industries is detailed below.

2.3.1.1 Iron and Steel Industry

The iron and steel industry is the predominant consumer of industrial oxygen worldwide [Kato et al. 2005]. In 2022, around 47% of the global oxygen demand was consumed by the steelmaking process [Market.us 2024]. To illustrate this massive quantity at an individual plant level, the Voestalpine steel plant in Linz, Austria, consumes $577 \cdot 10^6 \frac{\text{Nm}_{O_2}^3}{\text{y}}$ or $824533 \frac{\text{to}_2}{\text{y}}$ to produce up to $6 \cdot 10^6 \, \text{t}$ of steel, translating to a rough value of $138 \, \frac{\text{kg}_{O_2}}{\text{t}_{\text{Steel}}}$ [Loeffler 2022].

The substantial demand for steel arises from its crucial role in urban infrastructure, including the construction of buildings, bridges, and transportation systems, as well as its vital application in energy production and in machinery [WORLD STEEL ASSOCIATION 2020].

Steel production currently follows two major pathways: the conventional blast furnace-basic oxygen furnace (BF-BOF) route and the electric arc furnace (EAF) route. While the former is employed to produce new steel, the latter is predominantly used for recycling steel scrap. [Eurofer 2024]

A schematic overview of the raw materials and processes involved in iron and steel production is presented in figure 2.2.

In the BF-BOF route, which currently accounts for approximately 72% of global steel production, the underlying chemical process involves the reduction of iron ore (iron oxide) into iron, with carbon (in the form of coke) serving as the primary reducing agent. This occurs in a blast furnace (BF) where hot air, at temperatures ranging from 1000 °C to 1300 °C, is injected at the lower part of the blast furnace. This hot air facilitates the combustion of coke, generating the necessary heat and carbon monoxide required for the reduction of iron ore to molten iron, known as pig iron. The molten iron also absorbs a percentage of carbon from the coke, with carbon serving as an essential element in the composition of steel. [LOEFFLER 2022]

The primary chemical reaction responsible for the production of molten iron is:

$$Fe_2O_3 + 3CO \longrightarrow 2Fe + 3CO_2$$
 (C 2.2)

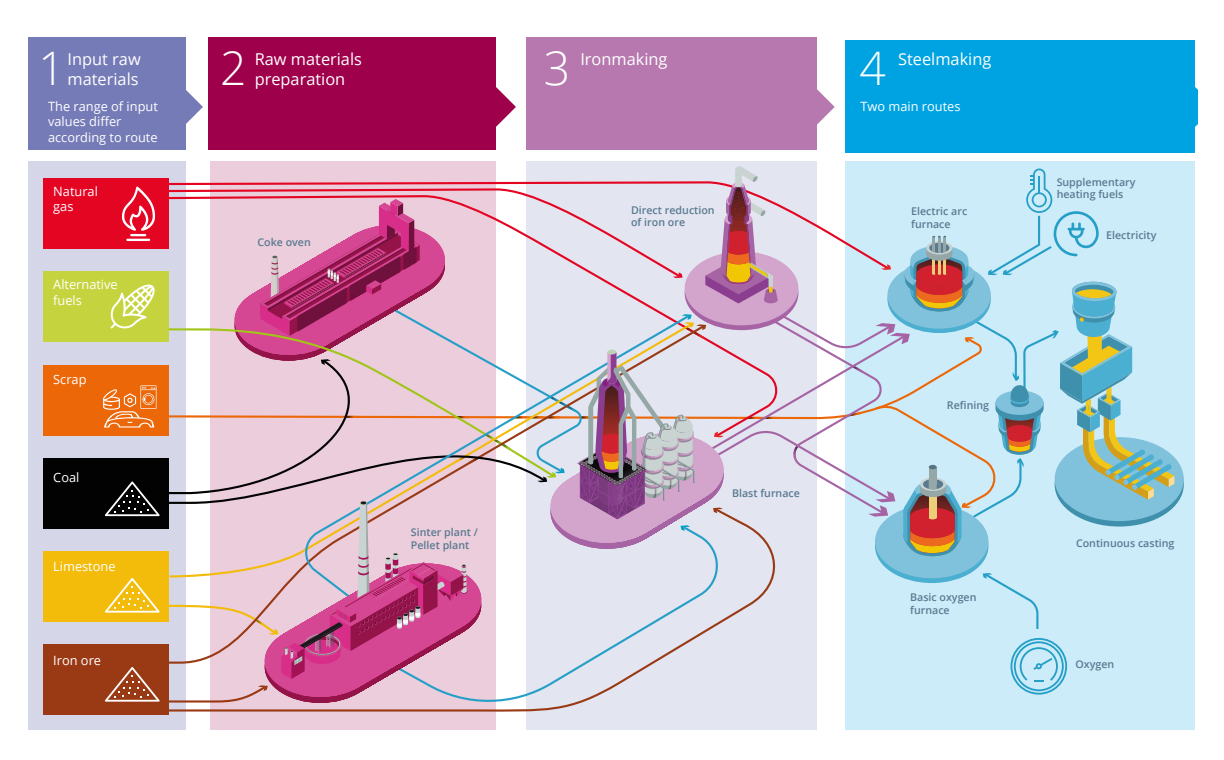


Figure 2.2: Overview of the raw materials and processes involved in iron and steel production [Adapted from WORLD STEEL ASSOCIATION 2020]

As described by LOEFFLER 2022, slag is formed as a by-product through the reaction of impurities in the iron ore with flux materials such as limestone. These flux materials are deliberately added to facilitate the removal of impurities in the form of slag. Because of its lower density, the slag floats on top of the molten pig iron, acting as a protective layer that minimizes heat loss and prevents oxidation of the underlying iron. The slag and pig iron are tapped separately, with the molten pig iron being collected at the base of the furnace.

Since the pig iron obtained is brittle and unsuitable for end-use applications, it must be converted into steel. The pig iron, therefore, is transported to the basic oxygen furnace (BOF) for further processing.

In the BOF, high-purity oxygen ($\geq 99.5\%$ by volume) is blown onto the molten pig iron at a pressure of approximately 12 to 15 bar. This oxidizes unwanted elements such as silicon, phosphorus, carbon, manganese, and others, resulting in the production of crude steel.

An alternative to the conventional BF-BOF route is producing crude steel in an electric arc furnace. The primary feedstock for the EAF is currently steel scrap; however, EAFs are also capable of smelting solidified iron or direct reduced iron (DRI). The prevailing practice is to use the BF-BOF route for producing new steel, while the EAF is primarily employed for recycling scrap steel [EUROFER 2024].

A direct EAF operates by generating high-temperature arcs between graphite electrodes and the metal charge, which provides the heat necessary for melting. The metal charge conducts electricity and hence completes the electrical circuit. Chemical energy,

alongside electrical energy, plays a crucial role in the melting process through exothermic reactions facilitated by the combustion of natural gas and other carbon carriers with oxygen. Natural gas (or other carbon carriers) and oxygen are injected into the semi-molten charge using specialized injection units. More oxygen is then injected to oxidize and eliminate impurities. Additional scrap may be added to regulate the temperature. [Dutta & Chokshi 2020]

Irrespective of the production route, crude steel has to be refined to obtain desirable steel properties. During the refining phase, alloying elements such as manganese and chromium are added, with measures taken to minimize oxidation and regulate carbon levels. Final deoxidation occurs in a further step by adding ferrosilicon and aluminum to obtain optimal purity and composition of the molten steel. [Dutta & Chokshi 2020]

Although Figure 2.2 illustrates the theoretical feasibility of alternative routes such as BF-EAF or DRI-BOF, these configurations lack practical industrial application. Consequently, the industrially-common steelmaking pathways are limited to BF-BOF and DRI-EAF (or the recycling of scrap steel in the EAF).

Steelmaking, as illustrated in reaction equation (C 2.2), emits CO_2 , which accounts for approximately 8% of global CO_2 emissions. Presently, European steel mills emit approximately 2112 t_{CO_2} per tonne of steel produced via the BF-BOF route [FRIES 2022]. This reveals the need to explore and implement alternative, more sustainable, and environmentally friendly production methods.

A promising alternative for low-carbon iron production is the DRI-EAF route, which is being intensively studied and evaluated by both academia and the steel industry.

Generally, DRI is a form of iron produced through the direct reduction of iron ore in its solid state, without reaching its melting point, using a reducing gas or elemental carbon. Direct reduction processes are highly dependent on the chemical and physical properties of the raw materials. The lumps or pellets utilized must exhibit high iron content, low gangue levels, strong mechanical integrity, high reducibility, and resistance to decrepitation. [Dutta & Chokshi 2020]

There are several technologies for the direct reduction of iron ore, such as MIDREX®, PERED®, and HYL/Energiron, which mainly differ in the types of input materials or reducing agents used, as well as the form of the starting materials (lump ore, pellets, or fine ore). In all these processes, the reducing gas typically consists of high proportions of carbon monoxide and hydrogen (so-called synthesis gas). [LOEFFLER 2022]

The main reduction reactions are the following if methane, which must first be reformed into CO and H_2 before being injected into the direct reduction shaft, is used:

$$CH_4 + H_2O \longrightarrow CO + 3H_2$$
 (C 2.3)

$$Fe_2O_3 + 3CO \longrightarrow 2Fe + 3CO_2$$
 (C 2.4)

$$Fe_2O_3 + 3H_2 \longrightarrow 2Fe + 3H_2O$$
 (C 2.5)

Equation (C 2.5) showcases the possibility to reduce iron ore using only hydrogen, without the involvement of carbon. In fact, this reduction pathway, combined with steelmaking in the EAF, is at the core of many sustainable and so-called green steel initiatives.

Vogl et al. 2018 investigated the hydrogen-based direct reduction ironmaking process summarized in equation (C 2.5), followed by an EAF that melts the DRI exclusively using electrical energy to finally produce steel. The flow chart in diagram 2.3 demonstrates the process.

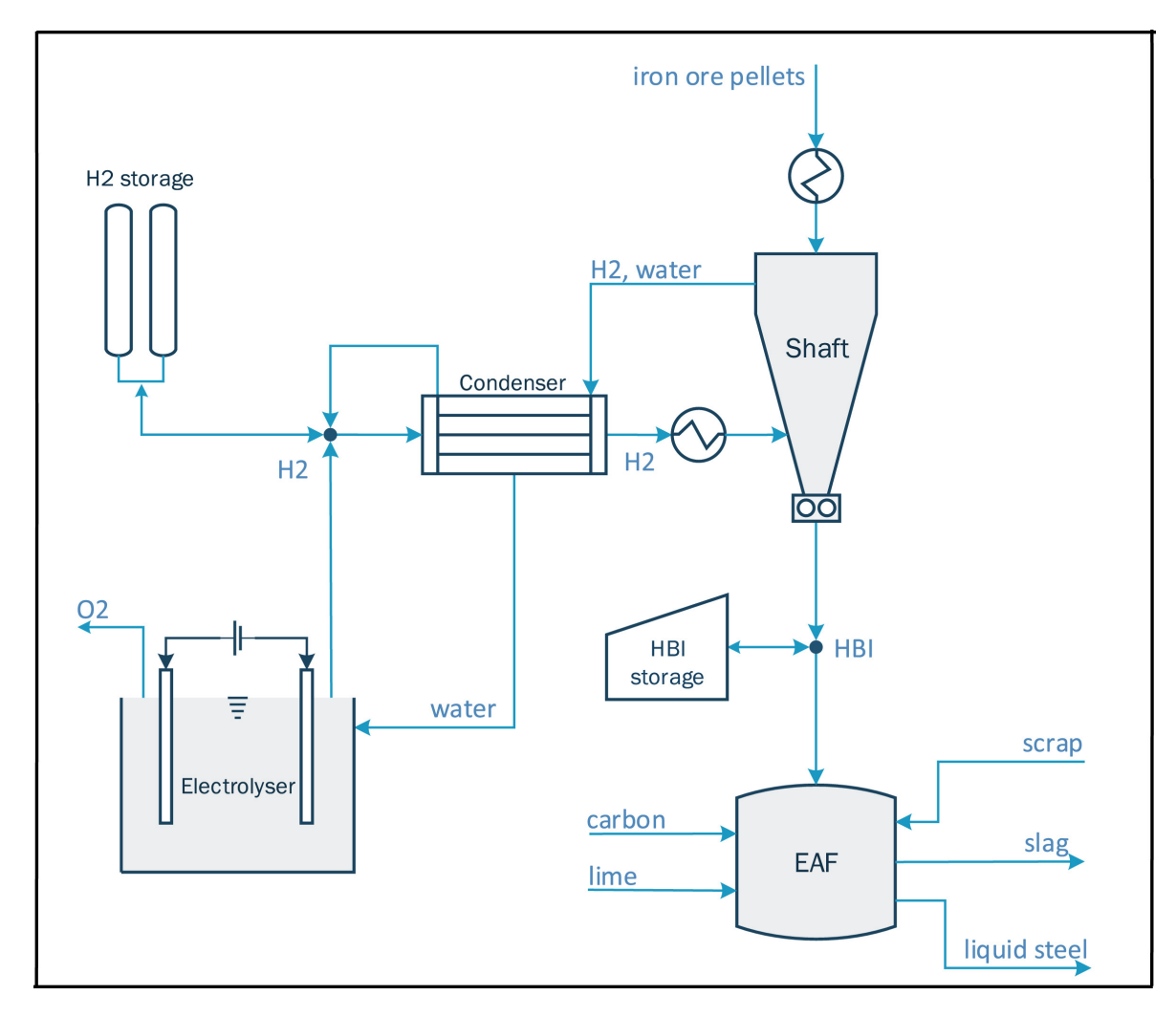


Figure 2.3: Proposed process design for the hydrogen-based direct reduction of iron [VOGL ET AL. 2018]

Since the hydrogen in this process is produced via water electrolysis and no carbon-based compounds are utilized, this iron-making route is classified as "green".

The inputs to the iron-making shaft are iron ore pellets, consisting of 95% iron oxide and 5% inert substances, and hydrogen gas. The reduction process produces DRI, which is subsequently compressed at high temperatures for easier handling and transportation. This compressed form of DRI is referred to as hot-briquetted iron (HBI). The HBI is then charged into the EAF for steelmaking. [VOGL ET AL. 2018]

It is worth noting that substituting fossil feedstocks with electrical power for hydrogen production and EAF heating alone is insufficient for achieving low-carbon steel production. CO₂ emissions remain embedded in process-steps such as the extraction of iron ore and limestone (emitted by equipment such as drills, trucks, excavators, and crushers), the processing of these materials, and lime calcination. In addition to the CO₂ released during limestone calcination, fossil fuels are often burned to heat the limestone to the necessary temperatures, further contributing to carbon emissions. Furthermore, the addition of carbon, which is an essential component of steel, makes carbon-free steelmaking impossible. Nonetheless, the process depicted in figure 2.3 emits only 2.8% of the CO₂ produced by the conventional BF-BOF route, consuming 3.48 MW h of electricity per tonne of steel produced. This energy consumption is comparable to that of the BF-BOF route, as a similar amount of energy is required by a blast furnace in the form of coal and coke to produce one tonne of steel. [VOGL ET AL. 2018]

VOGL ET AL. 2018s' study excludes the oxygen requirements of the EAF (even though some O₂ is required), treating the oxygen produced via electrolysis as a commodity for sale. In practical applications, however, the process depicted in figure 2.3 presents a promising pathway for producing low-carbon steel by integrating both elemental products of water electrolysis: hydrogen and oxygen.

This proposed production pathway is transcending the academic sphere and is steadily advancing towards industrial application. Stegra is building the world's first large-scale green steel plant in Boden, Sweden [STEGRA 2025]. This facility will integrate a 700 MW AWE plant for green hydrogen production to directly reduce iron and manufacture steel, aiming to produce $5 \cdot 10^6$ t of green steel annually by 2030. By replacing coal with green hydrogen derived from renewable electricity, the plant intends to reduce CO_2 emissions by up to 95% compared to traditional iron and steelmaking processes. Production is scheduled to fully commence in 2030.

Furthermore, ArcelorMittal, the world's second-largest steel producer, has announced plans to construct multiple DRI-EAF plants in Gijón, Bremen, Eisenhüttenstadt, Dunkerque, Ghent, Dąbrowa Górnicza, Fos-sur-Mer, and Dofasco. The strategy involves gradually replacing blast furnaces with DRI facilities that will initially operate using natural gas as a transitional fuel, shifting to hydrogen once sufficient volumes are available and economically viable. [FRIES 2022]

The oxygen demand varies depending on the steel production route.

The BF-BOF process requires approximately 85 kg to 157.2 kg of oxygen per tonne of crude steel produced [Wente & Nutting 2024, Eckl et al. 2025]. This only considers the oxygen requirement of steelmaking in the BOF.

It is also possible to enhance the performance of the blast furnace by adding pure oxygen to the hot blast, as demonstrated by the oxycoal+ technology. In this approach, oxygen-enriched air (OEA) is injected simultaneously with pulverized coal in the blast furnace. Although this method improves efficiency and reduces carbon emissions, it leads to an increase in oxygen demand of approximately 90 kg per tonne of crude steel. [Schott & Reufer 17.09.2016 - 19.09.2016, Loeffler 2022]

This term paper excludes the blast furnace oxycoal+ technology and only considers an oxygen demand ranging from $85\,\mathrm{kg}$ to $157.2\,\mathrm{kg}$ per tonne of crude steel for the BF-BOF route.

LOEFFLER 2022 compiles and summarizes multiple sources and studies on the DRI-EAF route. The DRI-EAF route requires significantly less oxygen per tonne of crude steel compared to other methods, with current values ranging between 49 kg and 64 kg per tonne of crude steel. A study by Kleimt et al. 2012 thoroughly examined the oxygen consumption of the EAF and presented the following segmented oxygen requirements per tonne of crude steel:

- Oxygen for the burner: 20.86 $\frac{\rm kg~O_2}{\rm t_{Steel}}$
- Oxygen for the lance: 20.43 $\frac{\text{kg O}_2}{\text{t}_{\text{Steel}}}$
- Jet O_2 : 18.29 $\frac{\text{kg } O_2}{t_{\text{Steel}}}$
- Post-combustion O_2 : 8 $\frac{\text{kg } O_2}{t_{\text{Steel}}}$

This sums to a total of around 67.58 $\frac{\text{kg O}_2}{\text{t}_{\text{Steel}}}$ for the DRI-EAF route. If the charge in the EAF is melted entirely through electrical means, without the partial use of natural gas combustion for heat generation as it is currently practiced, the oxygen demand per tonne would be even lower.

For the BF-BOF steelmaking route, while academic literature presents a range of oxygen demand from 85 kg to 157.2 kg per tonne of crude steel, this term paper will adopt the industrially validated value of 134.33 kg per tonne of crude steel. This preference for the industrial benchmark stems from its direct reflection of real-world operational practices and inherent accuracy compared to values derived solely from academic modeling. In the context of the DRI-EAF route, literature suggests an oxygen consumption range of 49 kg to 64 kg per tonne of crude steel. Considering the anticipated shift towards exclusively electric heating in EAFs, however, the lower end of this range, 49 kg per tonne of crude steel, is selected as the specific demand for subsequent analysis, whenever DRI-EAF plants are considered.

As discussed earlier, hydrogen-based direct reduction is central to many low-carbon steel initiatives. Depending on the proportion of scrap steel used in the EAF, the hydrogen demand ranges from 25 to 51 kg per tonne of crude steel [VOGL ET AL. 2018]. The

iron and steel industry, therefore, is one of the sectors that could employ both of the elemental products of water electrolysis.

2.3.1.2 Wastewater Treatment

Wastewater treatment is an integral component of any modern urban and industrial infrastructure across all geographical regions.

In municipal and industrial wastewater treatment plants (WWTP), oxygen is supplied in the biological treatment stage to microorganisms which metabolize it in order to decompose organic matter. Additionally, oxygen in the form of ozone could be applied for the removal of micropollutants. In most municipal WWTP, oxygen is typically introduced into the wastewater through compressed air via blowers, with air compression accounting for 45 to 75% of the plant's total energy consumption. Since air consists of approximately 21% oxygen and 79% nitrogen, the nitrogen is also compressed unnecessarily, increasing energy consumption without contributing to the treatment process. [LOEFFLER 2022]

Even though the use of pure oxygen theoretically reduces electricity consumption, it is rarely implemented in municipal WWTP due to the high cost of pure oxygen from the energy-intensive cryogenic air separation. Exceptions include, but are not limited to, regions experiencing temporary load increases, such as those caused by rapid population growth or other factors, as well as industrial complexes generating highly contaminated wastewater. [LOEFFLER 2022, DIPL.-ING. BERTHOLD MÜLLER 1999]

The Deer Island WWTP, the second largest in the United States, relies on pure oxygen to manage its substantial wastewater volumes. To meet this demand, the plant produces 130 to 220 metric tons of oxygen daily through cryogenic air separation. [MWRA 02.03.2025]

BASF's site in Ludwigshafen, the world's largest integrated chemical complex, operates its own wastewater treatment plant. As part of the research conducted, the WWTP was contacted to determine whether pure oxygen is used for treating wastewater from the chemical complex. The response clarified that surface aerators are initially activated, utilizing air oxygen, while pure oxygen is only employed for peak load buffering, controlled automatically based on discharge values [OLIVER SÜSS 2024].

As outlined by DIPL.-ING. BERTHOLD MÜLLER 1999, using pure oxygen instead of air in the biological treatment process enables either a reduction in plant size or an increase in wastewater treatment capacity within the same plant footprint. This is attributed to physical factors:

- The saturation concentration of pure oxygen in water is nearly five times higher than that of air oxygen under identical temperature and pressure conditions.
- The saturation deficit is significantly greater for pure oxygen compared to air oxygen. A larger saturation deficit lowers the energy required to dissolve a given amount of oxygen in water.

As a result, the required gas volume can be reduced by up to 25 times, ensuring sufficient oxygen dissolution even at elevated temperatures. This means that pure oxygen could be particularly beneficial for industrial wastewater treatment plants managing high wastewater temperatures and odorous compounds. Skouteris et al. 2020 also studied the potentials and limitations of using pure oxygen in aerobic wastewater treatment and came to similar conclusions.

The use of pure oxygen in wastewater treatment, along with its associated advantages, represents a compelling application for oxygen generated through water electrolysis. This is particularly compelling due to the widespread geographic distribution of wastewater treatment plants, which ensures they can serve as potential off-takers for electrolytically-produced oxygen in the vicinity of the electrolysis plant's location.

In the context of WWTP, any oxygen source with a purity greater than 90% by volume is classified as "pure" [Skouteris et al. 2020]. For WWTP, the minimal hydrogen impurity in electrolytically-produced oxygen has no impact on the process [Hönig et al. 2023].

The pressure of oxygen in the aeration tank varies depending on factors such as the depth of the aeration tank, the type of diffuser used, and the desired oxygen transfer efficiency, with the maximum pressure typically not exceeding 13 to 15 bar [VAN ORMER & VAN ORMER 2011].

The amount of oxygen required to break down organic matter aerobically in wastewater treatment depends on several factors, such as the strength of the wastewater contamination and the processes and reactor types used by the respective plant for wastewater treatment.

For a population equivalent of eighty thousand people, an annual demand of $3.8 \cdot 10^6$ kg of oxygen is given by ECKL ET AL. 2025. That translates to roughly 47.4 kg of oxygen per population equivalent. The population equivalent represents the maximum organic load a sewage treatment plant can handle, quantified based on the sewage contribution from a fixed population [Butler 01.01.2024]. One population equivalent corresponds to $73\,\mathrm{m}^3$ of wastewater per year (with a contamination level of 60 grams of biological oxygen demand per person per day) [Henze et al. 2008].

This results in a specific demand of roughly 0.65 $\frac{kg_{O_2}}{m_{\text{Wastewater}}^3}$, if pure oxygen is to be used.

2.3.1.3 Cathode Active Material Manufacturing

Batteries play a pivotal role in energy storage, especially within the context of the energy transition. This is exemplified by the surge in global demand for automotive lithium-ion batteries [IEA - International Energy Agency 2023]. The demand escalated significantly, rising by approximately 65% to 550 GW h in 2022 from 330 GW h in 2021, driven primarily by the booming sales of electric passenger vehicles. The demand is set to increase in the coming years. [IEA - International Energy Agency 2023]

The fundamental components of a battery consist of an electrolyte and two electrodes: the negative electrode, commonly referred to as the anode, and the positive electrode, commonly referred to as the cathode. LiFePO₄ and Li(NiCoMn)O₂ are the predominant cathode chemistries in the lithium-ion battery market for electric passenger vehicles [Shu et al. 2021].

Oxygen is required in the manufacturing of the cathode material for $Li(NiCoMn)O_2$ lithium batteries. The presence of three key transition metal elements - Nickel (Ni), Manganese (Mn), and Cobalt (Co) - in the cathode structure is why these batteries are commonly referred to as NMC batteries, with each letter representing one of the transition metals involved in the formulation.

STEFAN LEICHSENRING 2022 reports on the dismantling of batteries used in Tesla Model Y electric vehicles, revealing that the nickel content in the cathode is 82%. This finding suggests the use of NCM811 chemistry, where the active cathode material typically consists of 80% nickel, 10% cobalt, and 10% manganese.

The steps involved in the component manufacturing process of a lithium-ion battery cell are outlined in Kampker & Offermanns 2023. The production of NMC (Nickel Manganese Cobalt) material involves calcination of the NMC material, a high-temperature process conducted in a controlled environment. The temperature during calcination is critical as it influences key properties such as particle size, electron mobility, and crystal structure development. During calcination, the material remains in a furnace for several hours to ensure complete reactions. The process occurs in a pure oxygen (≥ 99.5% by volume) atmosphere, which is essential for maintaining the precise chemical balance, critical for the cathode material's performance and stability. Although Liang et al. 2019 investigated different calcination atmospheres: air, 50% oxygen by volume (1:1 oxygen and nitrogen by volume), and pure oxygen. Interestingly, the electrochemical performance of the sample calcined in 50% oxygen by volume was found to be comparable to that of the sample calcined in pure oxygen, with the one calcined in pure oxygen performing only slightly better.

According to XIAO ET AL. 2022, while calcination can be performed at atmospheric pressure, a higher oxygen pressure of approximately 4 bar has been shown to yield more desirable material properties.

Air Liquide, a leading global provider of industrial gases, is investing 150 million USD to expand its oxygen production capacity in Tennessee, United States to meet LG Chem's demand for oxygen at their upcoming cathode active material manufacturing plant for lithium-ion electric vehicle batteries [AIR LIQUIDE 15.10.2024]. This highlights the potential of electrolytically-produced oxygen to partially address the rapidly growing demand for lithium-ion electric vehicle batteries.

According to Shu et al. 2021, $4.7 \,\mathrm{m}^3$ or $6.7 \,\mathrm{kg}$ of oxygen is required for manufacturing 1 kWh of a Li(NiCoMn)O₂-based battery cell. A Li(NiCoMn)O₂ battery cell has an energy density of 200 $\frac{\mathrm{Wh}}{\mathrm{kg}}$. This gives a specific demand of around 1.34 kg of oxygen per 1 kg of a Li(NiCoMn)O₂ battery cell.

2.3.1.4 Healthcare

The use of oxygen in hospitals and other healthcare facilities is likely more familiar to the general public compared to its application in other industrial sectors.

Oxygen is employed in human medicine for both emergency care and in private healthcare settings to manage acute oxygen deficiency (hypoxia) and treat chronic respiratory and pulmonary diseases such as asthma and COPD [LOEFFLER 2022].

The COVID-19 pandemic highlighted the critical importance of oxygen in healthcare facilities and demonstrated how its unavailability could be fatal to patients.

Quantifying the medical oxygen demand of a hospital and finding available data is challenging, as it depends on the facilities available and the number of patients being treated. GÓMEZ-CHAPARRO ET AL. 2018 monitored the oxygen demand in Spanish hospitals over several years, and the findings indicate that, on average, one hospital bed requires approximately 470 kg of O₂ annually. This implies that Charité Universitätsmedizin, the largest hospital complex in Germany by number of patients and beds, would require approximately 1548 t of medical oxygen annually [PA MEDIEN GMBH 2024].

Due to the stringent purity requirements of medical oxygen, cryogenic air separation is typically the primary method for producing medical oxygen, which is frequently delivered in pressurized storage tanks or in liquid form to healthcare facilities [ECKL ET AL. 2025]. Although in the past years, the World Health Organization also defined 93 vol.% oxygen as medical oxygen; in other words, both 93% oxygen and 99.5% oxygen are considered medically accepted for patient treatment [WEBMASTER 2022]. Cole et al. 2021 investigated the prolonged inhalation of hydrogen gas in healthy adults and concluded that low concentrations of H₂ are well tolerated without clinically significant adverse effects. P Koziarin 1989 also examined the effects of electrolytically-produced oxygen on the human body, finding that electrolytically-produced oxygen diluted with nitrogen poses no detrimental impact on vital physiological systems. Thus, P Koziarin 1989 advocated for the use of electrolytic oxygen for medical and respiratory purposes. This presents a significant opportunity for the utilization of electrolytically-produced oxygen, as the widespread geographic distribution of healthcare facilities, similar to WWTP, can serve as potential frequent off-takers.

For this purpose, the electrolytically-produced O_2 must be compressed to 200 bar for storage in gas cylinders, enabling efficient transport and distribution, typically within a radius of $200 \, \mathrm{km}$. [Panchawadkar 2024]

2.3.1.5 Oil and Gas Industry

Refineries are ideal offtakers for both elemental products of water electrolysis, as hydrogen and oxygen gases are needed in the following refinery processes: hydrodesulfurization and the Claus process. In hydrodesulfurization. hydrogen gas is used to remove sulfur from natural gas or other petroleum-based products. In the Claus process, oxygen is

used to convert hydrogen sulfide, a by-product of hydrodesulfurization, into elemental sulfur.

Sulfur in fossil-based fuels (such as petrol, diesel, and gas-oil) is a strictly regulated element, as its combustion releases sulfur oxides, which pose significant hazards to both the environment and human health. For example, the European Union mandates a maximum sulfur content of 10 parts per million (by mass) for both diesel and gasoline used in road vehicles, while the International Maritime Organization has set a global sulfur content limit of 0.5% by mass for marine fuels [European Parliament, Council of the European Union 23.04.2009, International Maritime Organization 20.19.2019]. This indicates the significance of hydrodesulfurization processes within the oil and gas industry.

Hydrodesulfurization, performed at high temperatures and pressures (depending on the feedstock) using cobalt-molybdenum or nickel-molybdenum-based catalysts, can remove up to 99% of sulfur from feedstocks [SPEIGHT 2011]. The general chemical transformation, where R represents an alkyl group, can be summarized as follows:

$$R-SH + H_2 \longrightarrow R-H + H_2S$$
 (C 2.6)

The resulting H₂S is, on one hand, a toxic gas that cannot be vented into the atmosphere; on the other hand, elemental sulfur is a valuable commodity that can be sold. For these reasons, H₂S is converted into elemental sulfur in the Claus process. The input feed gas typically contains H₂S, NH₃, CO₂, and H₂O in varying concentrations, with H₂S generally being the main component. The first step of the Claus process involves the partial oxidation or combustion of a portion of gaseous hydrogen sulfide (H₂S) to produce sulfur dioxide (SO₂). The SO₂ is then mixed with the remaining H₂S and passed over a catalyst bed, where H₂S and SO₂ react to form elemental sulfur and water vapor. [Shell 2025] The two-step reaction can be summarized as follows:

$$2 H2S + 3 O2 \longrightarrow 2 SO2 + 2 H2O$$
 (C 2.7)

$$2 H_2 S + 2 SO_2 \longrightarrow \frac{3}{x} S_x + 2 H_2 O . \qquad (C 2.8)$$

Theoretically, the Claus process can be carried out using the oxygen available in ambient air without any oxygen enrichment (at pressures lower than 1 bar). However, oxygen enrichment of the combustion air in Claus plants has been implemented since the early 1970s. The primary motivations for this practice include increased capacity and significantly improved ammonia destruction efficiency. The capital and operating costs associated with oxygen enrichment are significantly lower than those for constructing an additional Claus plant. [LINDE AG n.d., KOHL & NIELSEN 1997]

Figure 2.4 below illustrates the increase in capacity as the oxygen fraction by volume (vol. %) rises, depending on the hydrogen sulfide concentration in the feed gas.

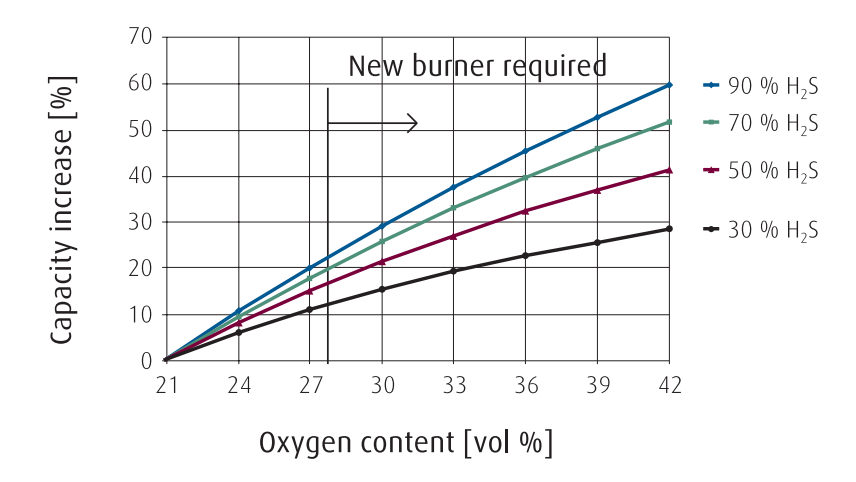


Figure 2.4: Overview of the Claus plant capacity increase as a function of increasing oxygen enrichment by volume [Adapted from LINDE AG n.d.]

Oxygen enrichment in the Claus process can be categorized in three distinct stages [Linde AG n.d., Kohl & Nielsen 1997]:

- Low-level oxygen enrichment (< 28 vol.% oxygen): Oxygen is introduced into the air supply for the Claus furnace without necessitating significant modifications to the existing system.
- Medium-level oxygen enrichment (28 to 45 vol.% oxygen): At this stage, a new burner is required (to replace the existing burner) which can handle the increased oxygen concentration.
- **High-level oxygen enrichment** (> 45 vol.% oxygen): Both a new burner and a new furnace are required. Additionally, product gas recycling is implemented to moderate furnace temperature and prevent excessive thermal loading on the system.

In addition to the Claus process, oxygen enrichment can also be applied to fluid catalytic cracking's (FCC) catalyst regeneration step. FCC is employed to convert long-chain hydrocarbons into short-chain hydrocarbons, thereby increasing conversion efficiency and capacity. [Reinhardt et al. 2015]

The integration of an electrolyzer into refinery processes could potentially meet a portion of the hydrogen and oxygen demand. While the integration of such a system involves relatively high costs, its financial feasibility is supported by the fact that many oil and gas companies are among the most profitable globally [Statista 2024b]. This suggests that many oil and gas companies have the financial capacity to invest in the integration of electrolyzer systems, thereby contributing to the energy transition technologically while also reducing the carbon footprint of refineries.

Depending on the sulfur content of the crude oil, between 0.03 and 0.55 kg of hydrogen are required per barrel for the hydrodesulfurization process [Praxair 2017].

For the Claus process, 1 kg of sulfur requires 0.49 kg of pure oxygen stoichiometrically. However, the actual amount required by refineries to process residual gas can vary. According to An & Jung 2020, 0.37 kg of pure O_2 is required to treat 1 kg of residual gas with the following molar composition (in mol.%): 78% H_2S , 10.8% NH_3 , 0.5% CO_2 , and 10.4% H_2O .

2.3.1.6 Pulp and Paper Industry

As reported by the European Commission EC 2025, the pulp and paper manufacturing sector is a vital industry, characterized by a high energy consumption and substantial raw material requirements.

LOEFFLER 2022 describes the production procedure from several sources.

In 2020, renewable energy sources, mainly biomass, accounted for approximately 60% of the energy used in the Austrian pulp and paper industry. The remaining 40% was derived from fossil fuels, including coal, heating oil, and natural gas. These fossil fuels are predominantly used to fuel rotary kilns, which are a significant source of CO_2 emissions. The purpose of a lime rotary kiln in the pulp and paper industry is to reburn lime mud into calcium oxide, which is used in the pulping process [ADAMS NA].

Paper is made from cellulose fibers found in plant cell walls, using raw materials like wood, reed, or sugarcane. The production process typically involves the kraft (sulfate) method, where lignin and hemicellulose are chemically separated from cellulose. This is achieved by cooking shredded plant material in a pressurized vessel with a solution of caustic soda, sodium sulfide, and sodium sulfate at high temperatures. The process dissolves lignin, forming black liquor, while leaving behind brown-colored pulp. The pulp is washed, screened, and delignified with oxygen to reduce the residual lignin content. Finally, it is bleached to achieve the desired white color before being processed into paper.

Just like the iron and steel industry, the pulp and paper industry is a major consumer of industrial oxygen. Along the entire paper production process, oxygen is used for the following purposes:

- Oxygen delignification: Used after kraft pulping to remove residual lignin from the pulp, reducing the need for chlorine-based bleaching chemicals.
- Ozone bleaching: Ozone is generated onsite from oxygen and is applied after oxygen delignification to further whiten the pulp.
- Black liquor oxidation: Oxygen is used to treat the by-products from the kraft process, helping to recover chemicals.
- White liquor oxidation: Oxygen is employed to regenerate and improve the efficiency of the cooking chemicals used in the kraft process. [Eckl et al. 2025]

The oxygen purity required is $\geq 92\%$ by volume and the oxygen pressure ranges between 4 to 8 bar. [Rodríguez et al. 2007]

LOEFFLER 2022 discusses a study on integrating electrolysis into the pulp mill process to produce and integrate both hydrogen and oxygen. In the proposed concept, hydrogen is sourced via electrolysis using internally generated electricity. The produced $\rm H_2$ could be used as fuel for the rotary kiln. Simultaneously, the oxygen produced can meet the demand for delignification and oxygen bleaching. In the studied application, the hydrogen via electrolysis fulfills 73% of the kiln's heat requirements, while oxygen production surpasses the mill's overall demand.

This utilization of both hydrogen and oxygen from water electrolysis in this study presents an innovative and sustainable alternative to partially replace fossil fuels as the fuel for the rotary kiln and eliminate the need for standalone oxygen production systems.

SUNANDAN 2010 reports a specific oxygen demand ranging from 21 to 34 kg per tonne of pulp. ECKL ET AL. 2025 provides a range of 20 to 37 kg per tonne of pulp.

Recognizing that the oxygen requirement in the pulp and paper industry fluctuates depending on wood type, lignin content, and the extent of bleaching, this term paper shall utilize an average value of 27.5 kg of pure oxygen per tonne of pulp for its analysis.

2.3.1.7 Generation of Synthesis Gas

Synthesis gas, or syngas, is a mixture primarily consisting of hydrogen and carbon monoxide. It can be produced from various feedstocks, with the majority currently derived from fossil sources like natural gas, coal, and refinery by-products. Solid and liquid waste, along with biomass, can also be gasified to produce synthesis gas [LOEFFLER 2022].

The importance of synthesis gas cannot be overstated. It is a key process step in the production of hydrogen and methanol, which are in turn the foundation for many other valuable chemicals. In other words, synthesis gas, derived from fossil fuels, serves as a feedstock for producing chemicals like methanol and hydrogen. Synthesis gas can also be used to produce synthetic fossil fuels, reduce iron ore, and generate electricity in certain power plants. [Mandal et al. 2020]

Figure 2.5 illustrates two commonly used industrial processes for the generation of synthesis gas which require oxygen as an oxidising agent.

EIGA 2024 provides an overview of both the processes in figure 2.5. It is to be noted that variations and combinations of such processes also exist.

Partial Oxidation (POX) is a well-established industrial process used for syngas production, typically applied in medium to large-scale applications due to its high capital cost. In this process, hydrocarbon feedstock is injected into a reaction chamber, where it undergoes partial oxidation with pure oxygen under sub-stoichiometric conditions to produce synthesis gas. POX operates at pressures between 40 and 100 bar and is an overall exothermic process. The feedstock and oxygen are usually preheated before injection into the reaction chamber. As it does not rely on a catalyst, it can accommodate

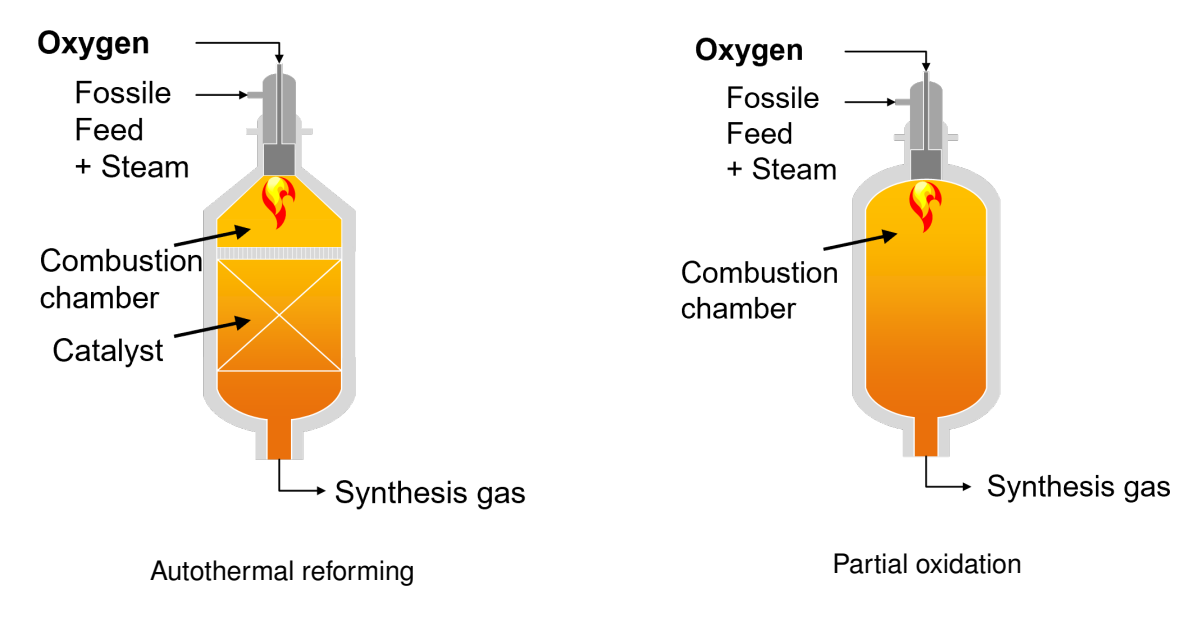


Figure 2.5: Commonly used industrial processes for the generation of synthesis gas [Adapted from HEMAUER ET AL. 2021]

a wide range of feedstocks with varying types and qualities. Typical applications include the processing of coal, liquid feedstocks such as oil or heavy hydrocarbon residues, and lean gaseous feeds like natural gas. At times, the addition of steam as a moderating agent is necessary to suppress soot formation. [EIGA 2024]

Autothermal reforming (ATR), on the other hand, does require a catalyst. After optional desulfurization, the feed gas is pre-heated and optionally pre-reformed before entering the ATR reactor at 30 to 100 bar via the burner. In the first step, the feed gas undergoes partial combustion with oxygen and steam to produce syngas. The gas mixture then passes through a catalyst bed within the same reactor for further reforming to achieve high yields and thermodynamic equilibrium. In other words, ATR combines partial oxidation of the feedstock (exothermic) with steam reforming (endothermic). ATR is considered auto-thermal because the heat generated from partial oxidation is used to drive the endothermic steam reforming process. Finally, the resulting syngas is cooled in a process gas boiler, generating internally required process steam and steam for power generation, heating, export, or as a feed for another downstream process. The feedstock for ATR can include natural gas, refinery offgas, pre-reformed gas, Fischer-Tropsch tail-gas, liquified petroleum gas, or naphtha. [EIGA 2024]

An oxygen purity level of approximately $\geq 95\%$ by volume is required [Zahid et al. 2023].

As stated earlier, another method of synthesis gas generation that requires oxygen is gasification (typically of biomass or coal). Synthesis gas production can be closely integrated with power generation, as synthesis gas serves as a crucial fuel for IGCC power plants (more information on power generation can be found in subsection 2.3.2.7).

Gasification is a thermochemical process that converts fuel into synthesis gas, volatile components, and ash by reacting it with a gasification agent (oxygen). The process

occurs in two stages. In the first stage, the fuel undergoes pyrolysis, releasing volatile compounds such as hydrocarbons, H_2 , CO, CO_2 , and tars at temperatures below 600 °C, without the need for oxygen. In the second stage, solid carbon (such as coal) reacts with oxygen, steam, and hydrogen to produce gas. The final product gas mainly consists of H_2 , CO, CO_2 , CH_4 , and other hydrocarbons, with the exact composition depending on factors like temperature, pressure, and the type of fuel used. To use the product gas from gasification as synthesis gas, several factors must be considered, including the H_2/CO ratio, the levels of inert substances (such as nitrogen), methane (CH_4) , higher hydrocarbons, and catalyst poisons (e. g., H_2S , COS). [LOEFFLER 2022]

The required H_2/CO ratio and the composition of other gases in synthesis gas depend on its intended application. Different end products necessitate specific gas compositions. Electrolysis can play a significant role in providing hydrogen, a key component of synthesis gas, as well as oxygen, which is needed as an oxidizing or gasifying agent in the synthesis gas generation. In simpler terms, both hydrogen and oxygen, the elemental products of water electrolysis, could be utilized simultaneously.

Since oxygen is essential for both POX and ATR synthesis gas production methods, the oxygen demand is well-known and often provided by the sources. EIGA 2024 reports that an ATR requires between 0.15 and 0.25 kg of oxygen per cubic meter of synthesis gas produced.

2.3.1.8 Nitric Acid Production

Nitric acid, together with ammonia, plays a crucial role as a feedstock in the production of nitrogen-based fertilizers. Nitric acid is produced in a process called the Ostwald process with the following overall chemical transformation:

$$NH_3 + 2O_2 \longrightarrow H_2O + HNO_3$$
 (C 2.9)

The Ostwald process involves the catalytic oxidation of ammonia to nitric oxide, followed by the oxidation of this nitric oxide to nitrogen dioxide and its subsequent dimerization to dinitrogen tetroxide. Finally, these nitrogen oxides are absorbed in water to yield nitric acid. [Neumann et al. 2024]

Conventionally, oxygen from air (21% by volume) is utilized at pressures of up to 10.1 bar [Chemeurope 2025]. Neumann et al. 2024 explored potential synergies between the sustainable production of ammonia feedstocks - hydrogen and nitrogen - and nitric acid production through the Ostwald process. The electric power used in the study is generated from solar panels. The study evaluated the effect of injecting surplus oxygen from renewable ammonia production into the subsequent Ostwald process, using a techno-economic assessment for a mono-pressure (5.8 bar) plant with a capacity of 700 t per day. The results showed that, in general, injecting surplus oxygen into the

Ostwald process led to better performance in nitric acid production compared to the conventional process across all investigated cases.

The absorption column is the final stage of the Ostwald process where the produced nitrogen oxides are dissolved in water to form nitric acid. Notably, the reduction in NO_x emissions from the exhaust gas of the absorption column highlighted the potential for more economical fertilizer production, with a smaller $DeNO_x$ unit. The highest efficiency was achieved when oxygen was injected directly into the primary air upstream of ammonia combustion, resulting in a 0.31% increase in nitric acid production, a 0.24% increase in acid strength, and a 44% reduction in NO_x concentration in the exhaust gas. Neumann et al. 2024's work presents an intriguing approach for integrating both elemental products of an electrolyzer into a fertilizer production facility.

2.3.1.9 Aquaculture

To address the rising global demand for seafood while alleviating pressure on natural ecosystems, aquaculture has emerged as a vital solution. Over the past seven decades, total fisheries and aquaculture production has expanded dramatically, increasing from $19 \cdot 10^6$ t in 1950 to an unprecedented $179 \cdot 10^6$ t in 2018, with an annual growth rate of 3.3%. [FAO UNITED NATIONS 2024]

In aquaculture, maintaining sufficient dissolved oxygen is fundamental for successful fish farming. While increased feed input can enhance production within a given volume, it simultaneously raises the oxygen demand of the system. This heightened demand stems from two primary sources: the increased respiration of a larger or faster-growing fish population and the microbial decomposition of uneaten feed and metabolic wastes. The aerobic breakdown of this organic matter by bacteria consumes dissolved oxygen, potentially leading to critically low levels. Insufficient dissolved oxygen not only compromises fish health, increasing susceptibility to disease and mortality, but also contributes to water quality deterioration by favoring anaerobic processes and the accumulation of harmful substances. Therefore, ensuring adequate dissolved oxygen concentrations is crucial for sustaining healthy and productive fish populations while minimizing negative environmental consequences associated with aquaculture practices. [BOYD ET AL. 2017]

Oxygen demand is influenced by multiple factors, including the farmed species, feed composition, feed conversion efficiency, water temperature, and stocking density. Depending on these variables, oxygen demand can range from 0.5 to 3.3 $\frac{\text{kg}_{O_2}}{\text{kg}_{\text{Culture species}}}$. For example, the oxygen requirement for shrimp is 2.53 $\frac{\text{kg}_{O_2}}{\text{kg}_{\text{Shrimp}}}$, whereas for atlantic salmon, it is typically 0.5 $\frac{\text{kg}_{O_2}}{\text{kg}_{\text{Salmon}}}$. O₂ is typically supplied at pressures of up to 2.5 bar. [BOYD ET AL. 2017, BOYD 2008, REIL 2024]

Purity levels of ≥ 90 vol.% are common in the industry [INMATEC GASETECHNOLOGIE 2025].

A Norwegian fish farm plans to install a 6 MW electrolysis system, with the produced oxygen to be directly utilized in the farm. Similar to WWTPs, this suggests that trace amounts of H₂ likely have no significant impact on aquaculture applications.

2.3.2 Oxygen in Combustion Processes

Oxyfuel combustion is a process in which fuel is burned using high-purity oxygen (or a mixture of oxygen and recirculated flue gas) instead of air [ADAMS 2014]. In contrast, oxygen-enriched combustion (also known as oxygen-blown combustion) uses a mixture of oxygen and air.

Oxyfuel or oxygen-enriched combustion (OEC) is employed by many industrial plants that aim to capture CO_2 rather than emitting it into the atmosphere. Carbon capture is typically more efficient when combustion takes place in oxygen-enriched air or with pure oxygen. This is due to the resulting flue gas containing mainly CO_2 and water vapor. This simplifies the separation process by producing a concentrated CO_2 stream, which reduces both energy consumption and equipment complexity. In the case of oxyfuel combustion, only H_2O needs to be condensed. Furthermore, because the fuel is more effectively combusted, oxyfuel or oxygen-enriched combustion reduces fuel consumption, CO_2 emissions, and NO_x (nitrogen oxides) emissions compared to conventional air combustion. [ECKL ET AL. 2025, KATO ET AL. 2005]

As thermal efficiency increases and higher temperatures are achieved when oxyfuel or oxygen-enriched combustion is employed, heat management challenges also arise. This becomes evident in case of the Claus process explained in subsection 2.3.1.5.

Seven industries where the use of oxygen-enriched or oxyfuel combustion has been successfully implemented or holds potential for future application are outlined below. These include:

- Glass production
- Cement production
- Waste incineration
- Ceramics production
- Production of lime
- Production of magnesia
- Power generation.

2.3.2.1 Glass Production

Similar to steel, glass serves as a cornerstone of modern urban and industrial infrastructure. As reported by Westbroek et al. 2021, the global demand for glass products in 2014 was approximately $150 \cdot 10^6$ t. Of this, 48% was attributed to hollow or container

glass, 42% to flat glass (mainly used for windows in construction and vehicles), 5% to tableware, and 6% to other applications, such as glass fibers.

Glass is produced through a high-temperature melting process using carefully measured raw materials. These materials are mixed into batches, with recycled glass (cullet) included to improve efficiency and reduce energy consumption. Before entering the furnace, the silica sand is purified to remove impurities. Glass production then occurs in specialized furnaces, known as glass-melting furnaces, which operate at temperatures exceeding 1400 °C, making the process highly energy-intensive. For several decades, oxygen has been used to improve combustion efficiency and reduce pollutant emissions. Various technological approaches, such as oxyfuel combustion, have been developed for this purpose. [LOEFFLER 2022, SAINT GOBAIN 2025]

Typically, glass furnaces are powered by fossil fuels such as natural gas or oil, resulting in significant CO_2 emissions. Globally, this amounts to approximately $60 \cdot 10^6$ t of CO_2 annually [ECKL ET Al. 2025].

Oxygen-blown combustion improves energy efficiency of the melting process by 40% and cuts CO_2 emissions by 17-20% or even 75% with full CO_2 capture. [ECKL ET AL. 2025, KATO ET AL. 2005]

Figure 2.6 represents the above-mentioned points graphically.

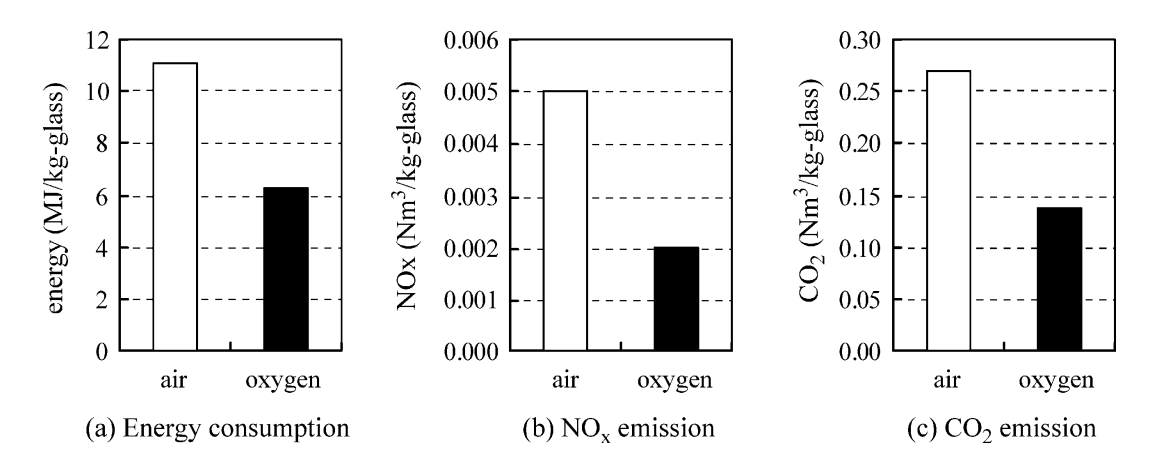


Figure 2.6: Comparison between air-blown and oxyfuel combustion in glass melting [KATO ET AL. 2005]

Kato et al. 2005 points out that for cost reasons, the oxygen-blown combustion furnace is not widely used, except in electric glass production, where the price of the glass product is relatively high compared to other types of glass. Electric glass is a high-purity, precision-made glass used in electronics, making it more expensive due to complex manufacturing and strict quality requirements. Since the publication of Kato et al. 2005, there has been an increasing focus on adopting more sustainable production methods. This shift is driven by the need to reduce fossil fuel consumption, increasing fossil fuel prices, and the implementation of carbon taxes. As a result, many producers have developed strategies to incorporate oxygen combustion as part of their efforts to enhance sustainability. AGC Glass Europe, for example, has transitioned to

pure oxygen combustion furnaces after overcoming profitability concerns [AGC GLASS 2025]. This was achieved by developing a system that reuses heat from waste gases to preheat both oxygen and natural gas before injection into the furnace, resulting in substantial additional energy savings.

electrolytically-produced oxygen could, therefore, be highly suitable for use in the glass industry. This is particularly true given that the minimum purity requirements are lower than what electrolysis typically outputs. According to Pioneer 2022, glass fiber manufacturers require oxygen with a purity of $\geq 93\%$ by volume. Falorni Tech 23.10.2017 reports an input oxygen pressure of 1 bar, when the oxyfuel firing technology is employed.

It is important to note though, that oxyfuel combustion appears to be an interim solution given the current infrastructure limitations. A more sustainable alternative is the possibility of melting glass electrically (using renewable electricity), eliminating the need for fuel combustion entirely - and, consequently, the need for oxygen. Additionally, other pathways include the use of hydrogen or renewable synthetic gases as fuel sources, which could further reduce the carbon footprint of glass production. [EVERLING 2022, SORG 05.07.2023]

The specific oxygen requirement for glass production varies depending on the type of glass being produced. In the oxygen combustion furnace, the ideal oxygen requirement can reach approximately 426 kg per tonne of glass [Kato et al. 2005].

Both elemental products of water electrolysis can be utilized in glass production. Daurer et al. 2025 numerically studied the use of hydrogen in oxy-fuel glass melting furnaces and provided hourly hydrogen demand values. By combining Daurer et al. 2025's values with the energy required to melt glass, as presented in Kermeli et al. 2022, a specific hydrogen requirement of 0.084 $\frac{kg_{H_2}}{kg_{Glass}}$ can be deduced.

2.3.2.2 Cement Production

Cement, a key ingredient in concrete, mortar, and screed, is a hydraulic binder and is amongst the most commonly used construction materials worldwide [LOEFFLER 2022].

Cement production contributes roughly 7% of global carbon dioxide emissions. A significant portion of this results from calcination, a chemical process that occurs when raw materials (lime, silica, alumina, magnesia, iron oxide, etc.) are heated to temperatures between 1400 and 1500 °C at 1 bar in a rotary kiln, producing clinker. The emissions are split, with 60% coming from the chemical reaction itself and 40% from the energy needed to provide the heat. Both of these emission sources can be substantially reduced by adopting oxyfuel combustion alongside carbon capture technologies. [ECKL ET AL. 2025, ZEMAN 2009]

The optimal oxygen concentration in the combustion air is 23 % by volume (based on the optimal temperature profile in the kiln), which is only marginally higher than the

standard 21% found in atmospheric air. Theoretically, as with all applications discussed in 2.3.2, oxyfuel combustion is also feasible in cement production. [LOEFFLER 2022]

In this way, electrolytically-produced oxygen could eventually be integrated into a clincker production facility.

To determine the specific oxygen demand for cement production, the clinker-to-cement ratio must be known. Skinner & Lalit 2023 provides a ratio of 0.72. If 100% O₂ by volume is used, 0.29 kg of oxygen would be required per 1 kg of clinker [Loeffler 2022]. This is equivalent to 0.414 kg of oxygen would per 1 kg of cement.

When establishing oxygen-enriched combustion, the optimal oxygen volume percentage is just slightly above 21%. Based on this, 0.0021 kg of oxygen is required per 1 kg of cement when the oxygen enrichment is 23% by volume. Using this specific value and the clinker-to-cement ratio, the specific oxygen demand can be calculated.

2.3.2.3 Waste Incineration

MA ET AL. 2019 studied the effect of oxygen-enriched combustion on flue gas emissions and combustion performance in a full-scale 8 MW municipal solid waste incineration plant without flue gas recirculation. The research focused on evaluating the impact of varying oxygen concentrations by volume in the input gas (21%, 24%, and 27%) on the combustion process. The results revealed that while the incinerator's average temperature increased with higher oxygen concentrations - resulting in a lower unburnt rate, improved thermal efficiency, and reduced levels of sulfur dioxide and hydrogen chloride in the flue gas - certain pollutant emissions rose. The higher temperatures led to an increase in nitrogen oxides and nitric oxide emissions. Furthermore, harmful dioxins, particularly in the flue gas and fly ash, showed a significant increase under higher oxygen conditions. Using pure oxygen could eliminate NO_x emissions and offer additional benefits; however, the feasibility of oxyfuel combustion is considered questionable due to the high costs associated with sourcing oxygen of purity greater than 95% by volume. This challenge presents an opportunity to utilize electrolytically-produced oxygen, provided there are no higher-value offtakers available in the vicinity. LOEFFLER 2022 analyzed further studies on the application of oxygen-enriched combustion for waste incineration and concluded that it could be largely advantageous.

MA ET AL. 2019 reports an annual oxygen demand of 16005 tonnes for the 8 MW waste-to-energy plant studied, which employs 27 vol.% oxygen-enriched combustion for waste incineration.

2.3.2.4 Ceramics Production

electrolytically-produced oxygen could potentially be utilized in another hard-to-decarbonize sector: the ceramics industry, which emits significant amounts of CO_2 , with the majority originating from the firing process operated at pressures up to 5 bar. Oxyfuel combustion or OEC can help decarbonize this sector. Additionally,

the integration of electrolytic oxygen with innovative fuels, such as eCombustible - a hydrogen-based fuel developed by eCombustible Energy LLC - offers a cleaner alternative. This fuel, created by recombining para-hydrogen (processed using a magnetic reactor) with oxygen from electrolysis, burns cleanly, emitting only water vapor. [ECKL ET AL. 2025, CERAMICTURKEY 2022]

ECKL ET Al. 2025 reports a study specifying an oxygen demand of 193 $\frac{kg_{O_2}}{t_{Ceramic}}$ for oxyfuel combustion.

2.3.2.5 Production of Lime

Lime, a term encompassing a range of calcium-based materials, is an indispensable resource in the construction industry and serves as a fundamental material for numerous other industrial sectors. Lime is essential in the production of iron, glass, chemicals, and medical products, as well as in agriculture and the food industry. [DORNISCH-BUND 2020]

LOEFFLER 2022 discusses the usage of oxygen in the lime industry.

Similar to cement clinker production, oxyfuel combustion technology with exhaust gas recirculation is being explored for shaft kilns in lime production. A study by ERIKSSON ET AL. 2014 indicates that combustion with pure oxygen leads to significant improvements in heat and mass transfer. These benefits include higher production rates, improved energy efficiency, and potential cost savings through smaller plant sizes while maintaining the same output, making the use of pure oxygen an attractive option for lime production.

The study by ERIKSSON ET AL. 2014 on oxyfuel combustion in a rotary kiln for lime production reports an annual oxygen demand of 44880 t when using coal as the fuel source to heat limestone, based on an annual operating time of 8000 h. This corresponds to $2.59 \, \frac{\rm kg_{O_2}}{\rm t_{Coal}}$. In lime production, rotary kilns typically operate under slightly negative pressure (lower than ambient) at both the kiln head and kiln tail.

2.3.2.6 Production of Magnesia

Similar to the lime industry, oxygen-enriched combustion can also be used in the magnesia (magnesium oxide) production. The natural deacidification process of magnesite is used to produce caustic magnesia at temperatures of 600 to 800 °C, while sinter firing takes place at 1800 to 2200 °C to produce sinter magnesia. The increased oxygen content in the combustion air reduces specific energy consumption. Therefore, there is also potential for utilizing electrolysis-produced oxygen in magnesia production, provided it can be made available under acceptable transport conditions. [LOEFFLER 2022]

As for the production of magnesia, LOEFFLER 2022 reports a specific oxygen demand ranging from 21.435 to 214.35 kg per tonne of sintered magnesia.

2.3.2.7 Power Generation

electrolytically-produced oxygen and hydrogen can also be utilized to generate power, which may initially seem counterintuitive since electric power is required to drive the electrolysis process that produces these gases in the first place. However, in specific applications, hydrogen and oxygen can be efficiently harnessed to generate power when needed.

LOEFFLER 2022 reviews several studies exploring the use of oxygen in integrated Power-to-Gas (PtG) applications and oxyfuel combustion within combined-cycle power plants. PtG converts excess electricity to hydrogen via water electrolysis, which is then methanated with CO₂ to produce synthetic natural gas. This gas can be combusted in a combined-cycle oxyfuel power plant using electrolysis oxygen during peak demand. While promising, the niche nature and absence of large-scale industrial implementation of these applications suggest limited near-term practicality, as current assessments are based on small-scale modeling that lack an industrial foundation.

The integration of electrolytically-produced oxygen for power generation seems most viable in Integrated Gasification Combined Cycle (IGCC) power plants. Figure 2.7 shows an oxygen-blown IGCC power plant that typically utilizes an air separation unit (ASU) to supply oxygen.

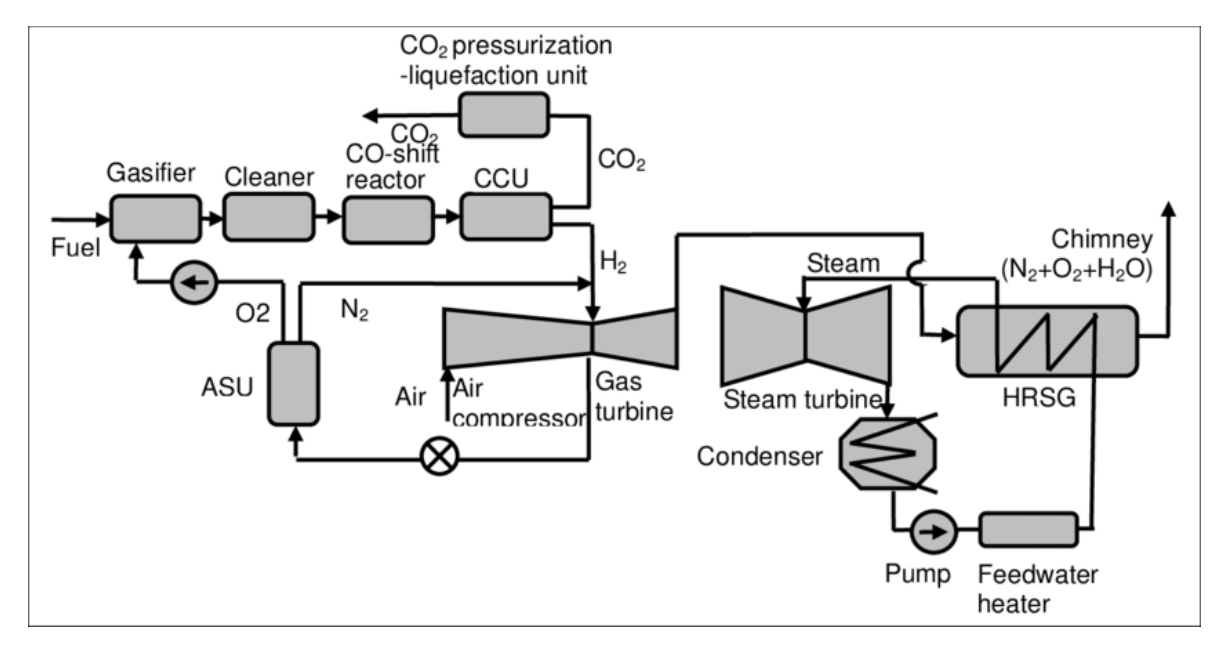


Figure 2.7: Simplified schematic diagram of oxygen-blown IGCC power generating plant integrated with pre-combustion carbon capture [HISATOME 2015]

In IGCC, a combination of gasification and combined-cycle technology is used. Solid and liquid fuels such as coal, biomass, and petroleum coke are gasified into a combustible gas, which is then cooled, cleaned, and burned in a gas turbine. The waste heat from the flue gas is utilized to generate steam, which is expanded in a steam turbine. Both turbines drive a generator that converts the mechanical energy into electricity. IGCC

technology is already in use on an industrial scale, though coal remains the dominant feedstock, accounting for 81% of the fuel used in gasification. [LOEFFLER 2022]

The purity of oxygen to be blown into the gasifier has to be $\geq 95\%$ with a pressure of 5 bar. Coal gasification, however, can be operated at pressures of up to 70 bar. [U.S. DEPARTMENT OF ENERGY AND TAMPA ELECTRIC COMPANY 2000, KREMLING ET AL. 2017].

Determining the oxygen demand for power generation is challenging, as, to the best of the author's knowledge, no operational power plants use oxygen-enriched combustion, with the exception of IGCC power plants. The available insights, therefore, are solely derived from a few simulation-based research studies that have explored this concept.

For a coal-based IGCC power plant, approximately 0.98 kg of oxygen is required to gasify one kilogram of coal [U.S. DEPARTMENT OF ENERGY AND TAMPA ELECTRIC COMPANY 2000]. When biomass is used, Zhou et al. 2009 determined an optimal biomass-to-oxygen ratio of 0.4.

HE ET AL. 2024 studied virtual power plants considering the combined operation of an oxygen-enriched coal power plant and power-to-ammonia systems. From the study, an approximate specific value of 1290 $\frac{\text{kg}_{O_2}}{\text{MWh}}$ can be derived. Given the niche nature of this study, the value is associated with considerable uncertainty.

Bailera et al. 2017 studied an oxyfuel power plant in combination with a PtG system which has a net generation capacity of approximately 0.256 TW h. The study provides the oxygen and hydrogen demand for the system analyzed.

2.3.3 Summary of Oxygen Demand, Pressure and Purity Requirements

Table 2.2 summarizes the oxygen pressure and purity requirements, as well as the specific demand for each application industry. It is important to note that real-world industrial plants may have varying pressure and purity requirements. The table provided below is derived solely from publicly available information and academic literature.

Table 2.2: Oxygen and hydrogen requirements for various application industries

Application industry	Specific O. & H. demand	O. presente	O. mirity
		Oz pressure in bar	oz purny in vol.%
Iron & steel Iron	BF-BOF: 85-157 $\frac{\text{kgo}_2}{\text{followidth}}$; DRI-EAF: 49-64 $\frac{\text{kgo}_2}{\text{followidth}}$ and 25-51 $\frac{\text{kgH}_2}{\text{followidth}}$	12 to 15	≥ 99.5
Wastewater treatment	0.65 kg _{O2} Steel	2 to 15	0 06 <
	my Wastewater	2	
CAM manufacturing 6	$6.7 \frac{\mathrm{kgo_2}}{\mathrm{kWh_{Li(NiCoMn)O2}}}$	1 to 4	50 to 99.5
Healthcare 4	$470 \frac{\mathrm{kg}_{\mathrm{O}_2}}{\mathrm{bed/vear}}$	200	93 to 99.5
Oil & gas $($	$0.37 \frac{{}^{'}$ kg _{O2} and 0.03 - $0.55 \frac{{}^{kg_{H_2}}}{{}^{kg_{Barrel}}}$	1	21 to 100
Pulp & paper \sim 2	$20-37 \frac{\mathrm{kgo_2}}{\mathrm{tpuin}}$	4 to 8	≥ 92
Synthesis gas ($0.15 \text{-} 0.25 \frac{\text{kgo}_2}{\text{m}_3^2 \text{miss}}$	30 to 100	≥ 99.5
HNO ₃ production	Cynthesis 845	up to 10.1	21 to 100
Aquaculture (0.5 -3.3 $\frac{kg_{O_2}}{kg_{Culture energies}}$	2.5	> 00
Glass	$426 \frac{\mathrm{kg}_{\mathrm{O}_2}}{\mathrm{t}_{\mathrm{Glass}}} \mathrm{and} \ 0.084 \frac{\mathrm{kg}_{\mathrm{H}_2}}{\mathrm{kg}_{\mathrm{Glass}}}$		> 93
Cement ($0.0021 \frac{\text{kg}_{\odot}}{\text{kg}_{\odot}}$		21 to 100
Waste incineration -	Comen	ı	21 to 100
Ceramics 1	$193 \frac{\text{kg}_2}{\text{tc.comis}}$	up to 5	21 to 100
Lime -	Ceranno	\ 	21 to 100
Magnesia 2	$21-214 \frac{kg_{O_2}}{t_{Magnesia}}$	ı	21 to 100
Power generation	1290 $\frac{^{\text{kgO}_2}}{^{\text{MWh}}}$; IGCC: 0.98 $\frac{^{\text{kgO}_2}}{^{\text{kgCoal}}}$; Biomass: 0.4 $\frac{^{\text{kgO}_2}}{^{\text{kgBiomass}}}$	5 to 70	≥ 95%

3 Quantitative Analysis of Oxygen Capacities and Demands

As outlined earlier, a key objective of this term paper is to identify major oxygen oxygen-consuming plants and quantify their respective demands to determine a series of suitable use cases where the integration of oxygen from electrolysis would be industrially sensible.

3.1 Methodology

Initially, market and literature research were conducted to assess the global oxygen demand and the global water electrolysis capacity. By comparing these global metrics, it is possible to evaluate whether electrolytically-produced oxygen can fulfill the global oxygen demand.

While the global values offer a general overview, they do not account for the operations, logistics, and economics at an individual industrial plant level. Therefore, after examining the global context, the market and literature research shifted focus to the scale of individual oxygen-consuming industrial plants.

The primary oxygen-consuming industries, along with their specific oxygen demands, purity, and pressure requirements, were identified in section 2.3. Within each oxygen-consuming industry, the smallest and largest oxygen-consuming plants were identified. In cases where this was not feasible, the largest oxygen-consuming plant within the industry was determined. A total of fifty-two oxygen-consuming plants and use cases across all sixteen industries were identified and listed in table A.1.

Concurrently, the capacities of individual electrolyzer projects, ranging from the smallest to the largest plants projected up to 2029, were assessed.

Having the capacity of individual electrolyzer systems and knowing the demand of a specific oxygen-consuming plant allows for a direct comparison to assess whether an existing electrolyzer system can meet the demand of a particular oxygen-consuming industrial plant.

Finally, using the above-mentioned information, an analysis and evaluation can be conducted to achieve the objective of this term paper: identifying a series of suitable use cases where the integration of electrolytically-produced oxygen is both quantitatively and qualitatively feasible. In cases where a hydrogen demand also exists, the possibility of integration of electrolytically-produced hydrogen is also examined.

Given the maturity levels and market availabilities discussed in section 2.1, AWE and PEMWE technologies are considered for the purposes of this term paper.

An average specific stack power consumption value of $50.04 \frac{\text{MW}\,\text{h}}{\text{t}_{\text{H}_2}}$ (equivalent to 6.26 $\frac{\text{MW}\,\text{h}}{\text{t}_{\text{O}_2}}$) is consistently used for any upcoming calculations. This value reflects the average stack efficiency derived from the data provided by PEMWE manufacturers in section 2.1.

Whenever hourly values were provided or when converting MW to MWh, an annual operational time of 8000 h was assumed. When a range of specific demand values was given, the upper bound was used in line with this term paper's conservative approach, except for the pulp and paper as well as the iron and steel industries. The reason for these two exceptions were outlined in subsections 2.3.1.1 and 2.3.1.6.

Table A.1 also includes the PEMWE stack capacity required to cover the O_2 demand (and H_2 demand when available) of each individual plant. To do this, the specific stack power consumption value of $50.04 \, \frac{\text{MW h}}{\text{t}_{H_2}}$ (equivalent to $6.26 \, \frac{\text{MW h}}{\text{t}_{O_2}}$) is essential as it enables a direct calculation of the required stack capacity in MW to meet the oxygen demand of individual plants. By calculating these required stack capacities, they can be compared with the electrolysis projects listed in table 3.1. The calculation follows:

Electrolyzer capacity =
$$\frac{6.26 \frac{\text{MW h}}{\text{t}_{\text{O}_2}} \cdot \text{Annual O}_2 \text{ demand}}{8000 \text{ h}}.$$
 (3.1)

Although PEMWE capacities have been calculated, it is important to note that the specific stack power consumption of both AWE and PEMWE are nearly identical. The stack consumption values were adopted because manufacturers typically provide these values rather than the total system power consumption. This conservative approach leads to the highest required PEMWE stack capacity. In other words, this conservative approach was chosen because it considers the maximum stack capacity of the electrolyzer. If this capacity aligns with the requirements of current electrolyzer projects, it will also be sufficient when the oxygen demand is lower.

3.2 Water Electrolysis Capacities

The International Energy Agency (IEA) publishes an annual report on hydrogen that provides an overview of global hydrogen production and demand, along with advancements in key areas such as infrastructure development, trade, policy, regulation, investments, and innovation. [IEA 2024]

The report indicates that the hydrogen electrolyzer market is growing rapidly, with substantial expansions planned. Global installed capacity, which reached 1.4 GW in 2023, was expected to rise to 5 GW by the end of 2024. Announced projects suggest that capacity could reach as high as 230 GW by 2030. It is important to mention, however,

that only 4% of the announced capacity has reached final investment decisions (FID) or is under construction, indicating challenges in the realization of such projects.

Dominating the water electrolysis market is the AWE technology, making up over 60% of the total installed capacity by 2023, while PEMWE accounts for 22%. By 2030, about 55% of the global electrolyzer capacity is expected to be represented by alkaline technology, while that of PEMWE is expected to grow to 43%.

Using the average specific stack energy consumption from section 3.1, along with the global electrolyzer capacity of 1.4 GW and an assumed average annual operation of 8000 h, the global oxygen production capacity via water electrolysis (by the end of 2023) can be calculated using the following equation:

Global O₂ production via water electrolysis =
$$\frac{1400 \,\mathrm{MW} \cdot 8000 \,\mathrm{h}}{6.26 \,\frac{\mathrm{MW} \,\mathrm{h}}{\mathrm{t}_{\mathrm{O}_2}}}$$
. (3.2)

This results in an estimated $1.79 \cdot 10^6 \,\mathrm{t}$ of oxygen produced electrolytically on an annual basis (2023).

At the individual plant level, this term paper's research aimed to determine the smallest and largest electrolyzer capacities that are either currently operational or projected to be operational by 2029. The findings are summarized in table 3.1. Apart from Sinopec Kuqa, which is based on AWE, all other electrolysis projects are based on PEMWE.

Since hydrogen is the desired product of water electrolysis, sources usually report the electrolyzer's hydrogen production capacity only without mentioning data on oxygen production. However, based on equation (2.1), the oxygen mass flow can be calculated as eight times the hydrogen mass flow. Oxygen output values in table 3.1 are hence all calculated using this stoichiometric relationship.

Table 3.1: Various electrolyzer capacities (*Not fully operational as of January 2025; Sinopec Kuqa: AWE, rest PEMWE)

Project	Stack capacity in MW	H_2 production in t/y	O_2 production in t/y	Source
HyBalance	1.2	182.5	1460	HyBalance 2020
REFHYNE	10	1300	10400	REFHYNE 2018
Air Liquide	20	2993	23944	Air Liquide 2021
REFHYNE 2*	100	15000	120000	REFHYNE 2018
Sinopec Kuqa*	260	20000	160000	HYDROGENINSIGHT.COM 2024
EWE Emden*	280	26000	208000	EWE AG 2024
SwitcH2 BV*	300	55000	440000	Team 2024

Currently, the world's largest electrolysis plant is the Sinopec Kuqa project, with an installed capacity of 260 MW. However, as of 2024, it is operating at less than a third of its capacity due to technical challenges faced by the three AWE manufacturers

involved, particularly concerning the flexibility of their electrolyzers, which has hindered the expected operating range of 30–100%. As of December 21, 2023, the plant had delivered approximately 2000 t of green hydrogen to Sinopec's Tahe Refining & Chemical Company. This figure is expected to rise to the targeted 20 000 t by the end of 2025. [HYDROGENINSIGHT.COM 2024]

The electrolyzer systems listed in table 3.1 exhibit variations in stack power consumption and operational hour values compared to the mean values utilized in this term paper. For instance, SwitcH2 BV's 300 MW electrolyzer is reported to produce 440 000 t of O₂ annually. In contrast, based on the specific power consumption and annual operational hours considered in section 3.1, a 300 MW electrolyzer would yield approximately 383 387 t of oxygen, representing a difference of about 15% than the figure reported by TEAM 2024. It remains unclear whether the power consumption figures in table 3.1 pertain to the entire electrolysis system or solely the electrolyzer stacks, as this distinction is not specified by the sources.

3.3 Global Demand of Industrial Oxygen

The global demand for industrial oxygen is extremely difficult to quantify due to the lack of a central organization that tracks the worldwide oxygen gas consumption. Despite an extensive literature review conducted as part of this term paper, no definitive figures for the annual global demand for oxygen could be identified. Nevertheless, it is still possible to assess demand and supply where reliable information is available.

KATO ET AL. 2005 provides data on oxygen demand in Japan for the year 2001. According to the report, 93% of the oxygen demand was attributed to the iron and steel industry, 1% to medical oxygen, and the remaining 6% to other applications such as glass melting (used in glass production) and pulp bleaching (pulp and paper industry).

Market research companies can serve as a further source of information; however, the origin and sources of their complete datasets are not publicly accessible, making independent verification of this information impossible. Nonetheless, their information offers valuable insights. According to MARKET.US 2024, the major oxygen consumers by sector in 2023 were as follows: 49% metal and mining (including processes such as smelting, refining, and ore processing), 12% medical oxygen, 14% chemical industry, 9% manufacturing, 6% research and development (R&D), and 10% other applications. This information is visualized in figure 3.1.

This underscores once again that the iron and steel industry is the largest consumer of industrial oxygen worldwide. According to the World Steel Association, global crude steel production in 2024 exceeded 1881 \cdot 10⁶ t, the majority of which was produced via the BF-BOF route [WORLD STEEL ASSOCIATION 2024]. Based on specific values from ECKL ET AL. 2025, this corresponds to approximately 164 \cdot 10⁶ t of oxygen required to meet the industry's annual demand. Assuming that the iron and steel sector accounts

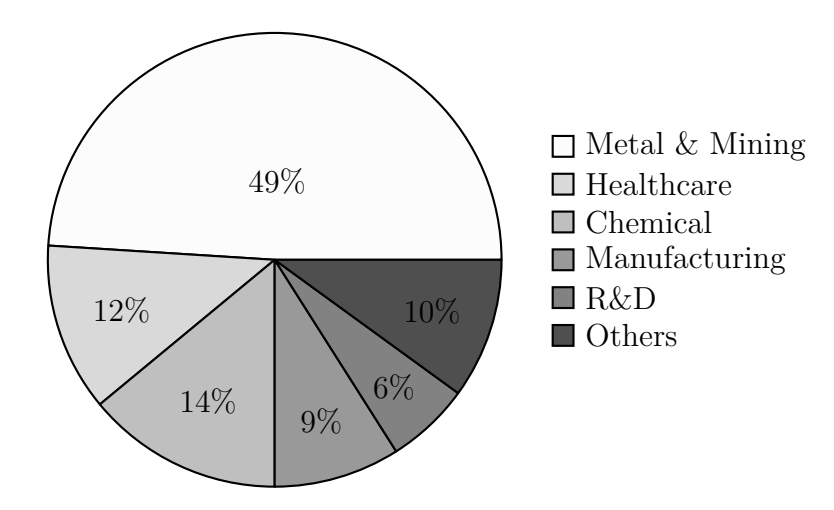


Figure 3.1: Global oxygen consumers by sector in 2023 [Based on MARKET.US 2024]

for approximately 50% of the global annual oxygen consumption, the total global oxygen demand can be estimated at roughly $328 \cdot 10^6$ t annually (for the year 2024).

3.4 Oxygen Demand at Plant Level

As previously mentioned, comprehensive research was undertaken to identify both the largest and smallest oxygen-consuming plants within each industry. In cases where this was not feasible, the largest oxygen-consuming plant within the industry was determined as they are typically well-documented and have publicly available information, unlike smaller oxygen-consuming industrial plants. For situations where oxygen usage is not currently implemented but is theoretically possible (as in many oxyfuel combustion applications), values from relevant research studies were adopted.

Table A.1 presents a comprehensive list of fifty-two oxygen-consuming industrial plants and use cases across sixteen industries where oxygen demand is either currently present or anticipated. Additionally, some of these industrial plants and use cases could be associated with a hydrogen demand. The country codes used in table A.1 are based on the ISO 3166-1 alpha-3 standard.

WORLD STEEL ASSOCIATION 2020 provides a comprehensive list of the world's top steel-producing companies. Seven steel plants, ranging from the largest producers to smaller facilities, have been identified and are listed in table A.1. Plants 6 and 7 are among the largest globally, operating via the BF-BOF route, whereas plants 1 to 5 utilize the EAF method, either recycling scrap steel or employing DRI technology. While the demand for plant no. 6 was provided by the source, the annual O₂ demand for the other plants was calculated based on specific demand values outlined in subsection 2.3.1.1.

Three wastewater treatment plants are listed in table A.1, with plant no. 9 being the largest globally. WWTP no. 10 represents an industrial wastewater treatment facility owned by BASF in Ludwigshafen, Germany. While the O₂ demand for WWTP no. 8

was provided, the annual O_2 demand for the remaining plants was calculated using specific values from subsection 2.3.1.2.

The largest producers of Li(NiCoMn)O₂-based CAM are listed as plant numbers 11 to 15. Their annual O₂ demands were calculated using specific values from subsection 2.3.1.3.

Several hospitals, each with varying numbers of beds, were identified and their annual oxygen demand estimated. These are numbered 16 to 18 in table A.1. While the demand for facilities no. 17 and 18 is based on specific values from GÓMEZ-CHAPARRO ET AL. 2018, plant no. 16's demand was sourced from PALIWAL & MATHUR 2021.

The largest glass-producing entities have been identified and listed in table A.1, alongside their calculated hydrogen and oxygen demands, as discussed in subsection 2.3.2.1. Plant no. 19 is a glass fiber manufacturing facility, while plant no. 20 represents the total glass production in Austria for 2019.

Two cement plants, along with their calculated oxygen demand (derived from specific values in subsection 2.3.2.4), are listed in table A.1. Notably, plant no. 23 is the largest cement production facility in the world. As discussed in subsection 2.3.2.2, an oxygen concentration of 23% by volume was considered when establishing the oxygen demand of cement production plants.

Table A.1 also includes research-based and industrial power plants (IGCC only) that utilize oxygen. Using specific values from HE ET AL. 2024, the oxygen requirements for two real-world power plants (26 and 27) were calculated, with plant 27 being one of the largest power plants globally. The O_2 demand for plants no. 28, 29, and 30 was provided by the source, while the O_2 demand for plants no. 31 and 32 was calculated using values from subsection 2.3.2.7.

The refineries listed in table A.1 are accompanied by their calculated hydrogen and oxygen demands, as discussed in subsection 2.3.1.5. Plant no. 33 is the Jamnagar refinery, the largest oil refinery in the world.

Plants no. 35 to 39 are among the largest in the world for synthesis gas production. The demand values for these plants were sourced from HARRISON 2022 rather than being calculated. Though hydrogen demand for each individual plant is not provided, electrolytically-produced hydrogen can be integrated into these plants as hydrogen is a key component of synthesis gas. It can either be mixed into the syngas to adjust the $\rm H_2/CO$ ratio or serve as product capacity booster in hydrogen production plants (such as plant no. 35, which uses ATR to produce blue hydrogen). Plant no. 37 is a partial oxidizer within the world's largest gas-to-liquid (GTL) plant, while plant no. 39 uses gasifiers to convert heavy refinery residues and petcoke into synthesis gas, which is fed into a 2.4 GW IGCC power plant.

Although the usage of both elemental products of electrolysis was discussed in the pulp and paper industry (see subsection 2.3.1.6), the hydrogen demand could not be quantified and is therefore not included in table A.1, which lists the two pulp mills examined in this paper. Plant no. 40 is the largest pulp mill in the world with a single

production line. The annual O_2 demands were calculated using specific demand values in subsection 2.3.1.6.

Plant no. 42 represents an academic study on oxygen-enriched combustion in a waste incineration plant, while plant no. 43 corresponds to the total magnesia production in Brazil in 2016. Plant no. 45 is a research study focused on solar-based ammonia and nitric acid production, where both H_2 and O_2 demands are provided.

Plants no. 46 to 52 represent the lime, ceramics, and aquaculture industries, with oxygen demand for these plants calculated using specific values. Mohawk Industries Inc. (plant no. 47), the world's leading ceramic tile manufacturer, and some of the globally largest fish farms, no. 50 to 52, are also included.

Figure 3.2 visually represents all the fifty-two industrial plants and uses cases, where the y-axis represents the annual oxygen demand of an individual plant logarithmically and the x-axis assigns a unique number to each individual plant and use case from various industries.

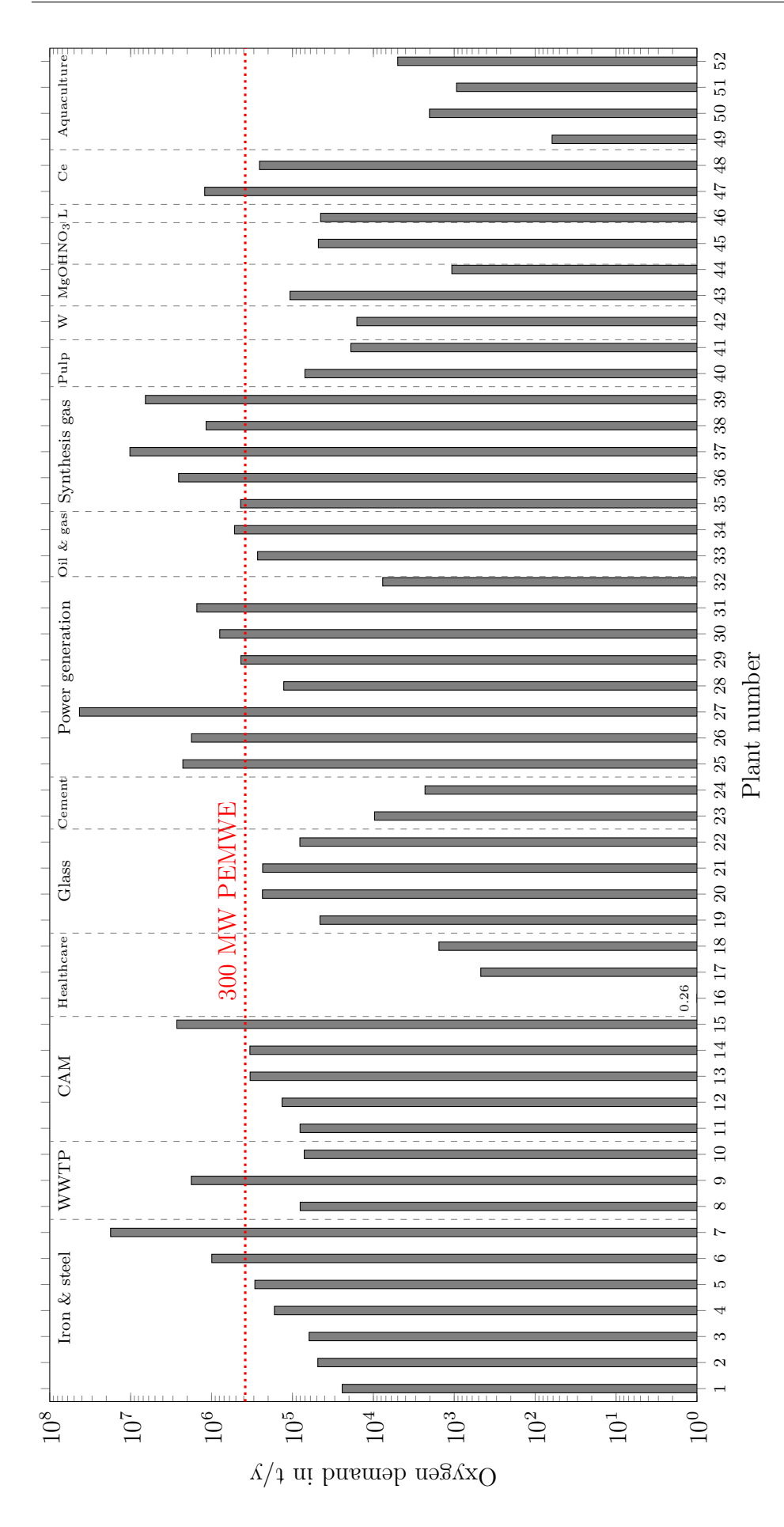


Figure 3.2: Quantified oxygen demand for each of the fifty-two shortlisted industrial plants for the named industries (see table A.1). The dotted line showcases the O₂ production capacity of a 300 MW PEMWE (based on 8000 h and 6.26 $\frac{MWh}{to_2}$). L represents the lime industry, W waste incineration, and Ce the ceramics

Each industry has a different number of studied plants, indicated by the dividing dotted lines and labels at the top of the graph to clarify each plant's industry. Stretched across the width of the graph is a red dotted line, representing the $\rm O_2$ production capacity of a 300 MW PEMWE. This allows for a quick visual assessment of which plants' $\rm O_2$ demand can be met with a realistic near-future PEMWE stack capacity.

The logarithmic scale emphasizes the following: orders of magnitude differ by factors of ten between and within industries. The O_2 demand of most (35 to be specific) plants fall below the red 300 MW dotted line, suggesting that many plants across various industries could realistically be supplied with electrolysis oxygen. It is often the largest oxygen-consuming plant(s) within each industry (such as iron and steel, WWTP, CAM manufacturing, oil and gas, synthesis gas, and ceramics) that have an O_2 demand exceeding the limits of electrolysis oxygen production. However, industries with more modest O_2 demands - such as healthcare, aquaculture, glass, pulp and paper, waste incineration, and the production of magnesia, cement, lime, and nitric acid - all fall below the red dotted line.

As theoretically predicted in section 2.3, a clear disparity in O_2 demand emerges across industries. Notably, sectors such as iron and steel, synthesis gas generation, and power generation demonstrate substantially higher demand compared to industries like healthcare and aquaculture.

A more detailed analysis of the results is carried out in chapter 4.

Figure 3.3 visually depicts all plants whose oxygen demands can be met by a PEMWE stack capacity of up to $350\,\mathrm{MW}$. The left y-axis arithmetically scales the oxygen demand, while the right y-axis shows the corresponding PEMWE stack capacity needed to meet this annual oxygen demand. Figure 3.3, therefore, excludes all plants whose O_2 demands exceed what a $350\,\mathrm{MW}$ PEMWE system can provide.

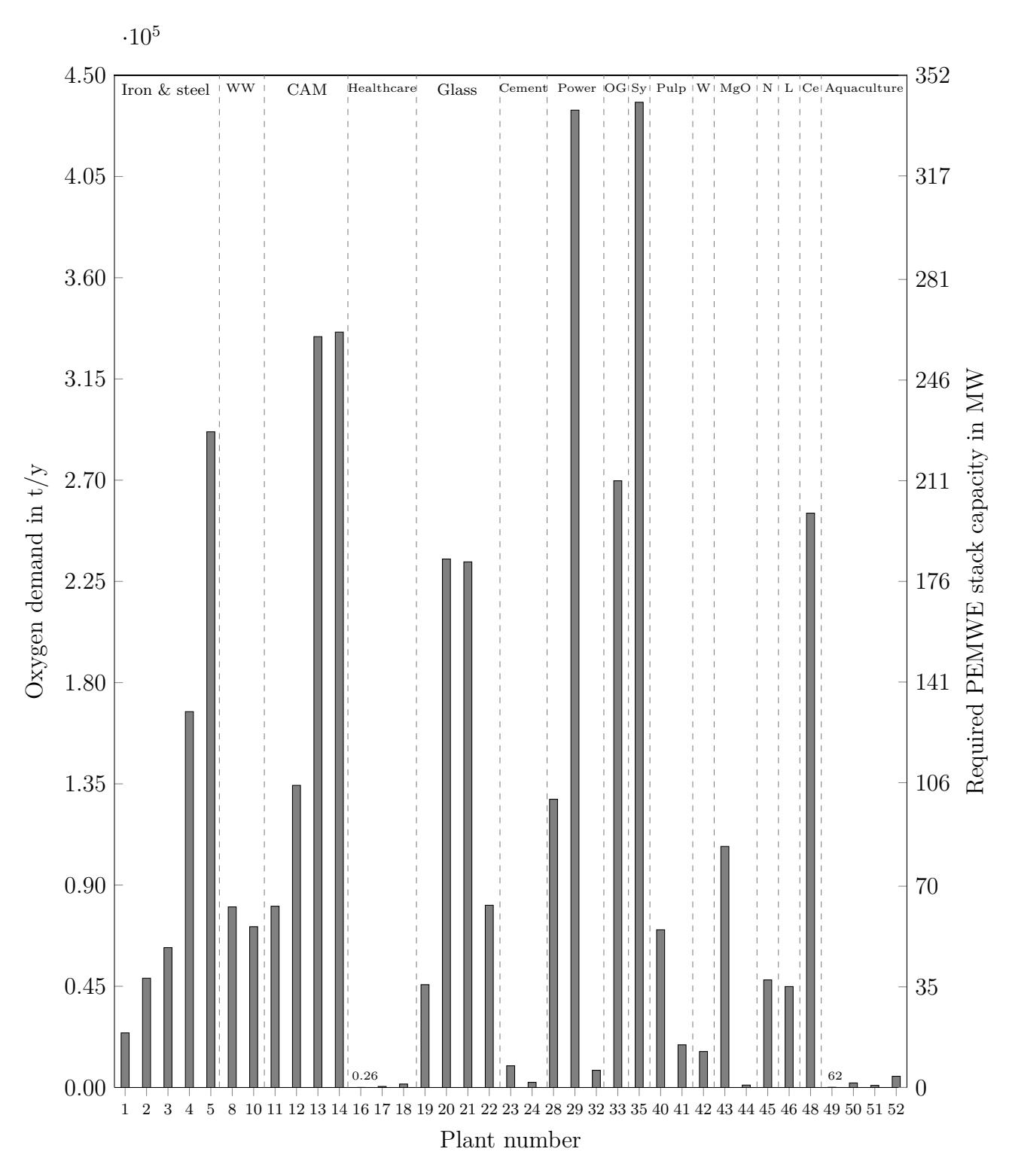


Figure 3.3: Industrial plants for the named industries (see table A.1) whose annual oxygen demand can be met by a PEMWE stack capacity of around 350 MW. OG represents the oil and gas industry, while Sy denotes synthesis gas generation, W stands for waste incineration, N for nitric acid production, L for lime production, and Ce for the ceramics industry

Interestingly, over 70% of the fifty-two studied plants (thirty-seven) have oxygen demand values within the capacity of a realistic $350\,\mathrm{MW}$ PEMWE system. This indicates an early hint of the possibility of incorporating electrolytically-produced oxygen across a significant number of industrial plants and use cases. Significantly, only a small fraction ascend to a PEMWE stack capacity of $350\,\mathrm{MW}$, with capacities predominantly in the range of $250\,\mathrm{MW}$. A more detailed analysis of the results is carried out in chapter 4.

As previously noted, some use cases and industrial plants require both oxygen and hydrogen. At first glance, these plants appear more promising, as they can integrate both elemental products of electrolysis. Figure 3.4 illustrates all the plants studied that have both hydrogen and oxygen demands.

Once again, dotted lines and labels distinguish between the industries the plants belong to. The y-axis represents the PEMWE stack capacity required to fulfill each plant's annual O_2 and H_2 requirements, capped at a maximum of 400 MW. PEMWE stack capacities exceeding this limit are not predicted for the near future (see table 3.1). While the filled bars represent needs below 400 MW, the patterned bars with arrows indicate requirements exceeding the capacity of a 400 MW PEMWE.

Without exception, the hydrogen demand (light green bars) consistently requires a greater PEMWE stack capacity. This implies that sizing the PEMWE stack capacity based on oxygen demand alone will not fully accommodate hydrogen needs, resulting in a hydrogen shortfall. Moreover, as oxygen is a by-product, it is unlikely that electrolysis plants will be sized based on the O₂ demand. On the other hand, sizing the PEMWE stack capacity based on hydrogen demand leads to excess oxygen production. Only plant 28 could ideally have its O₂ and H₂ demands met by a single PEMWE capacity size. Nonetheless, realistic PEMWE capacities could satisfy the hydrogen demands of industrial glass plants and smaller EAF steel facilities, inevitably resulting in excess oxygen production.

A more detailed analysis of the results is carried out in chapter 4.

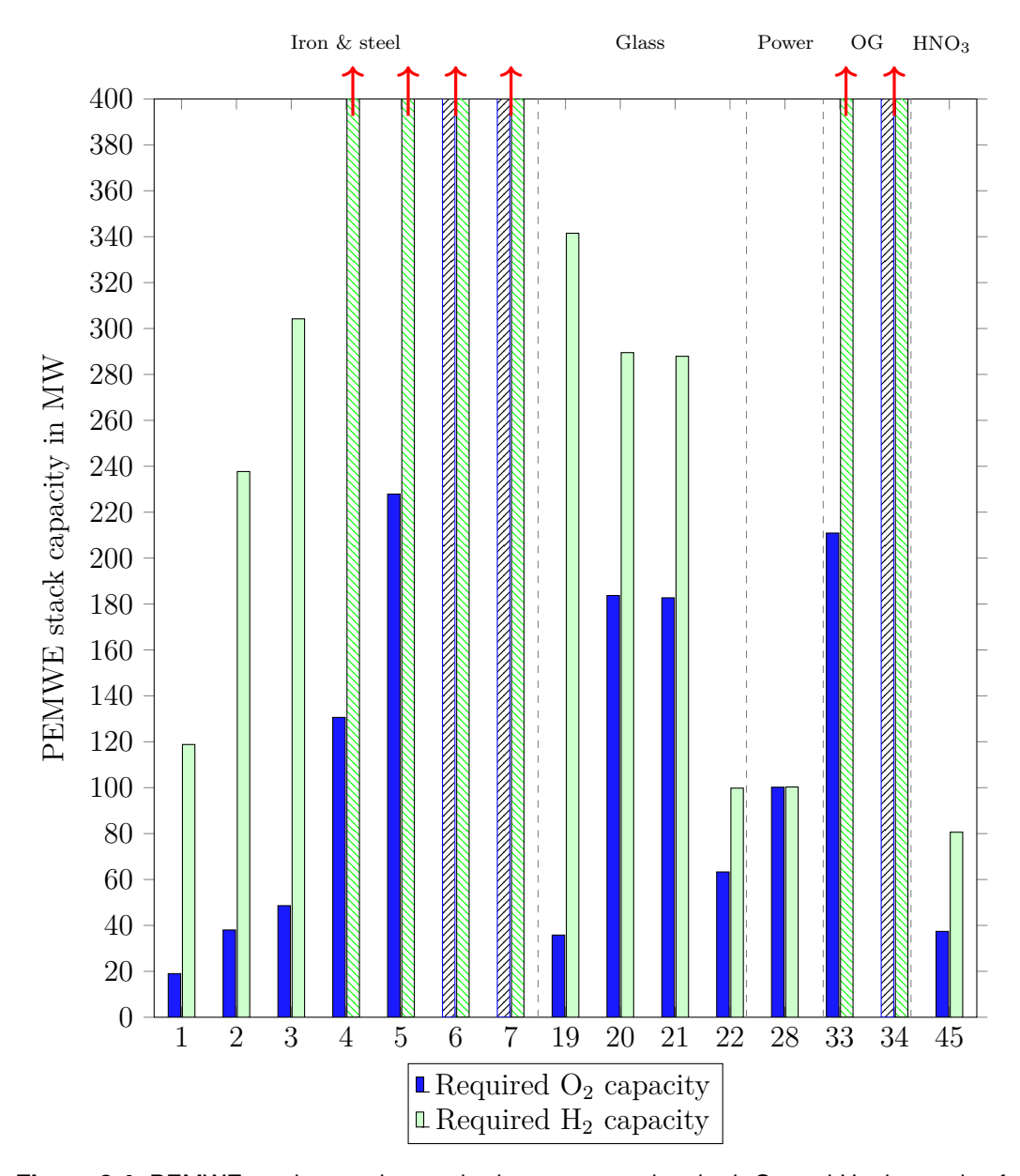


Figure 3.4: PEMWE stack capacity required to accommodate both O_2 and H_2 demands of selected industrial plants that require both O_2 and H_2 . PEMWE stack capacity based on 8000 h annual operation and 50.04 $\frac{\text{MW h}}{\text{t}_{H_2}}$ or 6.26 $\frac{\text{MW h}}{\text{t}_{O_2}}$. Arrows indicate demand exceeding 400 MW PEMWE stack capacity. OG stands for the oil and gas industry

4 Feasibility Assessment of Integrating Electrolytically-Produced Oxygen at an Industrial Scale

With quantitative data on demands and capacities from chapter 3, the feasibility of using electrolytically-produced oxygen on an industrial scale can be evaluated. This assessment will consider factors such as O_2 pressure and purity requirements, the integration of both elemental products of water electrolysis, and the alignment between oxygen demand and the supply capacity achievable through water electrolysis.

4.1 Assessment Based on Demand and Capacities

By comparing the estimated global oxygen demand of approximately $328 \cdot 10^6$ t annually with the total global capacity for electrolytically-produced oxygen, which stands at $1.79 \cdot 10^6$ t (as of 2023), an initial yet highly significant conclusion can be drawn: electrolytically-produced oxygen cannot be considered a replacement for current O_2 production methods, such as cryogenic air separation, as the electrolysis quantities fall far short of matching (or even approaching) current demand. Instead, electrolytically-produced oxygen should be regarded as a valuable by-product that enhances the economic and resource efficiency of electrolysis systems. Given the projected compound annual growth rate of over 11% in the oxygen market, valorizing electrolytic oxygen becomes increasingly important, especially in light of the rising global demand for oxygen in the coming years [MARKET.US 2024].

At the industrial scale, when considering capacity versus demand alone, electrolytically-produced oxygen can easily meet the requirements of hospitals and medical facilities. Even the largest hospitals and medical complexes can fulfill their O_2 needs through water electrolysis. The same holds true for on-land aquaculture applications. Both industries can have the demand of their largest oxygen-consuming plant met with a PEMWE stack capacity of less than 1.2 MW and 4 MW respectively - this is clearly evident from table A.1 and figure 3.2. Similarly, the O_2 demands of pulp and paper production plants can be met with PEMWE stack capacity ranges listed in table 3.1 as well. For instance, a PEMWE stack capacity of 55 MW is sufficient to fulfill the requirements of the world's largest pulp mill (plant no. 40), let alone those of smaller pulp mills.

Electrolytically-produced O_2 can seamlessly meet the oxygen demand of BASF's WWTP in Ludwigshafen, the largest integrated chemical complex in the world. This indicates that integrating oxygen from electrolysis into industrial WWTPs is a viable solution - if the needs of the world's largest chemical complex can be met with a 56 MW PEMWE stack capacity, it stands to reason that smaller demands of smaller industrial WWTPs can also be easily satisfied.

However, in the context of municipal WWTPs, while the oxygen demand of the world's largest WWTP might be challenging to meet (assuming pure oxygen is used), smaller municipal WWTPs can still utilize electrolytically-produced oxygen to handle unexpected temporary load increases or accommodate population growth without the need for building new facilities. For example, a 63 MW PEMWE stack capacity can fulfill the oxygen requirements of the Deer Island WWTP, which serves a 2.3 million-strong urban population. This suggests that PEMWE stack capacities below 100 MW could adequately address the fluctuating oxygen demands of most large metropolitan WWTPs, particularly for handling unexpected peaks. However, a fundamental shift towards the continuous use of pure oxygen throughout the entire treatment process in these large WWTPs would likely necessitate oxygen quantities exceeding the practical PEMWE capacities listed in table 3.1, even if the economic factors are ignored. Logically, it can be concluded that electrolytically-produced O_2 could serve as an effective backup system, capable of handling unexpected temporary load increases or rapid population growth in existing WWTPs, even in the world's largest cities. This could eliminate the need for cryogenic air separation units in municipal WWTPs.

As CAM manufacturing expands to meet the rising demand for electromobility, many mid-sized production plants can effectively fulfill their O₂ requirements using PEM electrolyzers with PEMWE stack capacities below 263 MW. However, the largest manufacturers - requiring PEMWE stack capacities up to 2101 MW - cannot yet rely on water electrolysis to meet their oxygen demands. The same holds true for the ceramics industry - while the oxygen demands of the largest plants cannot be met, smaller-scale production facilities could benefit from electrolytically-produced oxygen.

Power generation is a sector that may not be able to profit from electrolytically-produced oxygen as oxyfuel or oxygen-enriched combustion in power plants appears unrealistic for several reasons. Firstly, the volumes of oxygen required far exceed the capacity of current water electrolysis systems in the near future. Secondly, the energy-intensive nature of oxygen production via electrolysis makes the idea of oxyfuel or oxygen-enriched combustion seem counterintuitive, as electricity is required to generate oxygen in the first place. Additionally, the inherently fluctuating nature of (load following) thermal power plant operations or fluctuating electrolysis operations means that a continuous, steady supply of oxygen is not consistently needed or can be supplied, complicating its integration into power plants without introducing significant operational and logistical challenges. Expectedly, to the best of the author's knowledge, no major power plants have adopted oxyfuel or oxygen-enriched combustion, and academic research on the subject remains limited to niche applications. That being said, electrolytically-produced

oxygen could still play a role in biomass or coal gasification, where the O_2 demand for gasification may be partially addressed by water electrolysis.

The demand for other combustion applications, such as waste incineration, magnesia, cement, and lime production, can, however, be met via water electrolysis. The entire O_2 demand for magnesia production in Brazil could be fulfilled with a 84 MW PEMWE stack capacity, making it effortlessly possible to meet the demand of individual magnesia production plants. For waste incineration and cement production, only O_2 enrichment up to 27 vol.% and 23 vol.% was considered, rather than utilizing pure oxygen. Consequently, a modest PEMWE stack capacity of 13 MW for the waste incineration plant studied and 8 MW for the largest cement plant in the world would be adequate to meet their respective oxygen demands. Magnesia, cement, and lime production applications could also theoretically use the electrolytically-produced hydrogen as a fuel, hinting towards an attractive integration of both electrolysis products. However, the economic and logistic viability of such a theory remains an open question.

Synthesis gas generation is a significant consumer of oxygen; however, due to the large-scale nature of ATR and POX applications shortlisted in table A.1, none of their enormous O_2 demands can be met via water electrolysis. For instance, the POX system at Shell's plant in Qatar would require a PEMWE stack capacity of 7991 MW to satisfy its oxygen demand. Smaller ATR plants, on the other hand, may be able to cover their O_2 demand via water electrolysis.

Steelmaking, the largest oxygen-consuming industry in the world, has oxygen demands that vary significantly depending on production scale and the production route employed. The potential to integrate both products of electrolysis, additionally, makes this industry a particularly compelling end-user. However, for the top 50 steelmaking entities listed by WORLD STEEL ASSOCIATION 2020, the oxygen demand of the BF-BOF route is far too large to be met through water electrolysis alone. For example, Voestalpine's plant in Austria would require a 777 MW PEMWE stack capacity to meet its O₂ demand and 1764 MW to meet its H₂ demand, if direct reduction via hydrogen were implemented.

Therefore, upon initial inspection of table A.1 and figure 3.2, only steelmaking facilities using EAFs with production capacities of up to approximately $6 \cdot 10^6$ t of steel could meet their O_2 demands via water electrolysis. In practice, however, if both hydrogen and oxygen demands are to be satisfied, the higher capacity required for hydrogen ultimately determines the PEMWE stack capacity. For instance, Nucor Steel (plant no. 5) would need a calculated 131 MW PEMWE stack capacity to meet its oxygen demand, a capacity within the range of those discussed in table 3.1. However, meeting its hydrogen demand would require a 817 MW PEMWE stack capacity, meaning the hydrogen demand dictates the required PEMWE stack capacity. With such a capacity, the excess oxygen produced would either need to be vented off or sold for other applications.

This is the case for nearly all plants requiring both hydrogen and oxygen: it is the hydrogen demand that dictates the often higher electrolyzer capacity, meaning that more oxygen will always be produced than the plant would actually need. The glass industry is no exception to this observation. While the hydrogen demands of the

studied glass manufacturing plants necessitate a demonstrably larger PEMWE stack capacity than the O_2 demand, this capacity nonetheless resides within the same order of magnitude as the electrolyzer capacities documented in table 3.1. For instance, China Glass Su Qian (plant no. 21) requires a 183 MW PEMWE stack capacity to meet its O_2 demand and a 288 MW capacity to meet its O_2 demand. This means that a realistic PEMWE stack capacity of 288 MW could satisfy both the plant's O_2 and O_2 demands, with excess O_2 that could either be vented off or sold for other applications.

The oil and gas industry appears to be a promising end user for both elemental products of electrolysis. However, both of the refineries studied (plants no. 33 and 34), which are among the largest in the world, have H₂ demands that far exceed the capacities of electrolyzers listed in table 3.1. This makes meeting the H₂ demand via electrolysis unrealistic, at least in the near future. On the other hand, however, O₂ demands can be met with PEMWE capacities within the range outlined in table 3.1. Given the purchasing power of many oil and gas companies, it is conceivable that the oxygen needed for the Claus process could be purchased externally from electrolyzers that produce excess oxygen anyway, such as DRI-EAF steelmaking plants. This would eliminate the need for refineries to install and operate air separation units, reducing energy consumption and enhancing resource efficiency.

The integrated production of ammonia and nitric acid presents an additional use case for the valorization of both elemental products of water electrolysis. For the examined plant (plant no. 45), meeting the O_2 demand requires a 38 MW PEMWE stack capacity, while the H_2 demand necessitates a 81 MW capacity. This aligns with the trend of hydrogen demand being the primary driver of PEMWE stack capacity when both H_2 and O_2 are utilized.

There are industrial examples where both elemental products of water electrolysis are utilized, such as the Iberdrola & Fertiberia project in Spain. In this project, a 20 MW PEM electrolyzer produces green hydrogen, which is used at Fertiberia's ammonia plant, while the O₂ generated by the electrolyzer is entirely used in Fertiberia's nitric acid unit [IBERDROLA 2020]. The Lolland Hydrogen Community is another example where both H₂ and O₂ from electrolysis are valorized: the hydrogen is used for fuel cell combined heat and power generation, while the O₂ is used at the local municipal WWTP [MAGNONI & BASSI 2009]. These examples demonstrate that utilizing both products of water electrolysis is not just a theoretical concept, but an idea that can be practically implemented.

4.2 Assessment Based on Pressure and Purity Values

The purity and pressure of the oxygen gas output from an electrolyzer system were discussed in section 2.1. Depending on the operational load, stack degradation, and other factors outlined in section 2.1, the O_2 gas exiting the electrolysis stack contains varying amounts of H_2 and water vapor, resulting in an O_2 purity level that can safely oscillate between 98% and 99.5%. In other words, the purity of the O_2 output fluctuates

with load conditions and the age of the electrolysis stack but never falls (nor is allowed to fall) below 98% by volume. Therefore, assuming that an electrolyzer system consistently delivers O_2 with a purity of at least 98% by volume is reasonable.

In terms of the O_2 output pressure values, pressures between 0.03 to 32 barg were listed in table 2.1.

A direct comparison of tables 2.2 and 2.1 enables conclusions to be drawn.

At a first glance, the O_2 gas exiting an electrolyzer appears to be directly usable for most of the sixteen application industries examined. Apart from the iron & steel industry, all other sectors appear to have purity requirements that align with the ≥ 98 vol.% O_2 purity delivered by an electrolyzer. In terms of pressure, electrolytically-produced O_2 may require major additional compression only for medical applications, power generation, and synthesis gas generation. For other applications, slight compression is often sufficient.

A key question is whether the minor H_2 (and water vapor) impurity in electrolytically-produced oxygen is detrimental to each application.

In case of steelmaking, even trace amounts of hydrogen, at just a few parts per million, can diffuse into steel and induce hairline cracks (flakes), hydrogen embrittlement, hydrogen blistering, and a reduction in tensile ductility [Total Materia 2007]. Hence, purification steps are necessary if electrolytically-produced O_2 is to be used in steelmaking facilities.

The healthcare sector is a sector where oxygen properties are meticulously monitored. Studies by P Koziarin 1989 and Cole et al. 2021 suggest that the small traces of H₂ impurity in electrolytically-produced oxygen are medically harmless, implying that after moisture removal, no additional purification may be necessary for medical applications. However, in the absence of confirmation from concrete research and official sources like the World Health Organization and other regulatory bodies, the necessity of purification steps is assumed.

Although specific academic or industrial research on the effect of H_2 impurity in the oxygen atmosphere during CAM manufacturing was not identified, the inherent flammability of hydrogen, combined with high calcination temperatures, strongly indicates a significant hazard. Therefore, purification steps to remove H_2 are assumed to be necessary for CAM manufacturing.

 H_2 impurity is considered non-disruptive in synthesis gas generation since H_2 is a primary component of synthesis gas. This also applies when oxygen is used for oxyfuel or oxygen-enriched combustion purposes, as the combustible nature of H_2 ensures that its presence in the delivered O_2 should not be problematic.

As per Singh & Raj 2025, H_2 impurity in the oxygen stream used for the Claus process should not have any adverse effects.

In summary, it appears that the iron and steel industry, CAM manufacturing, and the healthcare sector are the only ones requiring additional purification steps to remove H_2 impurities from the oxygen stream.

Panchawadkar 2024 conducted a techno-economic analysis of purifying and pressurizing electrolytically-produced oxygen for use in the iron and steel industry and as medical oxygen.

In case of the iron & steel industry, the O_2 has to first be removed from its H_2 impurity and then dried to remove moisture. A streamlined purification system can comprise a deoxidizer unit and a drying unit (drying by condensation and adsorption). Oxygen purification is achieved via a Pt-Co catalyst bed, wherein product gas molecules interact with the catalyst surface, initiating an exothermic recombination reaction. Within this process, residual hydrogen (H_2 impurity) in the oxygen stream reacts with oxygen to form water, releasing thermal energy. Subsequent drying occurs in a two-stage process: initial cooling facilitates condensation drying, followed by adsorption drying to minimize the residual water content. This delivers a nearly-pure oxygen stream with the following gas compostion by volume: 99.87 % O_2 , 0.01 % O_2 , 0.12 % O_2 , 0.12 % O_2 , 0.12 % O_2 , 0.13 O_2 , 0.13 O_2 , 0.14 O_2 , 0.15 O_2 , 0.15 O_2 , 0.16 O_2 , 0.17 O_2 , 0.17 O_2 , 0.18 O_2 , 0.19 O_2 , 0.19 O_2 , 0.19 O_2 , 0.11 O_2 , 0.11 O_2 , 0.11 O_2 , 0.12 O_2 , 0.13 O_2 , 0.14 O_2 , 0.15 O_2 , 0.15 O_2 , 0.17 O_2 , 0.18 O_2 , 0.19 O_2 , 0.19 O_2 , 0.19 O_2 , 0.11 O_2 , 0.11 O_2 , 0.11 O_2 , 0.12 O_2 , 0.12 O_2 , 0.12 O_2 , 0.12 O_2 , 0.13 O_2 , 0.14 O_2 , 0.15 O_2 , 0.15 O_2 , 0.15 O_2 , 0.17 O_2 , 0.18 O_2 , 0.19 O_2 , 0.

4.3 Future Development of Oxygen Application Industries

The increasing emphasis on sustainable production methods, compounded by regulatory measures such as rising CO₂ taxes and prices, positions several CO₂-intensive industries that currently do not employ oxygen extensively as prime candidates for oxygen-assisted combustion technologies. These industries, which include magnesia, cement, and lime production, as well as glass manufacturing, currently depend on fossil fuel combustion for high-temperature processes and represent use cases where the benefits of oxyfuel or oxygen-enriched combustion, as discussed in section 2.3.2, could be particularly impactful. These industries could experience an emergence of oxygen demand, which could be potentially met by electrolytically-produced oxygen. This transition not only facilitates significant reductions in CO₂ emissions through oxyfuel or oxygen-enriched combustion but could also enhances the economic competitiveness of these industries over time.

As biomass gasification increasingly replaces coal gasification for enhanced sustainability, electrolysis oxygen could see future use in (small to medium-sized) biomass gasification units as well.

CAM manufacturing, an exponentially-growing industry with increasing oxygen demands, is set to become a major oxygen consumer that could purchase or integrate electrolytically-produced oxygen, particularly as the O_2 demand of small to medium-sized manufacturers can be met. However, logistical challenges related to transportation,

storage, or the intermittent operation of some electrolysis plants might lead CAM manufacturers to favor oxygen supplied via ASUs for their facilities. Likewise, the aquaculture industry is an expanding industry with a surging oxygen demand that can be effortlessly accommodated by electrolytically-produced oxygen, at least in terms of capacity, pressure, and purity requirements.

On the contrary, while the aforementioned industries are poised for increased oxygen demand, the traditional oxygen-intensive iron and steel sector is expected to experience a significant decline in O_2 demand as the DRI-EAF route gradually displaces the conventional BF-BOF process. This could mean the possibility of integrating electrolytically-produced oxygen in more and more steel mills on an initial inspection. Realistically, though, the widespread presence of ASUs in most existing steel mills, catering to their established oxygen demands, could make the incorporation of electrolysis oxygen more complicated than it seems. The declining O_2 demand could incentivize existing ASUs in many steel mills to sell their surplus gases externally, competing with electrolytically-produced oxygen.

Alongside the iron and steel industry, glass manufacturing offers another example of integrating both products of water electrolysis. Figure 3.4 illustrates several use cases where both electrolysis products can be advantageously utilized. The most practical scenario would involve installing a hydrogen-sized electrolyzer sufficient to meet H_2 demand, while selling the excess O_2 to other oxygen-consuming industries cases. New advancements in electric heating for glass production, however, may diminish the incentive for expensive electrolysis systems. This means that while the products of electrolysis could be integrated transitionally, the long-term shift to electric heating may make the concept of oxyfuel combustion in the short-term unattractive. This is another factor to consider.

Overall, there appears to be a net increase in the demand for industrial and medical oxygen, as predicted by Market.us 2024.

5 Summary and Outlook

Driven by the increasing demand for industrial oxygen and the expanding global capacity for water electrolysis, this term paper aimed to examine the quantitative and qualitative feasibility of utilizing electrolytically-obtained oxygen by-product in various industries, rather than venting it off into the atmosphere.

Recognizing a gap in the quantitative understanding of oxygen demand and supply, this research began with a market and literature review comparing the global oxygen demand versus the global oxygen production capacity via water electrolysis. More critically, individual industrial plants were studied to answer a fundamental question: can an electrolyzer meet the oxygen demand of a single oxygen-consuming industrial plant, including its purity and pressure requirements?

To answer this question, all major oxygen-consuming industries were studied, identifying sixteen key industries and use cases. Within each industry, the smallest and largest oxygen-consuming plants were identified where feasible; otherwise, the largest oxygen-consuming plant was determined (such as for synthesis gas generation, the oil and gas industry, and CAM manufacturing). Simultaneously, the projected capacities of individual electrolysis plants until 2029 were identified, enabling a comparison of demand versus supply. A total of fifty-two oxygen-consuming plants across these sixteen industries were identified and listed in table A.1.

An analysis of the oxygen demand, purity, and pressure requirements of all the fifty-two industrial plants and uses cases listed in table A.1 led to the supposition that oxygen gas from electrolyzers with capacities planned until 2029 can be directly used, without further purification, in the following direct application use cases:

- On-land aquaculture applications.
- Industrial WWTPs and municipal WWTPs using O_2 to handle unexpected temporary load increases or to accommodate population growth without the need for building new facilities.
- Pulp and paper mills.
- Refineries that use oxygen enrichment in the Claus process to produce sulfur.
- Ostwald process to produce nitric acid.

For the following oxygen combustion applications, oxygen gas from electrolyzers with capacities planned until 2029 can be directly used, without further purification:

• Glass manufacturing plants utilizing oxyfuel combustion. If hydrogen is used as fuel, their demand can also be met.

- Small to medium-sized ceramics manufacturing facilities.
- Oxygen-enriched combustion in magnesia production.
- Oxygen-enriched combustion in cement production.
- Oxyfuel or oxygen-enriched combustion in lime production.
- Oxygen-enriched incineration of municipal solid waste.

While power generation (excluding IGCC plants) is another application that does not currently employ oxygen on a broad scale, it was established that electrolytically-produced oxygen may not be a suitable option for this theoretical end-use. Gasification processes may constitute an exception, wherein electrolytically-produced oxygen (that might have to be pressurized) could be utilized to partially address the oxygen demand for either biomass or coal gasification units. For smaller-scale gasification facilities, electrolysis could potentially cover the entire oxygen demand.

Synthesis gas generation is another use case where, despite the theoretical viability of employing pressurized electrolytically produced oxygen in ATR and POX applications, the substantial $\rm O_2$ volumes required render electrolysis capacities projected until 2029 insufficient to meet the demand of many ATR and POX units. The only scenario where the integration of an electrolyzer in a synthesis gas production facility appears feasible is when the desired product is hydrogen, as seen in the blue hydrogen project in the UK (plant no.35), or when the $\rm H_2/CO$ ratio has to be adjusted. Operationally, any malfunction or intermittency within the electrolysis system would not appear to significantly impede production operations, as the blue hydrogen production route can proceed independently of a temporarily non-operational electrolysis system.

Considering the higher market value of medical oxygen, electrolyzer operators could potentially generate substantial long-term income by selling processed oxygen from electrolysis to medical facilities. While financially attractive, this avenue also presents complexities such as the necessary certifications, quality control costs for medical-grade oxygen, and the required legal permits and licenses for supplying hospitals.

Quantitavely (based on capacities in table 3.1), electrolytically produced oxygen can only meet the demand of EAF steelmaking facilities - primarily those recycling scrap steel - with an annual production of up to roughly $8 \cdot 10^6$ t of steel annually. In the case of BF-BOF steel mills, the oxygen demand of smaller mills possessing capacities up to $3 \cdot 10^6$ t of steel can be accommodated. The most practically feasible integration of water electrolysis appears to be new DRI-EAF steel mills with substantial electrolyzer capacities designed to meet hydrogen requirements. This would then generate oxygen, part of which could be utilized in the EAF, with the surplus potentially sold to other applications, as oxygen production will exceed demand if the electrolyzer is sized based on hydrogen needs.

While the projected electrolysis capacities until 2029 can meet the oxygen demand of the following cases, the oxygen produced cannot be directly employed and will require either purification, pressurization, or both:

- Application in small coal or biomass gasification units, or for partial oxygen supplementation in larger gasification processes.
- Blue hydrogen production facilities up to 600 MW utilizing electrolysis oxygen for oxyfuel combustion, with the electrolysis hydrogen boosting hydrogen production capacity. In this context, electrolytically derived hydrogen can augment the hydrogen production capacity, while the co-generated oxygen may be employed for oxyfuel combustion of the fossil fuel, resulting in reduced fuel consumption and facilitating CO₂ capture. Alternatively, applications where H₂/CO ratio has to be adjusted.
- Healthcare facilities requiring medical oxygen.
- Small to medium-sized manufacturing plants for Li(NiCoMn)O₂-based cathode active materials.
- DRI-EAF steel mills up to an annual steel production capacity of roughly $8 \cdot 10^6$ t. In the case of BF-BOF steel mills, the oxygen demand of smaller mills possessing capacities up to $3 \cdot 10^6$ t of steel can be accommodated.

Comparing the specific energy requirements and costs of water electrolysis with other oxygen production methods, it is clear that installing and operating an electrolyzer to solely meet an oxygen demand is not logical. A more sensible approach is to valorize the O_2 produced by current and upcoming electrolysis systems which are installed for hydrogen production and generate large quantities of oxygen as a by-product. Even if a direct O_2 end-user is not within the proximity of an electrolyzer, processing and selling the electrolytically produced O_2 by-product could, depending on the electrolyzer capacity, be a significant source of income, making electrolysis systems more economical and resource-efficient.

The principle of selling electrolytically produced oxygen externally also applies to electrolyzer systems currently in operation. Instead of venting the co-produced O_2 gas, potential users in the vicinity of these plants could be identified and contracted to purchase it. This would not only enhance the economic viability of electrolysis but also promote greater resource efficiency across industries. Central to this approach are inter-industry synergies, transforming one entity's by-product into another's raw material, thereby generating financial, environmental, and efficiency benefits - a mutually advantageous scenario. Nonetheless, logistical considerations pertaining to the storage and handling of O_2 , in conjunction with the significant capital expenditure associated with electrolysis systems, necessitate further detailed study on a case-to-case basis.

This study indicates that while the valorization of electrolytically derived oxygen is quantitatively and qualitatively feasible for the aforementioned scenarios, its widespread adoption likely necessitates supportive regulatory frameworks, complemented by incentives and subsidies. Furthermore, to solidify our quantitative and qualitative assessments, a plant-level simulation of oxygen production under variable loads, followed by a technoeconomic analysis encompassing storage, transport, and economic utilization on an individual plant level, would be beneficial.

A Appendix

Table A.1 presents a comprehensive list of fifty-two industrial plants and use cases identified for the purposes of this term paper, where oxygen demand is either currently present or anticipated to arise.

Table A.1: Oxygen-consuming facilities and use cases across various industries (PEMWE capacities based on $50.04 \, \frac{MWh}{t_{\rm Ho}}$ and annual operational time of 8000 h)

			th2 th2 th2	מישלים ואישוריים איני	מוש מוווממו סףכומוסוומו נווווס כו כככל וי)		
Plant no.	Plant	Industry	O ₂ demand	H ₂ demand	PEMWE capacity	PEMWE capacity	Source
			in t/y	in t/y	(O_2) in MW	(H_2) in MW	
1	Mini Steel mills	Iron & steel	24293	19000	19.0	118.8	DIASPARRO
c	(various) - MIN	1,000	70107	00006	0 06	99 20 20	ET AL. 2017
7		IIOII & Steel	40000	00000	90.00	7.167	Diasparro et al. 2017
33	(various) - MAA Tuwairqi (PAK)	Iron & steel	62190	48640	48.6	304.2	Wikipedia
•	•		1100	000	0	1	2025
4	Nucor Steel Berkeley (USA)	Iron & steel	167087	130682	130.6	817.4	Global Energy Monitor 2024a
ಗು	SABIC Hadeed Al Jubail (SAU)	Iron & steel	291516	228000	227.9	1426.1	GLOBAL ENERGY MONITOR 2024h
9	Voelstahlpine Linz Donawitz	Iron & steel	993155	281960	776.5	1763.7	GLOBAL GLOBAL ENERGY MONITOR 2024c
1-	(AUT) Baowu Group (CHN)	Group Iron & steel	17709540	5009920	13846.6	31337.0	CHINA BAOWU GROUP 2023
$ \infty $	Deer Island	WWTP	80300		62.8	1	MWRA
6	WWTP (USA) New Delta	WWTP	1779050	ı	1391.0	1	02.03.2025 The Arab
Ç	WWTP (EGY)	G177747	1		C L		6
10	WWTP (DEU)	W W 1F	00017	ı	99.9	ı	OLIVER SÜSS 2024
					7		

Continued on next page

	ba)
	previous	
	trom 1	
	continued	
٠	A.I-	
	lable .	

		Table A.1 –	- continued from previous page	n previous pag	ge		
Plant no.	Plant	Industry	O_2 demand in t/y	H_2 demand in t/y	PEMWE capacity (O_2) in MW	PEMWE capacity (H_2) in MW	Source
11	Sumitomo Metal	CAM	80596	ı	63.0	1	SUMITOMO
12	Mining (JPN) BASF Battery	CAM	134326	1	105.0	1	Metal Mining 2023 BASF 2022
13	Materials (DEU) POSCO Future	CAM	333800	1	261.0		Posco
14	M (KOR) Ningbo Ronbay		335815	ı	262.6		13.10.2024 YICAI
15	(CHN) Umicore (BEL)	CAM	2686520	1	2100.5	ı	24.01.2024 ELECTRIVE, COM 2018
16	Tirathram Shah	Healthcare	0.261	1	0.0002	1	Paliwal & Mathur 2021
17	pital (IND) A fictional hospi-	Healthcare	470	ı	0.4	ı	UCSF 2024
18	tal Charité (DEU)	Healthcare	1547.71	ı	1.2	1	Pa Medien GmbH 2024
19	Owens Corning	Glass production	45728	54600	35.8	341.5	RAETING 2024
20	${ m (USA)} \ { m Austria}$	Glass production	234954	46284	183.7	289.5	Loeffler 2022
21	China Glass Su Qian (CHN)	Glass production	233675	46032	182.7	287.9	IFC PROJECT IN- FORMATION & DATA PORTAL
					(2007

Continued on next page

page
orevious
from I
continued
A.1 –
Table

	z Source	SCHOTT 2025	GLOBAL CEMENT 2023	INTERNATIONAL CEMENT REVIEW 2010	HE ET AL. 2024	Wikipedia 18.01.2025	WIKIPEDIA 31.01.2025
	PEMWE capacity Source (H ₂) in MW	8.66	ı	1	1	ı	1
se	PEMWE capacity (O_2) in MW	63.3	7.6	1.8	1769.4	1384.8	33604.2
- continued from previous page	H_2 demand in t/y	15960	1	1	1	ı	1
continued fror	O_2 demand in t/y	81019	0996	2300	2263000	1771170	42978930
Table A.1 –	Industry	AG Glass production	Cement	Cement	Power generation	Power generation	Cuoketuo (CHN) Power generation
	Plant	Schott AG (DEU)	Ste. Genevieve Cement LafargeHolcim (USA)	Rezzato Italcementi (ITA)	Combined operation of oxygenenriched coal combustion PP and electricity- to-ammonia (Research paper)	Irsching 5 PP	Tuoketuo (CHN)
	Plant no.	22	23	24	25	26	27

Continued on next page

	page
	previous
٠	trom
	continued
7	A.1 –
- E	Table

		1able A.1 =	continued iroi	1able A.1 – continued from previous page	3.e		
Plant no.	Plant	${\rm Industry}$	O_2 demand in t/y	H_2 demand in t/y	PEMWE capacity (O_2) in MW	PEMWE capacity (H_2) in MW	Source
28	PtG oxycom-	- Power generation	128162	16042	100.2	100.3	BAILERA ET AL. 2017
	d cyc						
	power plant with AWE (Research						
59	paper) Api Energia	Power generation	434496	ı	339.7	ı	Като ет аг.
30	C P		792415	ı	619 6	ı	2005 International
37	IGCC (USA) Drax Biomass		1520000	ı	1188.5	ı	CEMENT REVIEW 2010 DRAX 2016
l)))))				
32	(GBR) Small-scale	Power generation	8992	I	6.0	ı	Patuzzi et al.
	biomass						2021
	gasification systems (ITA)						
33	Jamnagar refin-	- Oil & gas	269735	248930	210.9	1557.1	OIL & GAS
34	ery (IND) Motiva Port	Port Oil & gas	519828	144540	302.8	904.1	JOURNAL 2009 MOTIVA 2025
	Refi						
35	Blue H2 East Yorkshire (GBR)	Synthesis gas	438000	ı	342.5		Harrison 2022
					1 400 D	Continued on next room	

Continued on next page

	page	
	previous	
	trom	
_	_	
	continue	
7	A.I –	
-	lable	
	- '	

		Table A.1 $-$ 0	continued fror	Table A.1 – continued from previous page	ge		
Plant no.	Plant	Industry	O_2 demand in t/y	H_2 demand in t/y	PEMWE capacity (O ₂) in MW	PEMWE capacity PEMWE capacity (O ₂) in MW (H ₂) in MW	Source
36	Oryx gas-to-liquids (OAT)	Synthesis gas	2555000	ı	1997.7	1	Harrison 2022
37	Shell's Pearl	Synthesis gas	10220000	1	8.0662	1	Harrison 2022
38	G1L (AA1) Bintulu POX Gasfication	Synthesis gas	1168000	ı	913.2	ı	Harrison 2022
39	(MYS) Jazan (SAU)	Synthesis gas	6570000	1	5136.9	ı	Harrison 2022
40	Suzano Cerrado Pulp & paper (BRA)	Pulp & paper	70125	ı	54.8	1	ResourceWise 2023
41	Joutseno (FIN)	Pulp & paper	18975	1	14.8	1	ResourceWise 2023
42	Oxygen- enriched	Waste incineration	16005	ı	12.5	1	MA ET AL. 2019
	combustion of municipal						
	solid waste (Research paper)						
43	Brazil	Magnesia	107175	1	83.8	1	Wang 2019
44	Mag One Prod- Magnesia ucts (CDN)	Magnesia	1072	1	0.8	ī	GOVERNMENT OF INDIA 2021
					+===	, trock as Louister	

Continued on next page

	PEMWE capacity
ge	PEMWE capacity
n previous pag	H_2 demand
- continued from previous page	O ₂ demand
Table A.1	Industry
	Plant
	no.

	Source	NEUMANN ET AL, 2024	ERIKSSON ET AL. 2014	Statista 2024a	Statista 2024a	INMATEC GASETECH- NOLOGIE 2025	K+S 2023	SALMON BISE	NESS 2024 JIMÉNEZ 2025
Table A.1 – continued from previous page	PEMWE capacity (H_2) in MW	80.6	1	1	ı	ı	1	1	1
	PEMWE capacity (O_2) in MW	37.4	35.1	950.7	199.6	0.05	1.6	0.7	3.9
	H_2 demand in t/y	12885	1	ı	ı	1	1	1	1
	O_2 demand in t/y	47852	44880	1215900	255339	62	2024	237	2000
	Industry	Nitric acid	Lime	Ceramics	Ceramics	Aquaculture	& Aquaculture	Agnaculture	Aquaculture
	Plant	700 t/d 100 wt. Nitric acid plant (Research paper)	Oxyfuel Combustion in Rotary Kiln Lime Production (Research paper)	Mohawk Indus-	tries Inc. (USA) Somany Ceram-	fes (IND) Forellenhof Sigl fish farm (AUT)	K+S &	shrimp farm (DEU) Salmon Evolu- Aquaculture	tion (NOR) Soul of Japan Aquaculture K.K. (JPN)
	Plant no.	45	46	47	48	49	50	<u>rc</u>	52

Bibliography

Adams NA

ADAMS, T. N.: Lime Kiln Principles and Operations. (NA). URL: https://www.tappi.org/content/events/08kros/manuscripts/2-2.pdf.

Adams 2014

ADAMS, T. A.: Challenges and Opportunities in the Design of New Energy Conversion Systems. Proceedings of the 8th International Conference on Foundations of Computer-Aided Process Design. 34. Computer Aided Chemical Engineering. Elsevier, 2014, pp. 5–14. ISBN: 9780444634337. DOI: 10.1016/B978-0-444-63433-7.50002-X.

AGC Glass 2025

AGC GLASS: Hot Oxycombustion furnace design. Ed. by AGC GLASS EUROPE. 2025. URL: https://www.agc-glass.eu/en/news/story/quest-ecological-furnace.

Air Liquide 2021

AIR LIQUIDE: Inauguration du plus grand électrolyseur PEM au monde pour la production d'hydrogène décarboné | Air Liquide. 2021. URL: https://www.airliquide.com/fr/histoires/industrie/inauguration-du-plus-grand-electrolyseur-pem-au-monde-pour-la-production-dhydrogene-decarbone.

AIR LIQUIDE 15.10.2024

AIR LIQUIDE: Air Liquide to supply oxygen to LG Chem for their electric vehicle battery plant in the United States / Air Liquide. 15.10.2024. URL: https://www.airliquide.com/group/press-releases-news/2024-10-15/air-liquide-supply-oxygen-lg-chem-their-electric-vehicle-battery-plant-united-states.

An & Jung 2020

An, S.; Jung, J. C.: Kinetic modeling of thermal reactor in Claus process using CHEMKIN-PRO software. Case Studies in Thermal Engineering 21 (2020), p. 100694. ISSN: 2214157X. DOI: 10.1016/j.csite.2020.100694.

Bailera et al. 2017

BAILERA, M.; KEZIBRI, N.; ROMEO, L. M.; ESPATOLERO, S.; LISBONA, P.; BOUALLOU, C.: Future applications of hydrogen production and CO2 utilization for energy storage: Hybrid Power to Gas-Oxycombustion power plants. International Journal of Hydrogen Energy 42.19 (2017), pp. 13625–13632. ISSN: 03603199. DOI: 10.1016/j.ijhydene.2017.02.123.

Bibliography 65

Bareiss et al. 2019

BAREISS, K.; DE LA RUA, C.; MÖCKL, M.; HAMACHER, T.: Life cycle assessment of hydrogen from proton exchange membrane water electrolysis in future energy systems. Applied Energy 237 (2019), pp. 862–872. ISSN: 03062619. DOI: 10.1016/j.apenergy.2019.01.001.

BASF 2022

BASF: BASF expands production capacity in China for industry-leading cathode active materials and achieves multi-ton scale manufacturing for manganese-rich products. 2022. URL: https://www.basf.com/dk/en/media/news-releases/2022/06/p-22-253.

BOC 2025

BOC: Medical Gases Price List (ex. VAT @ 20%) - 1 January 2025. (2025). URL: https://www.bocgases.co.uk/files/medical_gas_price_list_uk.pdf.

BOYD 2008

BOYD, C. E.: Calculating the Feed Oxygen Demand (FOD) of Aquafeeds. PhD thesis. Bangkok: KASETSART UNIVERSITY, 2008. URL: https://fish.ku.ac.th/pdf/Bulletin29-38/Fishery%20Bulletin%20no%2032-3-4.pdf.

Boyd et al. 2017

BOYD, C. E.; CHATVIJITKUL, S.; DAVIS, D. A.: Understanding the oxygen demand of aquafeeds - Responsible Seafood Advocate: Proper aquafeed quality, management key to Minimizing dissolved oxygen and stress levels. Ed. by GLOBAL SEAFOOD ALLIANCE. 2017. URL: https://www.globalseafood.org/advocate/understanding-oxygen-demand-aquafeeds/.

Butler 01.01.2024

BUTLER, T.: Population Equivalent in Sewage Treatment. Ed. by BUTLER MAN-UFACTURING SERVICES. 1.01.2024. URL: https://butlerms.com/educationblog/sewage-parameters-3-population-equivalent-pe-part-1.

CARMO ET AL. 2013

CARMO, M.; FRITZ, D. L.; MERGEL, J.; STOLTEN, D.: A comprehensive review on PEM water electrolysis. International Journal of Hydrogen Energy 38.12 (2013), pp. 4901–4934. ISSN: 03603199. DOI: 10.1016/j.ijhydene.2013.01.151.

Caudle et al. 2023

CAUDLE, B.; TANIGUCHI, S.; NGUYEN, T. T.; KATAOKA, S.: Integrating carbon capture and utilization into the glass industry: Economic analysis of emissions reduction through CO2 mineralization. Journal of Cleaner Production 416 (2023), p. 137846. ISSN: 09596526. DOI: 10.1016/j.jclepro.2023.137846.

CERAMICTURKEY 2022

CERAMICTURKEY: CERAMIC PRODUCTION WITH HIGH PRESSURE METHOD. 2022. URL: https://www.ceramicturkey.org/post/ceramic-production-with-high-pressure-method.

CHEMEUROPE 2025

CHEMEUROPE: Ostwald Process. 2025. URL: https://www.chemeurope.com/en/encyclopedia/Ostwald_process.html.

CHINA BAOWU GROUP 2023

CHINA BAOWU GROUP: Company profile. 2023. URL: https://www.baowugroup.com/en/about/company profile.

Cole et al. 2021

Cole, A. R.; Sperotto, F.; Dinardo, J. A.; Carlisle, S.; Rivkin, M. J.; Sleeper, L. A.; Kheir, J. N.: *Safety of Prolonged Inhalation of Hydrogen Gas in Air in Healthy Adults.* Critical care explorations 3.10 (2021), e543. doi: 10.1097/CCE.000000000000543.

Colli et al. 2019

Colli, A. N.; Girault, H. H.; Battistel, A.: *Non-Precious Electrodes for Practical Alkaline Water Electrolysis*. Materials (Basel, Switzerland) 12.8 (2019). ISSN: 1996-1944. DOI: 10.3390/ma12081336.

CRC handbook of chemistry and physics: A ready-reference book of chemical and physical data 1995

: CRC handbook of chemistry and physics: A ready-reference book of chemical and physical data. 76. ed., 1995-1996. Boca Raton, Fla.: CRC Press, 1995. ISBN: 9780849304767.

Daurer et al. 2025

Daurer, G.; Schwarz, S.; Demuth, M.; Gaber, C.; Hochenauer, C.: On the use of hydrogen in oxy-fuel glass melting furnaces: An extensive numerical study of the fuel switching effects based on coupled CFD simulations. Fuel 380 (2025), p. 133576. ISSN: 00162361. DOI: 10.1016/j.fuel.2024.133576.

Diasparro et al. 2017

DIASPARRO, A.; TRISCIUZZI, A.; TAURINO, A.: Mini mills, Micro mills, Nano mills and the Energy Saving Compact Mini mill. (2017).

DIPL.-ING. BERTHOLD MÜLLER 1999

DIPL.-ING. BERTHOLD MÜLLER: Eine flexible und wirtschaftliche Alternative. 1999. URL: https://prozesstechnik.industrie.de/chemie/eine-flexible-und-wirtschaftliche-alternative/.

Dornisch-Bund 2020

DORNISCH-BUND, B.: Kalkindustrie: Auf dem Weg zur klimaneutralen Industrie. 2020. URL: https://www.klimaschutz-industrie.de/themen/branchen/kalkindustrie/.

Drax 2016

DRAX: This train isn't like any other in the UK / Drax. 2016. URL: https://www.drax.com/sustainable-bioenergy/this-train-isnt-like-any-other/.

Dutta & Chokshi 2020

Dutta, S. K.; Chokshi, Y. B.: *Basic Concepts of Iron and Steel Making*. 1st ed. 2020. Singapore: Springer Singapore and Imprint Springer, 2020. ISBN: 9789811524370. Doi: 10.1007/978-981-15-2437-0.

EC 2025

EC: Pulp and paper industry. 2025. URL: https://single-market-economy.ec.europa.eu/sectors/raw-materials/related-industries/forest-based-industries/pulp-and-paper-industry en.

ECKL ET AL. 2025

ECKL, F.; MOITA, A.; CASTRO, R.; NETO, R. C.: Valorization of the by-product oxygen from green hydrogen production: A review. Applied Energy 378 (2025), p. 124817. ISSN: 03062619. DOI: 10.1016/j.apenergy.2024.124817.

EIGA 2024

EIGA: Overview of Hydrogen Production Methods: EUROPEAN INDUSTRIAL GASES ASSOCIATION AISBL. (2024). URL: https://www.eiga.eu/uploads/documents/D0C251.pdf.

ELECTRIVE.COM 2018

ELECTRIVE.COM: Umicore sets up cathode factory in Poland - electrive.com. 2018. URL: https://www.electrive.com/2018/06/02/umicore-sets-up-cathode-factory-in-poland/.

Eriksson et al. 2014

ERIKSSON, M.; HÖKFORS, B.; BACKMAN, R.: Oxyfuel combustion in rotary kiln lime production. Energy Science & Engineering 2.4 (2014), pp. 204–215. ISSN: 2050-0505. DOI: 10.1002/ese3.40.

Eurofer 2024

EUROFER: What is steel and how is steel made? 2024. URL: https://www.eurofer.eu/about-steel/learn-about-steel/what-is-steel-and-how-is-steel-made.

EUROPEAN PARLIAMENT, COUNCIL OF THE EUROPEAN UNION 23.04.2009

EUROPEAN PARLIAMENT, COUNCIL OF THE EUROPEAN UNION: Directive
2009/30 - EN - EUR-Lex. 23.04.2009. URL: https://eur-lex.europa.eu/legalcontent/EN/ALL/?uri=CELEX:32009L0030.

EVERLING 2022

EVERLING, M.: Wie wird die Glasindustrie bis 2045 CO2-neutral? – glasstec Messe. 2022. URL: https://www.glasstec.de/de/Media_News/Presse/Pressematerial/Fachartikel/Wie_wird_die_Glasindustrie_bis_2045_CO2-neutral# ftnref1.

EWE AG 2024

EWE AG: Energieversorger EWE vergibt Auftrag für Wasserstoff-Großprojekt in Norddeutschland an Siemens Energy. 2024. URL: https://www.ewe.com/de/media-center/pressemitteilungen/2024/07/energieversorger-ewe-vergibt-auftrag-fr-wasserstoffgroprojekt-in-norddeutschland-an-siemens-energy.

Fahr et al. 2024

Fahr, S.; Engel, F. K.; Rehfeldt, S.; Peschel, A.; Klein, H.: Overview and evaluation of crossover phenomena and mitigation measures in proton exchange membrane (PEM) electrolysis. International Journal of Hydrogen Energy 68 (2024), pp. 705–721. ISSN: 03603199. DOI: 10.1016/j.ijhydene.2024.04.248.

FALORNI TECH 23.10.2017

FALORNI TECH: OXY Fuel Systems - Falorni Tech. 23.10.2017. URL: https://www.falornitech.com/solutions/heating-systems/oxy-fuel/.

FAO UNITED NATIONS 2024

FAO UNITED NATIONS: Total fisheries and aquaculture production: The state of world fisheries and aquaculture 2022. 2024. URL: https://openknowledge.fao.org/server/api/core/bitstreams/9df19f53-b931-4d04-acd3-58a71c6b1a5b/content/sofia/2022/world-fisheries-aquaculture-production.html.

Fries 2022

Fries, J.: The journey to green steel. Ed. by ArcelorMittal. 2022.

GLOBAL CEMENT 2023

GLOBAL CEMENT: Holcim US to invest US\$100m in Ste. Genevieve cement plant expansion. 2023. URL: https://www.globalcement.com/news/item/16503-holcim-us-to-invest-us-100m-in-ste-genevieve-cement-plant-expansion.

Global Energy Monitor 2024a

GLOBAL ENERGY MONITOR: Nucor Steel Berkeley plant. 2024. URL: https://www.gem.wiki/Nucor_Steel_Berkeley_plant.

GLOBAL ENERGY MONITOR 2024b

GLOBAL ENERGY MONITOR: SABIC Hadeed Al Jubail steel plant. 2024. URL: https://www.gem.wiki/SABIC Hadeed Al Jubail steel plant.

GLOBAL ENERGY MONITOR 2024c

GLOBAL ENERGY MONITOR: Voestalpine Stahl Linz steel plant. 2024. URL: https://www.gem.wiki/Voestalpine_Stahl_Linz_steel_plant.

Gómez-Chaparro et al. 2018

GÓMEZ-CHAPARRO, M.; GARCÍA-SANZ-CALCEDO, J.; ARMENTA MÁRQUEZ, L.: Analytical Determination of Medical Gases Consumption and Their Impact on Hospital Sustainability. Sustainability 10.8 (2018), p. 2948. DOI: 10.3390/su10082948.

GOVERNMENT OF INDIA 2021

GOVERNMENT OF INDIA: Indian Minerals Yearbook 2021. (2021).

Gustavsson et al. 2023

Gustavsson, M.; Särnbratt, M.; Nyberg, T.; Hernández Leal, M.; Lysenko, O.; Karlsson, M.; Karlsson, L.; Önnby, L.; Östling, E.; Lindblad, E.; Elevant, M.; Lundkvist, K.: *Potential use and market of Oxygen as a by-product from hydrogen production.* (2023).

Hancke et al. 2024

HANCKE, R.; BUJLO, P.; HOLM, T.; ULLEBERG, Ø.: High-pressure PEM water electrolyser performance up to 180 bar differential pressure. Journal of Power Sources 601 (2024), p. 234271. ISSN: 03787753. DOI: 10.1016/j.jpowsour.2024.234271.

Harrison 2022

HARRISON, S. B.: Safe oxygen production for Giga-scale hydrogen generation. Ed. by DECARBONISATION TECHNOLOGY. 2022. URL: https://decarbonisationtechnology.com/article/55/safe-oxygen-production-for-giga-scale-hydrogen-generation.

HAUG 2019

HAUG, P.: Experimental and theoretical investigation of gas purity in alkaline water electrolysis. PhD thesis. MyCoRe Community, 2019. DOI: 10.21268/20190328-0.

HE ET AL. 2024

HE, J.; MAO, Z.; HUANG, W.; ZHANG, B.; XIAO, J.; ZHANG, Z.; LIU, X.: Low-Carbon Economic Dispatch of Virtual Power Plants Considering the Combined Operation of Oxygen-Enriched Combustion and Power-to-Ammonia. Sustainability 16.10 (2024), p. 4026. DOI: 10.3390/su16104026.

Hemauer et al. 2021

HEMAUER, J.; MEIER, C.; PESCHEL, A.; REHFELDT, S.; KLEIN, H.: Vergleich verschiedener Prozesse zur Synthesegas-Herstellung im Hinblick auf deren Nachhaltigkeit und Weiterverarbeitung am Beispiel von Methanol. Jahrestreffen der ProcessNet-Fachgemeinschaft Prozess-, Apparate- und Anlagentechnik. 2021.

Henze et al. 2008

HENZE, M.; VAN LOOSDRECHT, M. C. M.; EKAMA, G. A.; BRDJANOVIC, D.: *Biological Wastewater Treatment: Principles, Modelling and Design.* IWA Publishing, 2008. ISBN: 9781780401867. DOI: 10.2166/9781780401867.

HISATOME 2015

HISATOME, M.: Development of Ultra-Efficient Fossil Fuel-Fired Power Generating Plant for CCS. PhD thesis. Yokohama: Hisatome Power & Environmental Engineering Office, 2015.

HÖNIG ET AL. 2023

HÖNIG, F.; RUPAKULA, G. D.; DUQUE-GONZALEZ, D.; EBERT, M.; BLUM, U.: Enhancing the Levelized Cost of Hydrogen with the Usage of the Byproduct Oxygen in a Wastewater Treatment Plant. Energies 16.12 (2023), p. 4829. DOI: 10.3390/en16124829.

Hybalance 2020

HyBalance: From wind power to green hydrogen. 2020.

HYDROGENINSIGHT.COM 2024

HYDROGENINSIGHT.COM: EXCLUSIVE | World's largest green hydrogen project in China only produced about 35% of expected output in first year of operation. 2024. URL: https://www.hydrogeninsight.com/production/exclusive-world-s-largest-green-hydrogen-project-in-china-only-produced-about-35-of-expected-output-in-first-year-of-operation/2-1-1702616.

Iberdrola 2020

IBERDROLA: Iberdrola and Fertiberia launch the largest plant producing green hydrogen for industrial use in Europe - Iberdrola. 2020. URL: https://www.iberdrola.com/press-room/news/detail/iberdrola-fertiberia-launch-largest-plant-producing-green-hydrogen-industrial-europe.

IEA 2024

IEA: Global Hydrogen Review 2024. (2024).

IEA - International Energy Agency 2023

IEA - International Energy Agency: Global EV Outlook 2023: Catching up with climate ambitions. (2023).

IFC PROJECT INFORMATION & DATA PORTAL 2007

IFC PROJECT INFORMATION & DATA PORTAL: Summary of Proposed Investment. 2007. URL: https://disclosures.ifc.org/project-detail/SPI/25665/china-glass.

INMATEC GASETECHNOLOGIE 2025

INMATEC GASETECHNOLOGIE: OXYGEN IN FISH FARMING. 2025. URL: https://www.inmatec.de/files/inmatec/img/news/FM_1912_Sigl_EN_web.pdf.

International Cement Review 2010

INTERNATIONAL CEMENT REVIEW: *Italcementi to upgrade Rezzato plant*, *Italy*. 2010. URL: https://www.cemnet.com/News/story/130777/italcementi-to-upgrade-rezzato-plant-italy.html.

International Maritime Organization 20.19.2019

INTERNATIONAL MARITIME ORGANIZATION: Global limit on sulphur in ships' fuel oil reduced from 01 January 2020. 20.19.2019. URL: https://www.imo.org/en/MediaCentre/PressBriefings/pages/34-IMO-2020-sulphur-limit-.aspx.

ITM Power 2025

ITM POWER: $NEPTUNE\ V\ /\ ITM$. 2025. URL: https://itm-power.com/products/neptune-5.

JIMÉNEZ 2025

JIMÉNEZ, R. Á.: Largest land-based salmon farm project in Asia receives \$210M in financing - WeAreAquaculture. 2025. URL: https://weareaquaculture.com/news/aquaculture/largest-land-based-salmon-farm-project-in-asia-receives-210m-in-financing.

JOHN COCKERILL 2025

JOHN COCKERILL: *Electrolysers and hydrogen refuelling stations*. 2025. URL: https://hydrogen.johncockerill.com/en/.

K+S 2023

K+S: Sustainable lighthouse project in the Innopark K+S and Aquapurna build shrimp farm in Sigmundshall. Wunstorf (Germany), 2023.

Kampker & Offermanns 2023

Kampker, A.; Offermanns, C.: *Microsoft PowerPoint - KOMPONENTEN-HERSTELLUNG EINER LITHIUM-IONEN-BATTERIEZELLE*. 2023.

Kato et al. 2005

Kato, T.; Kubota, M.; Kobayashi, N.; Suzuoki, Y.: Effective utilization of by-product oxygen from electrolysis hydrogen production. Energy 30.14 (2005), pp. 2580–2595. ISSN: 03605442. DOI: 10.1016/j.energy.2004.07.004.

Kermeli et al. 2022

KERMELI, K.; CRIJNS-GRAUS, W.; JOHANNSEN, R. M.; MATHIESEN, B. V.: Energy efficiency potentials in the EU industry: impacts of deep decarbonization technologies. Energy Efficiency 15.8 (2022). ISSN: 1570-646X. DOI: 10.1007/s12053-022-10071-8.

Kleimt et al. 2012

KLEIMT, B.; DETTMER, B.; HAVERKAMP, V.; DEINET, T.; TASSOT, P.: *Increased Energy and Material Efficiency of Steelmaking in the Electric Arc Furnace*. Chemie Ingenieur Technik 84.10 (2012), pp. 1714–1724. ISSN: 0009-286X. DOI: 10.1002/cite.201200076.

Kohl & Nielsen 1997

KOHL, A. L.; NIELSEN, R.: Gas purification. 5. ed. Houston, Tex.: Gulf Publ. Co, 1997. ISBN: 978-0-88415-220-0. URL: http://www.loc.gov/catdir/description/els032/96052470.html.

Kremling et al. 2017

Kremling, M.; Briesemeister, L.; Gaderer, M.; Fendt, S.; Spliethoff, H.: Oxygen-Blown Entrained Flow Gasification of Biomass: Impact of Fuel Parameters and Oxygen Stoichiometric Ratio. Energy & Fuels 31.4 (2017), pp. 3949–3959. ISSN: 0887-0624. DOI: 10.1021/acs.energyfuels.6b02949.

LIANG ET AL. 2019

LIANG, R.; YU, F.-D.; GOH, K.; SUN, G.; WANG, M.-J.; ZHU, H.; LIU, X.-Y.; HUANG, G.-S.; WANG, Z.-B.: Influence of oxygen percentage in calcination atmosphere on structure and electrochemical properties of LiNio.8Coo.1Mno.1O2 cathode material for lithium-ion batteries. Ceramics International 45.15 (2019), pp. 18965–18971. ISSN: 02728842. DOI: 10.1016/j.ceramint.2019.06.134.

LINDE AG n.d.

LINDE AG: Oxygen-enrichment-claus-plants. URL: https://static.prd.echannel.linde.com/wcsstore/NL_RES_Industrial_Gas_Store/Attachment/Downloads/Applications/Oxygen-enrichment-claus-plants.pdf.

Loeffler 2022

LOEFFLER, J.: Nutzungspotentiale des Nebenprodukt-Sauerstoffs der Wasserelektrolyse. Master Thesis. Leoben: Montan Universität, 2022.

LONGI 2025

LONGI: Green Hydrogen Production Equipment -. 2025. URL: https://www.longi.com/en/products/hydrogen/.

Ma et al. 2019

MA, C.; LI, B.; CHEN, D.; WENGA, T.; MA, W.; LIN, F.; CHEN, G.: An investigation of an oxygen-enriched combustion of municipal solid waste on flue gas emission and combustion performance at a 8 MWth waste-to-energy plant. Waste management (New York, N.Y.) 96 (2019), pp. 47–56. DOI: 10.1016/j.wasman.2019.07.017.

Magnoni & Bassi 2009

MAGNONI, S.; BASSI, A. M.: Creating Synergies from Renewable Energy Investments, a Community Success Story from Lolland, Denmark. Energies 2.4 (2009), pp. 1151–1169. DOI: 10.3390/en20401151.

Mandal et al. 2020

MANDAL, R.; KUMAR, R.; ANSARI, M. S.; KUMAR, D.; CHAULYA, S. K.; PRASAD, G. M.; SINGH, A. K.; MAITY, T.: *Underground coal gasification techniques for different geo-mining conditions*. International Journal of Oil, Gas and Coal Technology 23.2 (2020), p. 199. ISSN: 1753-3309. DOI: 10.1504/IJOGCT.2020.105452.

Market.us 2024

MARKET.US: Oxygen Market in 2023. 2024. URL: https://market.us/report/oxygen-market/.

Martinez Lopez et al. 2023

MARTINEZ LOPEZ, V. A.; ZIAR, H.; HAVERKORT, J. W.; ZEMAN, M.; ISABELLA, O.: Dynamic operation of water electrolyzers: A review for applications in photovoltaic systems integration. Renewable and Sustainable Energy Reviews 182 (2023), p. 113407. ISSN: 13640321. DOI: 10.1016/j.rser.2023.113407.

MOTIVA 2025

MOTIVA: Refining. 2025. URL: https://www.motiva.com/what-we-do/operations/refining.

MWRA 02.03.2025

MWRA: Deer Island Wastewater Treatment Plant / MWRA. Ed. by MWRA. 2.03.2025. URL: https://www.mwra.com/your-sewer-system/sewer-treatment-facilities/deer-island-wastewater-treatment-plant.

NEL HYDROGEN 2018

NEL HYDROGEN: Atmospheric Alkaline Electrolyser | Nel Hydrogen. 2018. URL: https://nelhydrogen.com/product/atmospheric-alkaline-electrolyser-aseries/.

Nel Hydrogen 2019

NEL HYDROGEN: PEM Electrolyser - MC Series | Nel Hydrogen. 2019. URL: https://nelhydrogen.com/product/mc-series-electrolyser/.

NEUMANN ET AL. 2024

NEUMANN, N. C.; BAUMSTARK, D.; LÓPEZ MARTÍNEZ, P.; MONNERIE, N.; ROEB, M.: Exploiting synergies between sustainable ammonia and nitric acid production: A techno-economic assessment. Journal of Cleaner Production 438 (2024), p. 140740. ISSN: 09596526. DOI: 10.1016/j.jclepro.2024.140740.

NEXANTECA 2024

NEXANTECA: Making money out of thin air: Valorizing the oxygen byproduct of green hydrogen production. 2024. URL: https://www.nexanteca.com/blog/202401/making-money-out-thin-air-valorizing-oxygen-byproduct-green-hydrogen-production.

Ohmium 02.04.2025

OHMIUM: / Making green hydrogen a reality today. 2.04.2025. URL: https://www.ohmium.com/.

OIL & GAS JOURNAL 2009

OIL & GAS JOURNAL: Indian refinery starts up new sulfur-recovery unit / Oil & Gas Journal. 2009. URL: https://www.ogj.com/refining-processing/refining/article/17222462/indian-refinery-starts-up-new-sulfur-recovery-unit.

OLIVER SÜSS 2024

OLIVER SÜSS: Sauerstoffnutzung in der BASF Kläranlage: Email. Ed. by AMIR DASTGHEIBIFARD. 2024.

P KOZIARIN 1989

P KOZIARIN: [Effect of electrolysis oxygen on the human body] - PubMed. 1989. URL: https://pubmed.ncbi.nlm.nih.gov/2718430/.

PA MEDIEN GMBH 2024

PA MEDIEN GMBH: Die 25 größten Unikliniken in Deutschland. praktischArzt (2024). URL: https://www.praktischarzt.de/magazin/unikliniken-deutschlandranking/.

Paliwal & Mathur 2021

Paliwal, A.; Mathur, A.: Covid-19: Oxygen shortage cripples hospitals, Delhi sees over 700% rise in demand. India Today (2021).

Panchawadkar 2024

PANCHAWADKAR, D.: Review of opportunities to valorise the oxygen generated from water electrolysis. Master's Thesis. Stockholm: KTH Royal Institute of Technology, 2024.

Patuzzi et al. 2021

Patuzzi, F.; Basso, D.; Vakalis, S.; Antolini, D.; Piazzi, S.; Benedetti, V.; Cordioli, E.; Baratieri, M.: *State-of-the-art of small-scale biomass gasification systems: An extensive and unique monitoring review.* Energy 223 (2021), p. 120039. ISSN: 03605442. Doi: 10.1016/j.energy.2021.120039.

Peric 2025a

PERIC: Alkaline Type Hydrogen Generation System-Purification Equipment Research Institute of CSIC. 2025. URL: https://www.peric718.com/Alkaline-Type-Hydrogen-G/r-85.html.

Peric 2025b

PERIC: PEM Type Hydrogen Generation System-Purification Equipment Research Institute of CSIC. 2025. URL: https://www.peric718.com/PEM-Type-Hydrogen-Genera/r-89.html.

PIONEER 2022

PIONEER: VPSA Oxygen Generation Process: Applied to Glass Fiber Oxyfuel Combustion for Energy Saving and Emission Reduction. 2022. URL: https://www.vpsatech.com/news-information/VPSA-Oxygen-Generation-Process-Applied-to-Glass-Fiber-Oxyfuel-Combustion-for-Energy-Saving-and-Emission-Reduction.html.

Posco 13.10.2024

Posco: POSCO Future M Commences Operations at Pohang NCA Cathode Material Plant. 13.10.2024. URL: https://www.poscofuturem.com/en/pr/view.do?num=857.

Praxair 2017

PRAXAIR: Role of Hydrogen in Removing Sulfure Liquid Fuels. (2017). URL: https://assets.linde.com/-/media/global/corporate/corporate/documents/sustainable-development/climate-change/the-role-of-hydrogen-in-removing-sulfur-from-liquid-fuels-w-disclaimer-r1.pdf.

QUEST ONE 2025

QUEST ONE: PEM-Elektrolyseur Modular Hydrogen Platform: Quest One Produkte. 2025. URL: https://www.questone.com/produkte/detail/mhp-serie/mhp-elektrolyseur/.

Raeting 2024

RAETING: World's top five glass manufacturers. 2024. URL: https://raeting.com/news/the-worlds-top-five-glass-fiber-manufacturers/.

REFHYNE 2018

REFHYNE: Clean refinery hydrogen for europe. 2018. URL: https://www.refhyne.eu/about/.

Reil 2024

REIL, M.: Efficient-oxygen-supply-in-fish-farming. 2024. URL: https://www.kerafol.com/wp-content/uploads/2024/08/Efficient-oxygen-supply-in-fish-farming.pdf.

Reinhardt et al. 2015

REINHARDT, H.-J.; OBERMEYER, H.-D.; SCHREINER, B.; WOLF, S.: Oxygen enrichment for intensification of air oxidation reactions. Ed. by LINDE AG. 2015.

ResourceWise 2023

RESOURCEWISE: 2023 Pulp and Paper Industry Year in Review. 2023. URL: https://www.resourcewise.com/forest-products-blog/2023-pulp-and-paper-industry-year-in-review.

Rodríguez et al. 2007

RODRÍGUEZ, A.; JIMÉNEZ, L.; FERRER, J.: Use of oxygen in the delignification and bleaching of pulps. (2007).

Saint Gobain 2025

SAINT GOBAIN: Glass Manufacturing Process | How is Glass made | Saint-Gobain Glass. Ed. by SAINT GOBAIN. 2025. URL: https://in.saint-gobain-glass.com/knowledge-center/glass-manufacturing-process.

Salmon Business 2024

SALMON BUSINESS: Meet the world's largest land-based producer of Atlantic salmon / SalmonBusiness. 2024. URL: https://www.salmonbusiness.com/meet-the-worlds-largest-producer-of-land-based-atlantic-salmon/.

SCHOTT 2025

SCHOTT: The center of a global glass tubing industry. 2025. URL: https://www.schott.com/en-gb/about-us/company/regions-and-locations/mitterteich.

SCHOTT & REUFER 17.09.2016 - 19.09.2016

SCHOTT, R.; REUFER, F.: *EFFICIENCY IMPROVEMENT OF REDUCING AGENTS IN THE BLAST FURNACE TO REDUCE CO2 EMISSIONS AND COSTS.* ABM Proceedings. São Paulo: Editora Blucher, 17.09.2016 - 19.09.2016, pp. 379–390. DOI: 10.5151/2594-357X-27827.

SHELL 2025

SHELL: Claus Process | Shell Global. 2025. URL: https://www.shell.com/business-customers/catalysts-technologies/licensed-technologies/emissions-standards/sulphur-recovery/claus-process.html#iframe=L2NvbnRlbnQvZXhwZXJpZW5jZS1mcmFnbWVudHMvc2hlbGwvY29ycG9yYXRlL2J1c2luZXNzLWN1c3Rv=

Shu et al. 2021

Shu, X.; Guo, Y.; Yang, W.; Wei, K.; Zhu, G.: Life-cycle assessment of the environmental impact of the batteries used in pure electric passenger cars. Energy Reports 7 (2021), pp. 2302–2315. ISSN: 23524847. DOI: 10.1016/j.egyr.2021.04.038.

SINGH & RAJ 2025

SINGH, S.; RAJ, A.: Investigating the impact of co-combustion of acid gas and hydrogen in the Claus process for efficient sulfur production, contaminant destruction, and low carbon emissions. Gas Science and Engineering 134 (2025), p. 205535. ISSN: 29499089. DOI: 10.1016/j.jgsce.2024.205535.

Skinner & Lalit 2023

SKINNER, B.; LALIT, R.: With Concrete, Less Is More - RMI. 2023. URL: https://rmi.org/with-concrete-less-is-more/.

Skouteris et al. 2020

SKOUTERIS, G.; RODRIGUEZ-GARCIA, G.; REINECKE, S. F.; HAMPEL, U.: The use of pure oxygen for aeration in aerobic wastewater treatment: A review of its potential and limitations. Bioresource technology 312 (2020), p. 123595. DOI: 10.1016/j.biortech.2020.123595.

SMOLINKA & GARCHE 2022

SMOLINKA, T.; GARCHE, J., eds.: Electrochemical power sources: fundamentals, systems, and applications: Hydrogen production by water electrolysis. Amsterdam, Oxford, and Cambridge, MA: Elsevier, 2022. ISBN: 9780128194249.

SORG 05.07.2023

SORG: Nachhaltigkeit. 5.07.2023. URL: https://www.sorg.de/de/nachhaltige-glasschmelze/.

Speight 2011

SPEIGHT, J. G.: *The refinery of the future*. Norwich, N.Y, Oxford, and Oxford: William Andrew and Elsevier Science distributor, 2011. ISBN: 9780815520412. URL: https://www.sciencedirect.com/science/book/9780815520412.

Statista 2024a

STATISTA: Ceramic tile companies: global producer ranking 2023 | Statista. 2024. URL: https://www.statista.com/statistics/939668/global-leading-ceramic-tile-manufacturing-companies/.

Statista 2024b

STATISTA: Most profitable companies worldwide 2023 | Statista. 2024. URL: https://www.statista.com/statistics/269857/most-profitable-companies-worldwide/.

STEFAN LEICHSENRING 2022

STEFAN LEICHSENRING: Teslas 4680-Zellen haben NCM811-Chemie und reine Graphit-Anode. Ed. by INSIDEEVS.DE. 2022. URL: https://insideevs.de/news/598966/tesla-4690zellen-zerlegung-aufbau-ncm811chemie/.

STEGRA 2025

STEGRA: Our platforms -; green hydrogen, iron and steel. 2025. URL: https://stegra.com/green-platforms.

STEINHARDT 06.03.2025

STEINHARDT, M.: Oxygen purity of Siemens Energy's PEMWE: Email. Ed. by Amir Dastgheibifard. 6.03.2025.

Sumitomo Metal Mining 2023

SUMITOMO METAL MINING: SMM to Make Strategic Investment in Battery Cathode Material Technology Developer Nano One Collaboration on Producing Technology for Electric Vehicle Battery Material. 2023. URL: https://www.smm.co.jp/en/news/release/uploaded_files/20230925_EN.pdf.

Sunandan 2010

Sunandan, L.: Overview on the use of liquid oxygen to Pulp and Paper Industries. IPPTA (2010).

Sunfire 2025

Sunfire: $Pressurized \ Alkaline \ Electrolyzers \ (AEL) \ Sunfire. \ 2025.$ url: https://sunfire.de/en/products/pressurized-alkaline-electrolyzers-ael/.

TEAM 2024

TEAM, H. E.: Ohmium to develop electrolyzer solutions for 300-MW offshore floating green ammonia plant. 2024. URL: https://hydrogentechworld.com/ohmium-to-develop-electrolyzer-solutions-for-groundbreaking-300-mw-offshore-floating-green-ammonia-plant.

The Arab Contractors 2023

THE ARAB CONTRACTORS: New Delta Water Treatment Plant | The Arab Contractors. 2023. URL: https://www.arabcont.com/english/project-777.

THYSSENKRUPP NUCERA 2025

THYSSENKRUPP NUCERA: Grüner Wasserstoff. 2025. URL: https://www.thyssenkrupp-nucera.com/de/gruener-wasserstoff/.

Total Materia 2007

TOTAL MATERIA: hydrogen in steels. 2007. URL: https://www.totalmateria.com/en-us/articles/hydrogen-in-steels/.

U.S. Department of Energy and Tampa Electric Company 2000

U.S. DEPARTMENT OF ENERGY AND TAMPA ELECTRIC COMPANY: Tampa Electric Integrated Gasification Combined-Cycle Project. Clean Coal Technology (2000).

UCSF 2024

UCSF: O₂ Demand Calculator | Oxygen Calculator. 2024. URL: https://www.oxygencalculator.com/oxygen/o2demand.

VAN ORMER & VAN ORMER 2011

VAN ORMER, S.; VAN ORMER, H.: COMPRESSED AIR IN WASTEWATER TREATMENT. 2011.

Vogl et al. 2018

VOGL, V.; ÅHMAN, M.; NILSSON, L. J.: Assessment of hydrogen direct reduction for fossil-free steelmaking. Journal of Cleaner Production 203 (2018), pp. 736–745. ISSN: 09596526. DOI: 10.1016/j.jclepro.2018.08.279.

Wang 2019

WANG, L.: The world's 10 largest producer of magnesite. 2019. URL: https://www.apsense.com/article/the-worlds-10-largest-producer-of-magnesite.html.

Webmaster 2022

WEBMASTER: Medicinal Oxygen: WHO International Pharmacopoeia PH.INT redefinition Autonomy in your Oxygen and Nitrogen supply, with the most sustainable solution. 2022. URL: https://www.pcigases.com/news/medicinal-oxygen-who-international-pharmacopoeia-ph-int-re-definition/.

Wente & Nutting 2024

WENTE, E. F.; NUTTING, J.: Steel - Basic Oxygen, Refining, Alloying | Britannica. 2024. URL: https://www.britannica.com/technology/steel/Basic-oxygensteelmaking.

Westbroek et al. 2021

WESTBROEK, C. D.; BITTING, J.; CRAGLIA, M.; AZEVEDO, J. M. C.; CULLENA, J. M.: Global Material Flow Analysis of Glass: From Raw Materials to End-of-Life. PhD thesis. Cambridge, UK: University of Cambridge, 2021.

Wikipedia 2025

WIKIPEDIA: Tuwairqi Steel Mills - Wikipedia. 2025. URL: https://en.wikipedia.org/wiki/Tuwairqi_Steel_Mills.

Wikipedia 18.01.2025

WIKIPEDIA: Kraftwerk Irsching. 18.01.2025. URL: https://de.wikipedia.org/wiki/Kraftwerk Irsching.

Wikipedia 31.01.2025

WIKIPEDIA: Tuoketuo Power Station. 31.01.2025. URL: https://en.wikipedia.org/wiki/Tuoketuo_Power_Station.

World Steel Association 2020

World Steel Association: The steelmaking process. 2020.

World Steel Association 2024

WORLD STEEL ASSOCIATION: Total production of crude steel 2024. 2024. URL: https://worldsteel.org/data/annual-production-steel-data/?ind=P1_crude_steel_total_pub/CHN/IND/WORLD_ALL.

XIAO ET AL. 2022

XIAO, P.; LI, W.; CHEN, S.; LI, G.; DAI, Z.; FENG, M.; CHEN, X.; YANG, W.: Effects of Oxygen Pressurization on Li+/Ni2+ Cation Mixing and the Oxygen Vacancies of LiNi0.8Co0.15Al0.05O2 Cathode Materials. ACS applied materials & interfaces 14.28 (2022), pp. 31851–31861. DOI: 10.1021/acsami.2c05136.

YICAI 24.07.2024

YICAI: China's Ronbay Gets Go-Ahead to Hike Battery Materials Capacity in South Korea. (24.07.2024). URL: https://www.yicaiglobal.com/news/chinas-ronbay-gets-go-ahead-to-hike-battery-materials-capacity-in-south-korea.

Zahid et al. 2023

Zahid, U.; Khalafalla, S. S.; Alibrahim, H. A.; Ahmed, U.; Jameel, A. G. A.: *Techno-economic evaluation of simultaneous methanol and hydrogen production via autothermal reforming of natural gas.* Energy Conversion and Management 296 (2023), p. 117681. ISSN: 01968904. DOI: 10.1016/j.enconman.2023.117681.

ZEMAN 2009

ZEMAN, F.: Oxygen combustion in cement production. Energy Procedia 1.1 (2009), pp. 187–194. ISSN: 18766102. DOI: 10.1016/j.egypro.2009.01.027.

ZHAO 2024

ZHAO, T.: Hydrogen case study: operational efficiency and electrolyser technology at the Sinopec Kuqa project | Wood Mackenzie. 2024. URL: https://www.woodmac.com/news/opinion/hydrogen-case-study-sinopec-kuqa-project/.

ZHOU ET AL. 2009

ZHOU, J.; CHEN, Q.; ZHAO, H.; CAO, X.; MEI, Q.; LUO, Z.; CEN, K.: Biomass-oxygen gasification in a high-temperature entrained-flow gasifier. Biotechnology advances 27.5 (2009), pp. 606-611. DOI: 10.1016/j.biotechadv.2009.04.011.